

Commercializing a Next-Generation Source of Safe Nuclear Energy

Low Energy Nuclear Reactions (LENRs)

Experimental examples: gas-phase Nickel-seed Hydrogen systems and their measured transmutation products; ‘hard’ radiation is absent

What products might be found if Fe, Cr, Pd seeds were also present?

Technical Overview

**Lewis Larsen, President and CEO
Lattice Energy LLC**

April 20, 2011

“There are two possible outcomes: if the result confirms the hypothesis, then you've made a measurement. If the result is contrary to the hypothesis, then you've made a discovery.”

Enrico Fermi



Commercializing a Next-Generation Source of Safe Nuclear Energy

Contents

Main objectives of presentation	3
References	4
Overview and useful background information	5 - 25
Discussion of W-L networks and experimental data	26 - 34
Gas-phase LENR systems with metallic vessels	35 - 49
Pd-seed experiments consistent with ULMN capture	50 - 57
Conclusions, W-L technical papers, and final quotation	58 - 61

Main objectives of presentation

Discuss certain W-L LENR transmutation networks in context of experiments

- ✓ Present selected segments of W-L model LENR nucleosynthetic networks starting with ULM neutron captures on stable Chromium (Cr), Iron (Fe), and Nickel (Ni) 'seed' isotopes; discuss likely pathways and isotopic products that might be produced
- ✓ Explain extreme importance of accurate 'before and after' characterization of ALL materials, both compositionally and isotopically, that are exposed to regions of apparatus in which LENRs are occurring; appreciate often severe consequences of poor characterization in terms of being unable to understand what may appear to be bewildering, inconclusive experimental results re observed transmutation products
- ✓ For gas-phase LENR experiments, explain importance of extensive wall interactions that can occur inside metal reaction vessels, including likelihood of significant wall material ablation over time, and how this might affect experimental observations
- ✓ Relate described W-L model networks and related concepts to specific experiments involving measurements of LENR transmutation products and photon radiation and how W-L theory can potentially help readers to better understand such observations
- ✓ Discuss implications of W-L Palladium (Pd) and Cr 'seed' networks in context of selected examples of anomalous isotopic abundances observed in a variety of interesting and different physical environments, including catalytic converters

References

Two important source documents referenced in this presentation

✓ 2004 ICCF-11 conference paper (not refereed):

“Surface analysis of hydrogen-loaded nickel alloys”

E. Campari (Dipartimento di fisica, Università di Bologna, Centro IMO, Bologna, Italy), S. Focardi (Dipartimento di fisica, Università di Bologna, Centro IMO, Bologna, Italy), V. Gabbani (Dipartimento di fisica, Università di Siena, Centro IMO, Bologna, Italy), V. Montalbano (Dipartimento di fisica, Università di Siena, Centro IMO, Bologna, Italy), F. Piantelli (Dipartimento di fisica, Università di Siena, Centro IMO, Bologna, Italy), and S. Veronesi (Dipartimento di fisica, Università di Siena, Centro IMO, Bologna, Italy, and INFN, UdR Siena, Siena, Italy)

CONDENSED MATTER NUCLEAR SCIENCE pp. 414 - 420

Proceedings of the 11th International Conference on Cold Fusion

Marseilles, France, 31 October - 5 November 2004

edited by Jean-Paul Biberian (Université de la Méditerranée, France)

World Scientific Publishing 2006

DOI No: 10.1142/9789812774354_0034

Source URL (World Scientific website) = <http://eproceedings.worldscinet.com/9789812774354/9789812774354.shtml>

Source URL (purchase online) = http://eproceedings.worldscinet.com/9789812774354/9789812774354_0034.html

Source URL (free public copy of conference paper on LENR-CANR.org; this may differ slightly from final version published by World Scientific in 2006) = <http://www.lenr-canr.org/acrobat/CampariEGsurfaceana.pdf>

✓ 2011 Lattice PowerPoint presentation (not refereed):

“Nucleosynthetic networks beginning with Nickel ‘seed’ nuclei --- why cascades of fast Beta-decays are important and why end-products of LENR networks are mostly stable isotopes”

L. Larsen, Lattice Energy LLC Technical Document dated March 24, 2011

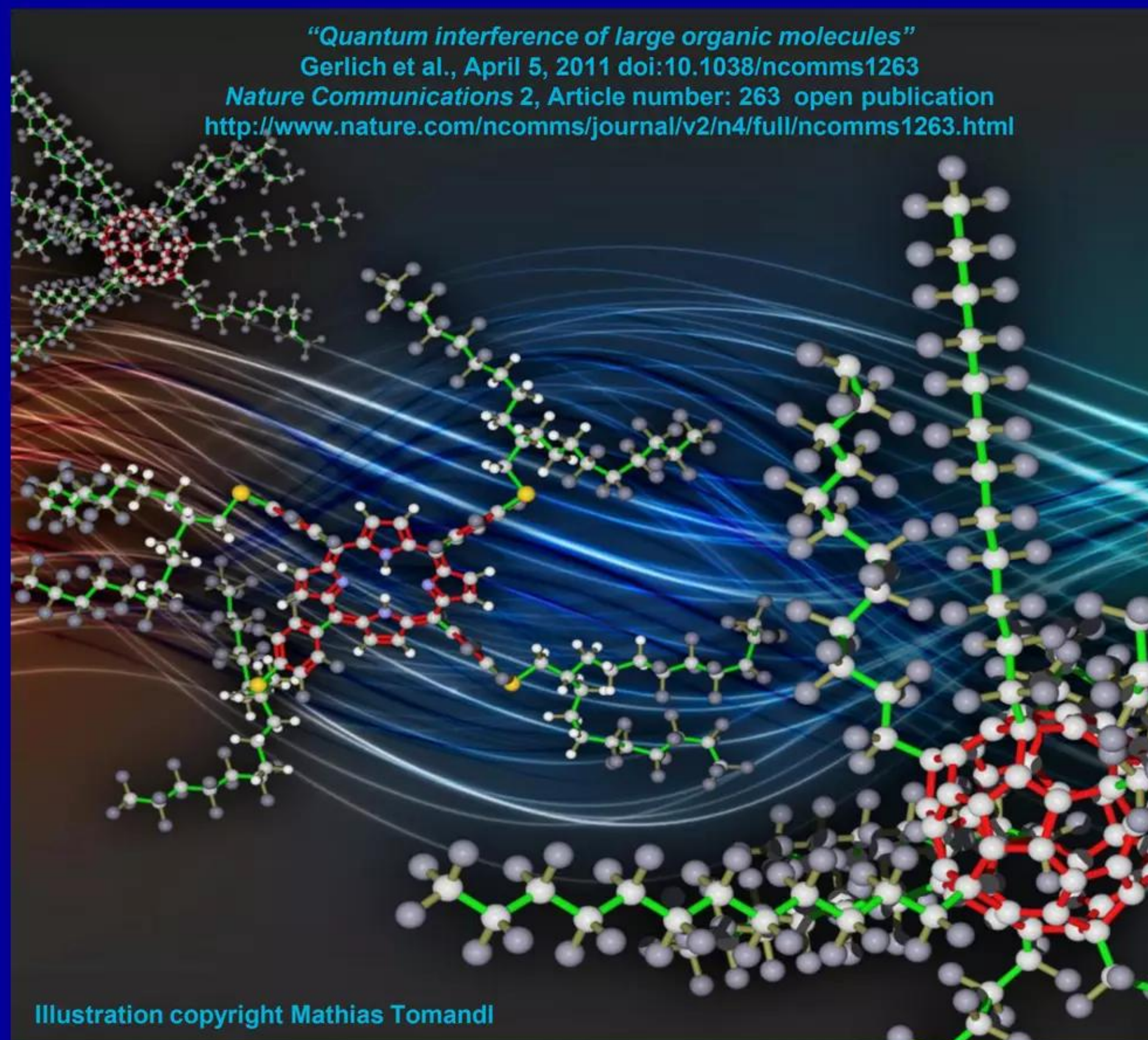
Source URL = <http://www.slideshare.net/lewisglarsen/lattice-energy-llcnickel-seed-wl-lenr-nucleosynthetic-networkmarch-24-2011>

Commercializing a Next-Generation Source of Safe Nuclear Energy

Overview and useful background information

Many-body collective Q-M effects are widespread in Nature

“PFNS10 and TPPF152 contain 430 atoms covalently bound in one single particle. This is ~350% more than that in all previous experiments and it compares well with the number of atoms in small Bose–Einstein condensates (BEC), which, of course, operate in a vastly different parameter regime: The molecular de Broglie wavelength λ_{dB} is about six orders of magnitude smaller than that of ultracold atoms and the internal molecular temperature exceeds typical BEC values ($T < 1 \mu\text{K}$) by about nine orders of magnitude. Although matter wave interference of BECs relies on the de Broglie wavelength of the individual atoms, our massive molecules always appear as single entities.”



“Our experiments prove the quantum wave nature and delocalization of compounds composed of up to 430 atoms, with a maximal size of up to 60 \AA , masses up to $m=6,910 \text{ AMU}$ and de Broglie wavelengths down to $\lambda_{dB}=h/mv \approx 1 \text{ pm}$... In conclusion, our experiments reveal the quantum wave nature of tailor-made organic molecules in an unprecedented mass and size domain. They open a new window for quantum experiments with nanoparticles in a complexity class comparable to that of small proteins, and they demonstrate that it is feasible to create and maintain high quantum coherence with initially thermal systems consisting of more than 1,000 internal degrees of freedom.”

Artistic view of most complex and massive molecules (PFNS-10, TPP-152)
brought to quantum interference by Gerlich et al. (2011)

Commercializing a Next-Generation Source of Safe Nuclear Energy

Many-body collective Q-M effects widespread in Nature

Welcome to the New World!

"I am increasingly persuaded that all physical law we know about has collective origins, not just some of it."

"... I think a good case can be made that science has now moved from an Age of Reductionism to an Age of Emergence, a time when the search for ultimate causes of things shifts from the behavior of parts to the behavior of the collective Over time, careful quantitative study of microscopic parts has revealed that at the primitive level at least, collective principles of organization are not just a quaint sideshow but everything --- the true essence of physical law, including perhaps the most fundamental laws we know ... nature is now revealed to be an enormous tower of truths, each descending from its parent, and then transcending that parent, as the scale of measurement increases."

"Like Columbus or Marco Polo, we set out to explore a new country but instead discovered a new world."

Robert Laughlin, *"A Different Universe - Reinventing Physics from the Bottom Down,"* Basic Books, 2005, pp. xv and 208

Commercializing a Next-Generation Source of Safe Nuclear Energy

Many-body collective Q-M effects widespread in Nature

- ✓ Many-body collective oscillations and mutual quantum entanglement of protons (as well as deuterons and tritons) and electrons (e.g., SPPs on metallic hydride surfaces), in conjunction with a breakdown of the Born-Oppenheimer approximation, appear to be relatively common in nature, occurring in many different types of systems
- ✓ While these many-body collective processes chronicled by Chatzidimitriou-Dreismann et al. operate very rapidly and nanoscale coherence can only persist for time spans on the order of femtoseconds (10^{-15} sec) to attoseconds (10^{-18} sec), nuclear processes such as weak interaction ULM neutron production and neutron capture operate on even faster time-scales: 10^{-19} to 10^{-22} sec. Therefore, LENRs as explained by the Widom-Larsen theory can easily take advantage of such many-body collective quantum effects as an integral part of their amazing dynamical repertoire
- ✓ It is well-known that metallic surface nanostructures and SPP electrons can have configurations that are able to effectively absorb E-M energy over a wide area, transfer and concentrate it, and in conjunction with contiguous surface 'patches' of collectively oscillating protons, create extremely high local electric fields. According to W-L theory, ULM neutron production may then follow

→ C. A. Chatzidimitriou-Dreismann (Technical University of Berlin) and his collaborators have published extensively on collective proton dynamics since 1995. Please also see:

→ "Attosecond quantum entanglement in neutron Compton scattering from water in the keV range" - 2007; can be found at

http://arxiv.org/PS_cache/cond-mat/pdf/0702/0702180v1.pdf

"Several neutron Compton scattering (NCS) experiments on liquid and solid samples containing protons or deuterons show a striking anomaly, i.e. a shortfall in the intensity of energetic neutrons scattered by the protons; cf. [1, 2, 3, 4]. E.g., neutrons colliding with water for just 100 – 500 attoseconds ($1 \text{ as} = 10^{-18} \text{ s}$) will see a ratio of hydrogen to oxygen of roughly 1.5 to 1, instead of 2 to 1 corresponding to the chemical formula H_2O Recently this new effect has been independently confirmed by electron-proton Compton scattering (ECS) from a solid polymer [3, 4, 5]. The similarity of ECS and NCS results is striking because the two projectiles interact with protons via fundamentally different forces, i.e. the electromagnetic and strong forces."

→ Also, J. D. Jost et al., "Entangled mechanical oscillators" *Nature* 459 pp. 683 – 685 4 June 2009, in which "mechanical vibration of two ion pairs separated by a few hundred micrometres is entangled in a quantum way."

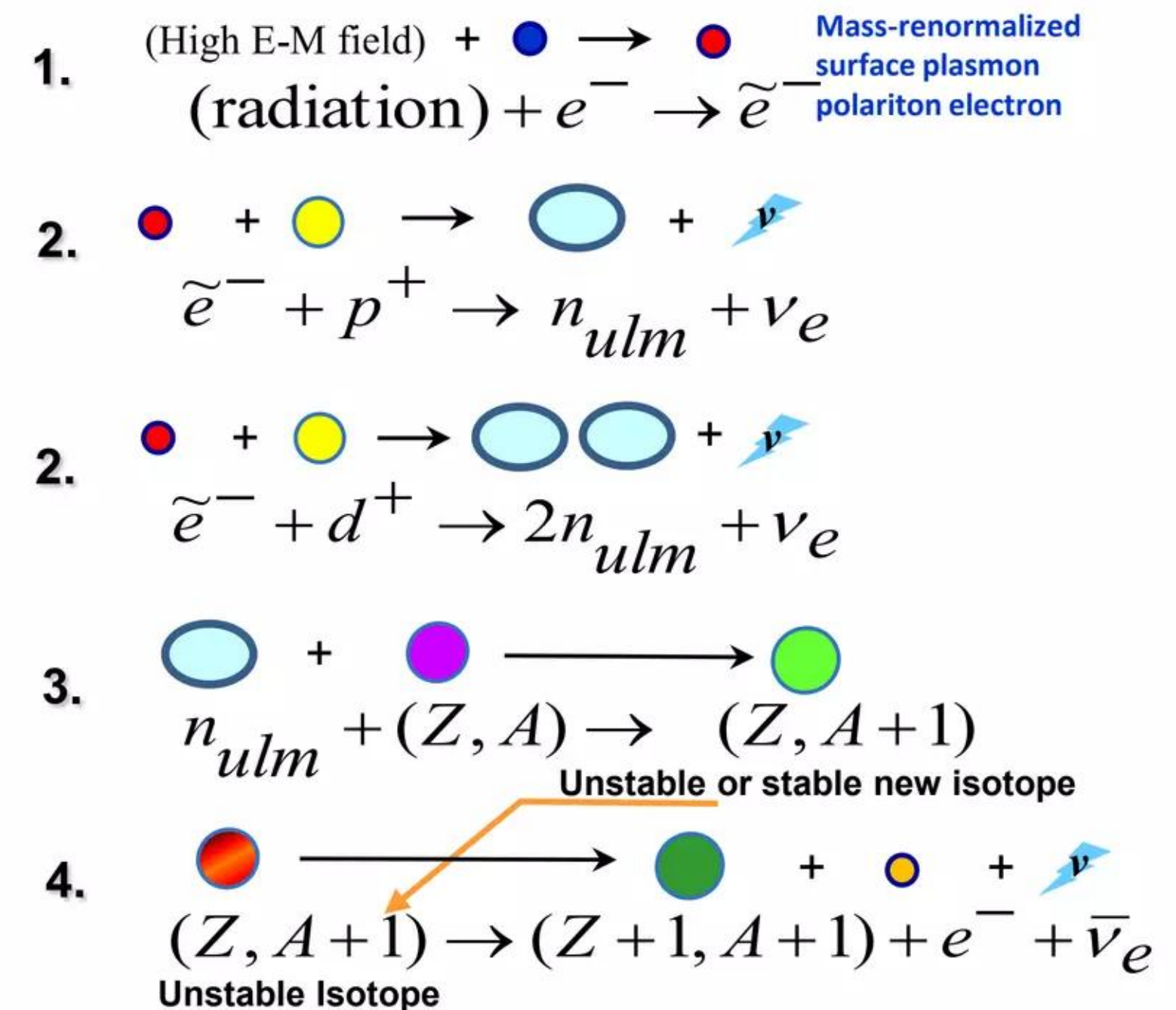
W-L mechanism in condensed matter LENR systems

Weak interaction processes are very important in LENRs

1. E-M radiation on metallic hydride surface increases mass of surface plasmon electrons
2. Heavy-mass surface plasmon polariton electrons react directly with surface protons (p^+) or deuterons (d^+) to produce ultra low momentum (ULM) neutrons (n_{ulm} or $2n_{ulm}$, respectively) and an electron neutrino (ν_e)
3. Ultra low momentum neutrons (n_{ulm}) are captured by nearby atomic nuclei (Z, A) representing some element with charge (Z) and atomic mass (A). ULM neutron absorption produces a heavier-mass isotope ($Z, A+1$) via transmutation. This new isotope ($Z, A+1$) may itself be a stable or unstable, which will perform eventually decay
4. Many unstable isotopes β^- decay, producing: transmuted element with increased charge ($Z+1$), \sim same mass ($A+1$) as 'parent' nucleus; β^- particle (e^-); and an antineutrino

→ Note: colored shapes associated with diagram on next Slide

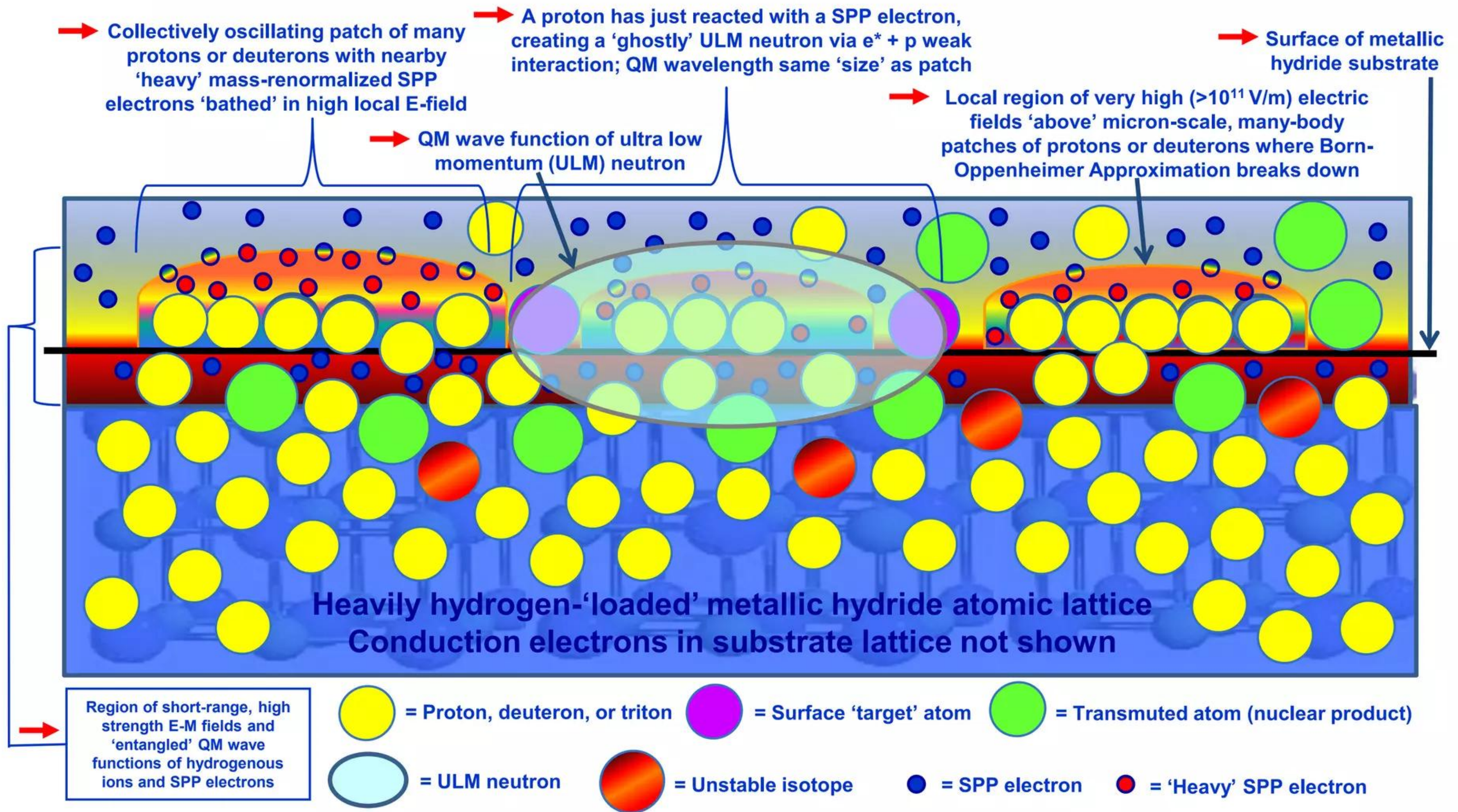
→ No strong interaction fusion or heavy element fission occurring below; weak interaction $e + p$ or $e + d$



→ Weak interaction β^- decays (shown above), direct gamma conversion to infrared (not shown), and α decays (not shown) produce most of the excess heat calorimetrically observed in LENR systems

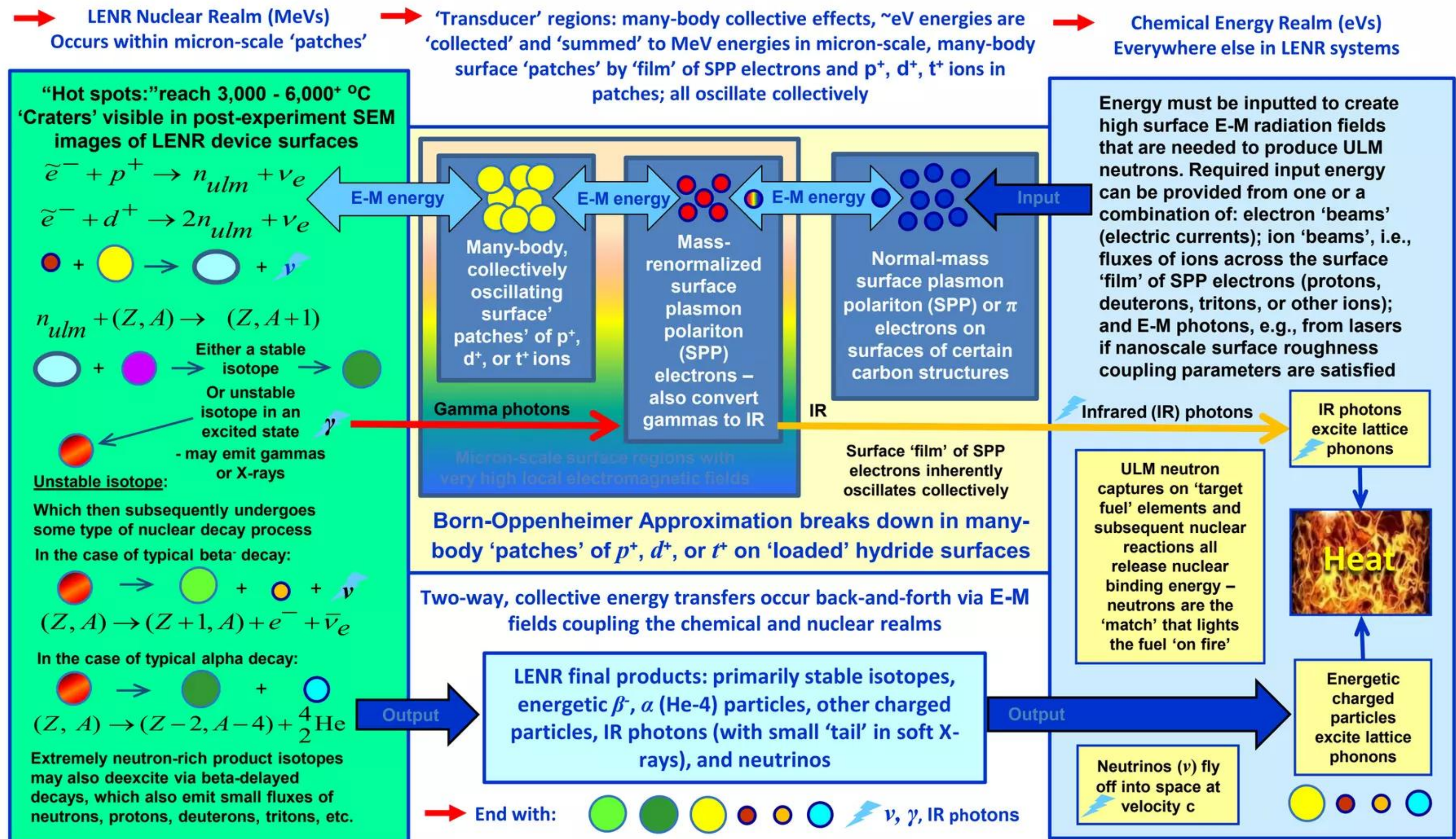
Conceptual details: W-L mechanism in metallic hydrides

Side view – not to scale – charge balances in diagram only approximate



High level overview: W-L mechanism in condensed matter

Chemical and nuclear energy realms can interconnect in small regions



What is required for LENRs to occur in condensed matter?

Key factors for initiation and operation

- ✓ Substantial quantities of Hydrogen isotopes must be brought into intimate contact with ‘fully-loaded’ metallic hydride-forming metals; e.g., Palladium, Platinum, Rhodium, Nickel, Titanium, Tungsten, etc.; please note that collectively oscillating, 2-D surface plasmon (SP) electrons are intrinsically present and cover the surfaces of such metals. At ‘full loading’ of H, many-body, collectively oscillating ‘patches’ of protons (p^+), deuterons (d^+), or tritons (t^+) will form spontaneously at random locations scattered across such surfaces
- ✓ Or, delocalized collectively oscillating π electrons that comprise the outer ‘covering surfaces’ of fullerenes, graphene, benzene, and polycyclic aromatic hydrocarbon (PAH) molecules behave very similarly to SPs; when such molecules are hydrogenated, they can create many-body, collectively oscillating, ‘entangled’ quantum systems that, within context of W-L theory, are functionally equivalent to loaded metallic hydrides
- ✓ Born-Oppenheimer approximation breaks down in tiny surface ‘patches’ of contiguous collections of collectively oscillating p^+ , d^+ , and/or t^+ ions; enables E-M coupling between nearby SP or π electrons and hydrogen ions at these locations --- *creates local nuclear-strength electric fields*; effective masses of coupled electrons are then increased to some multiple of an electron at rest ($e \rightarrow e^*$) determined by required simultaneous energy input(s)
- ✓ System must be subjected to external non-equilibrium fluxes of charged particles or E-M photons that are able to transfer input energy directly to many-body SP or π electron ‘surface films.’ Examples of such external energy sources include (they may be used in combination): electric currents (electron ‘beams’); E-M photons (e.g., emitted from lasers, IR-resonant E-M cavity walls, etc.); pressure gradients of p^+ , d^+ , and/or t^+ ions imposed across ‘surfaces’; currents of other ions crossing the ‘electron surface’ in either direction (ion ‘beams’); etc. Such sources provide additional input energy that is required to surpass certain minimum H-isotope-specific electron-mass thresholds that allow production of ULM neutron fluxes via $e^* + p^+$, $e^* + d^+$, or $e^* + t^+$ weak interactions
- ✓ N.B.: please note again that surface plasmons are collective, many-body electronic phenomena closely associated with interfaces. For example, they can exist at gas/metal interfaces or metal/oxide interfaces. Thus, surface plasmon oscillations will almost certainly be present at contact points between purely metallic surfaces and adsorbed ‘target’ nanoparticles composed of metallic oxides, e.g., PdO, NiO, or TiO₂, etc., or vice-versa

Technical side note: ULM neutron capture cross-sections

- ✓ Unlike energetic neutrons produced in most nuclear reactions, collectively produced LENR neutrons are effectively 'standing still' at the moment of their creation in condensed matter. Since they are vastly below thermal energies (ultra low momentum), ULM neutrons have huge DeBroglie wavelengths (from *nm* to *~100 microns*) and accordingly large capture cross-sections on nearby nuclei; most or all will be locally absorbed; few will be detectable as 'free' neutrons
- ✓ For the vast majority of stable and unstable isotopes, their neutron capture cross-section (relative to measurements of cross-sections at thermal energies where $v = 2,200 \text{ m/sec}$ and neutron DeBroglie wavelength is *~2 Angstroms*) is proportional to $\sim 1/v$, where v is velocity of a neutron in *m/sec*. Since v is extraordinarily small for ULM neutrons, their capture cross-sections on atomic nuclei will therefore be correspondingly larger. After being collectively created, an enormous percentage of the ULMNs produced will be locally absorbed before scattering on nearby atoms can elevate them to thermal kinetic energies; per Prof. S. Lamoreaux (Yale) thermalization would require *~0.1 to 0.2 msec*, i.e. 10^{-4} sec. , a very long time on typical $10^{-16} - 10^{-19} \text{ sec.}$ time-scale of nuclear reactions

*Please note: ultra low momentum (ULM) neutrons have enormous absorption cross-sections on $1/v$ isotopes. For example, Lattice has estimated the ULMN fission capture cross-section on U-235 to be *~1 million barns (b)* and on Pu-239 at *49,000 b*, vs. *~586 b* and *~752 b*, respectively, for 'typical' neutrons at thermal energies*

*A neutron capture expert recently estimated the ULMN capture cross-section on He-4 at *~20,000 b* vs. a value of *<1 b* for thermal neutrons; this is a huge increase*

*By comparison, the highest known thermal n capture cross section for any stable isotope is Gadolinium-157 at *~49,000 b**

*The highest measured cross-section for any unstable isotope is Xenon-135 at *~2.7 million b**





Crucial technical point: ULMNs have many-body scattering, NOT 2-3 body scattering as, for example, in stellar plasmas or thermalized neutrons traveling through condensed matter

Decays of Neutron-rich Halo Nuclei: More Complicated

Can dynamically vary their decay 'choices' depending on their 'environment'

Per W-L theory, once ULM neutron production begins at high rates, populations of unstable, very neutron-rich 'halo' isotopes build-up locally on 2-D surfaces. Such nuclei likely have substantially lengthened half-lives because they may have a difficult time emitting beta electrons or neutrons (both of which are fermions) into locally unoccupied Q-M states. By contrast, alpha (He-4) particle and gamma photon emissions are bosons and are unaffected by the exclusion principle. If fermionic decay channels are 'blocked', neutron-rich halo nuclei may emit bosons or continue capturing ULM neutrons as long as it is energetically favorable or until they finally get so neutron-rich and excited, or a previously occupied local state opens-up, that 'something breaks' and β^- decay cascades ending in stable isotopes can begin. This is one important reason why LENR systems typically do not end-up with large amounts of long-lived, radiologically 'hot' isotopes

Importantly, the neutron-capture phase of LENRs can release substantial amounts of nuclear binding energy, much of it in the form of prompt and delayed gammas (which are bosons). Unique to LENR systems and according to W-L theory, those gammas are converted directly to infrared photons by heavy SP electrons also present in nuclear-active 'patches' on surfaces in LENR systems. As explained elsewhere, beta-decay cascades of unstable isotopes with short half-lives can proceed very rapidly, release large amounts of binding energy, and produce complex arrays of different transmutation products that, if neutron fluxes are high enough, can rapidly traverse rows of the periodic table; in one spectacular experiment, Mizuno went from K to Fe in <2 minutes

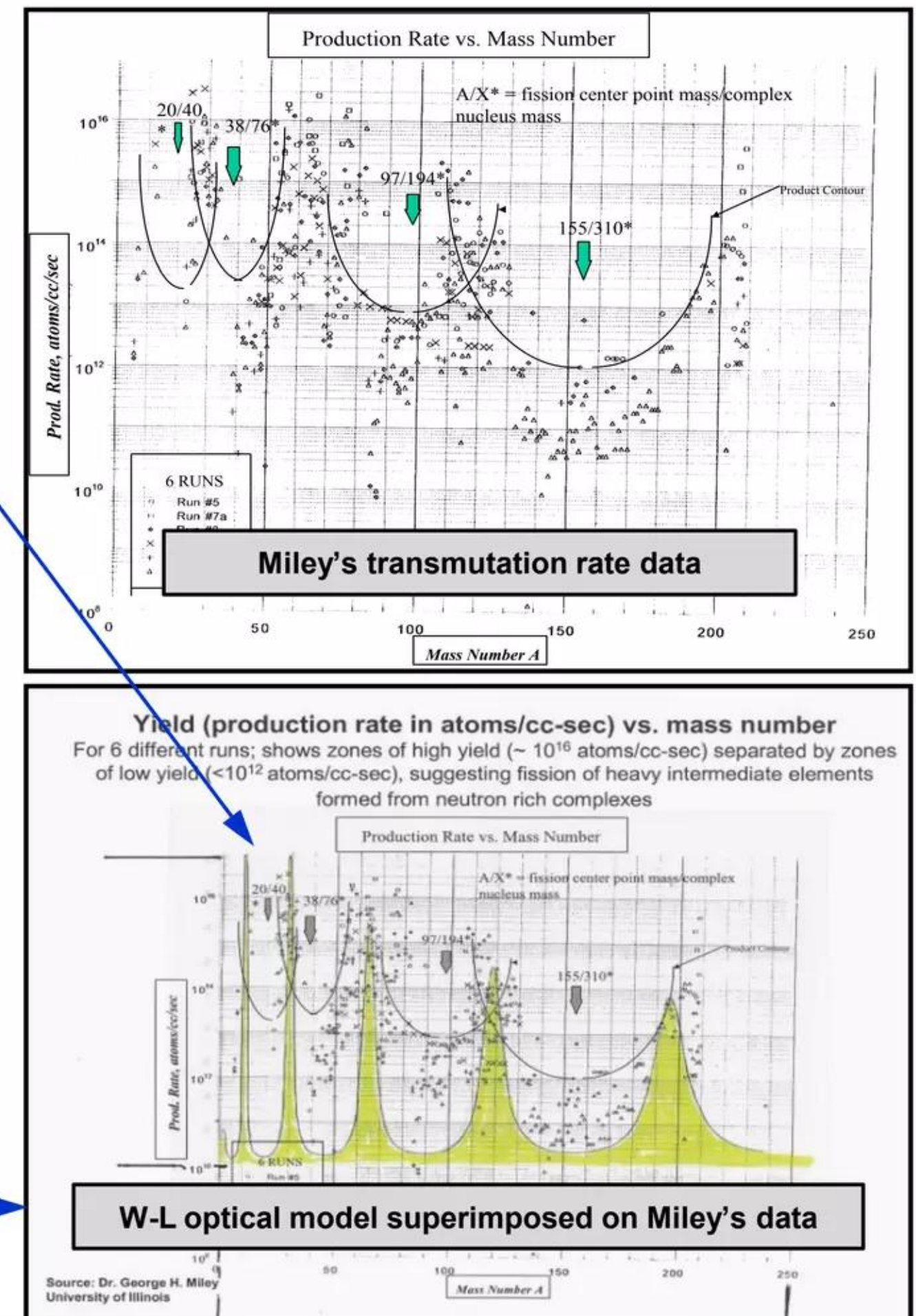
Weak interaction	W-L neutron production	LENR Nuclear Realm (MeVs) Occurs within micron-scale 'patches' $\tilde{e}^- + p^+ \rightarrow n_{ulm} + \nu_e$ $\tilde{e}^- + d^+ \rightarrow 2n_{ulm} + \nu_e$ 
Strong interaction	Neutron capture	$n_{ulm} + (Z, A) \rightarrow (Z, A+1)$  Either a: stable or unstable HEAVIER isotope
Transmutations: isotope shifts occur; chemical elements disappear/appear	Decays of unstable, very neutron-rich isotopes: beta and alpha (He-4) decays	<u>In the case of unstable isotopic products:</u> they subsequently undergo some type of nuclear decay process; e.g., beta, alpha, etc. In the case of a typical beta ⁻ decay:  $(Z, A) \rightarrow (Z+1, A) + e^- + \bar{\nu}_e$ In the case of a typical alpha decay:  $(Z, A) \rightarrow (Z-2, A-4) + {}^4_2\text{He}$ <u>Note:</u> extremely neutron-rich product isotopes may also deexcite via beta-delayed decays, which can also emit small fluxes of neutrons, protons, deuterons, tritons, etc.

Five-peak mass-spectrum: ULM neutron 'fingerprint' - I

Miley's dataset is 'smoking gun' for ULM neutron absorption by nuclei

- ✓ Top chart to right is Miley's raw data; chart below is same data only with results of W-L neutron optical potential model of ULMN neutron absorption by nuclei (yellow peaks) superimposed on top of Miley's data; good correspondence of Miley obs. vs. W-L calc.
- ✓ Model not fitted to data: only 'raw' calc output
- ✓ W-L model only generates a five-peak resonant absorption spectrum at the zero momentum limit; neutrons at higher energies will not produce the same result
- ✓ This means that 5-peak product spectrum experimentally observed by Miley and Mizuno is a unique 'signature' of W-L ULM neutron production and absorption (capture) in LENRs

See: "Nuclear abundances in metallic hydride electrodes of electrolytic chemical cells" arXiv:cond-mat/0602472 (Feb 2006) A. Widom and L. Larsen

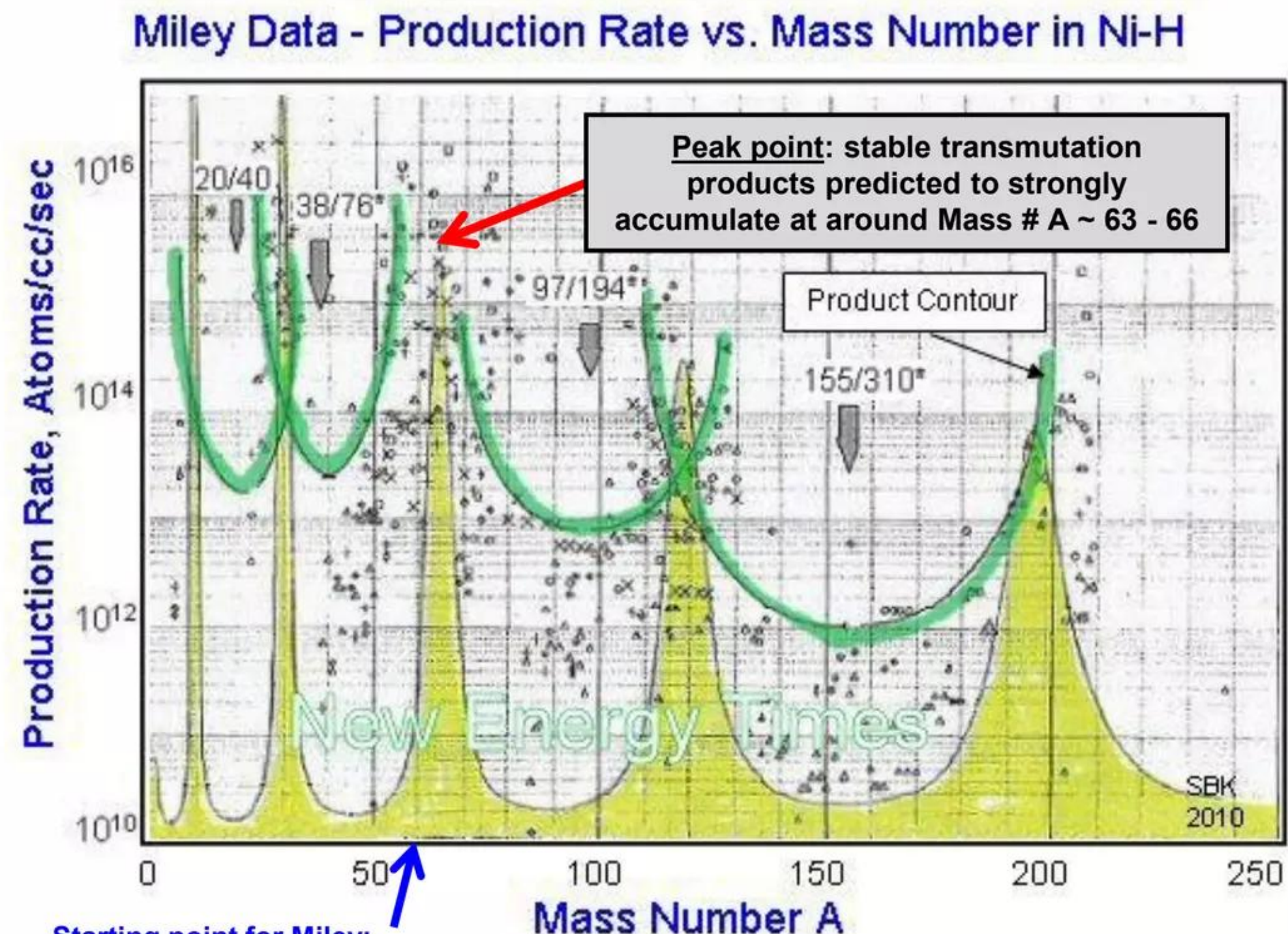


Five-peak mass-spectrum: ULM neutron 'fingerprint' - II

W-L ULM neutron absorption model (2006) strongly predicts a stable product isotopic abundance peak at around mass # $A \sim 63 - 66$ (i.e., stable isotopes will tend to accumulate around that value of mass), that is, at around $\sim \text{Cu}$ thru $\sim \text{Zn}$, which is clearly observed in Miley's 1996 experimental data shown to the right. The next major mass-peak number where somewhat larger quantities of stable LENR transmutation products are predicted by W-L to accumulate lies out at $A \sim 120$, which is also observed in Miley's (and Mizuno's) data.

Please recall that Miley's ending transmutation product rate data came from multiple P-F type electrolytic Ni-H experimental cell systems that were run for up to several weeks. Also, the beginning Nickel 'seed' in Miley's experiments was a prosaic Ni cathode comprised of (this is starting point):

Ni-58 $\sim 68.0\%$
 Ni-60 $\sim 26.2\%$
 Ni-61 $\sim 1.14\%$
 Ni-62 $\sim 3.63\%$
 Ni-64 $\sim 0.92\%$



Starting point for Miley:
 was a Nickel 'seed' at $A \sim 58 - 60$

Erratum: in fact, we drew the yellow curve showing our 'raw' model output in 2006, not in 2000 as Krivit states

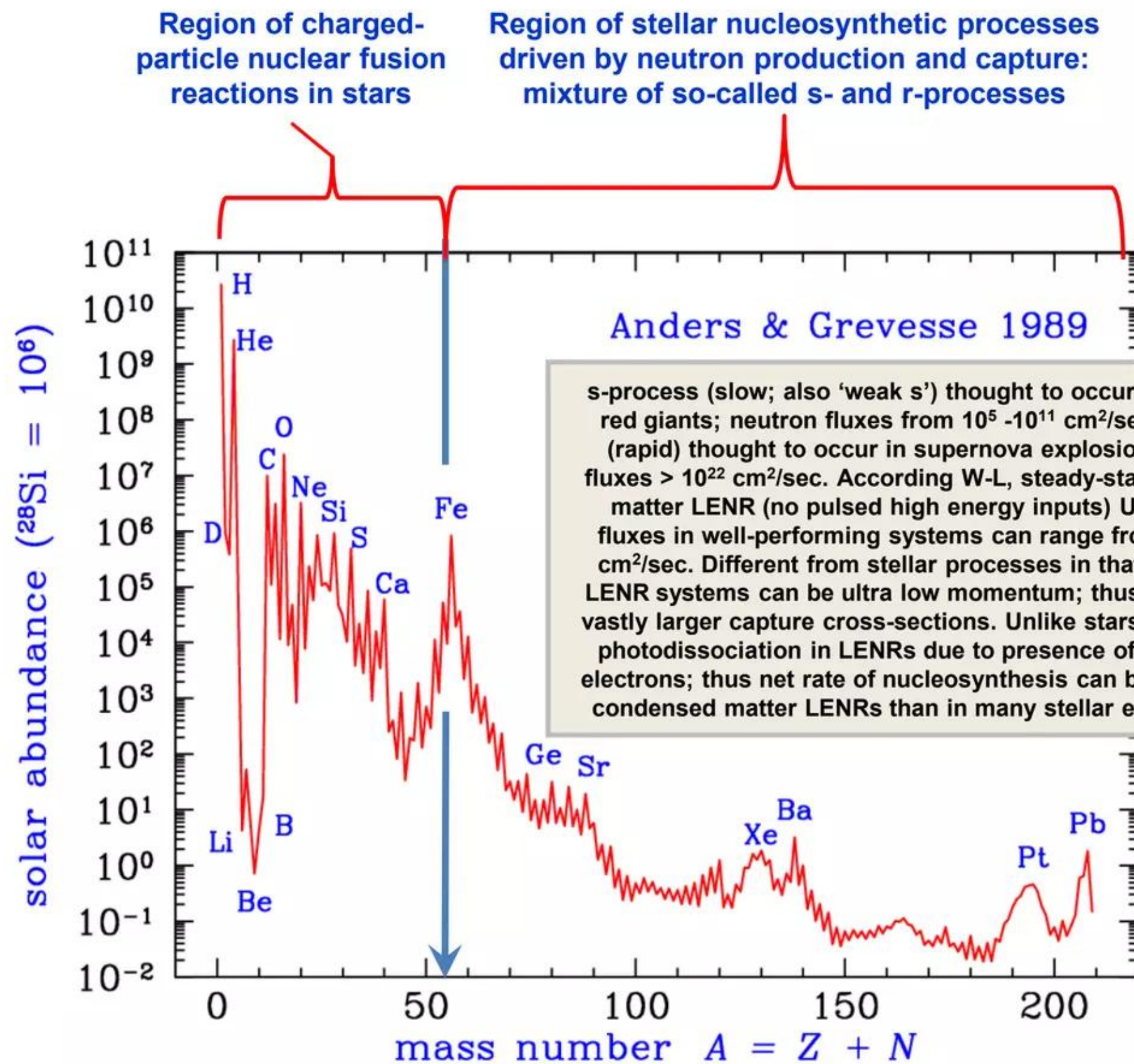
Upper 5-peak peak curve drawn by Miley in 1996 based on 6 experimental runs of transmutation yields from Ni-H LENR systems [1]. Lower curve, shaded in yellow, drawn by Larsen in 2000 with no fitting, based on Widom-Larsen ultra-low momentum neutron absorption model. [2]

1. Miley, G.H, and Patterson, James, "Nuclear Transmutations in Thin-Film Nickel Coatings Undergoing Electrolysis," Journal of New Energy, Vol. 1(3), pg. 5, (1996)
2. Larsen, Lewis, Feb. 7, 2009 slides

Source of modified graphic: New Energy Times

W-L optical model and Miley data vs. solar abundance

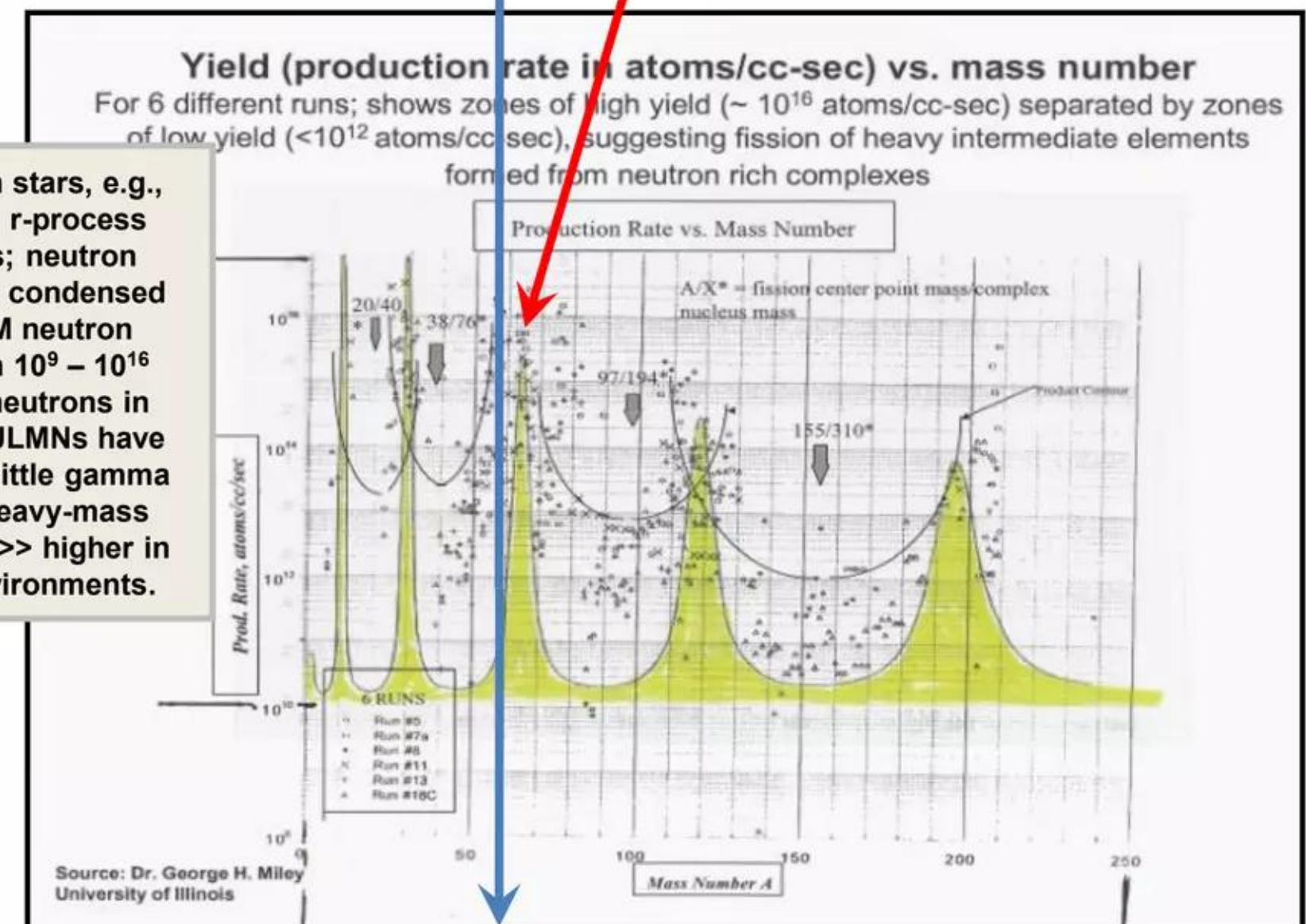
Solar abundance result of fusion up to Fe and neutron capture beyond



Solar abundance data ca. 1989 per Anders & Grevesse

Peak Point #3: W-L optical model predicts that stable LENR transmutation products should strongly accumulate at approximately Mass # $A \sim 63 - 66$; this corresponds well to Miley condensed matter transmutation data.

Condensed matter LENR neutron capture processes can operate at all values of A from 1 (H) to 200+ (beyond Pb)



Fe at $A \sim 56$

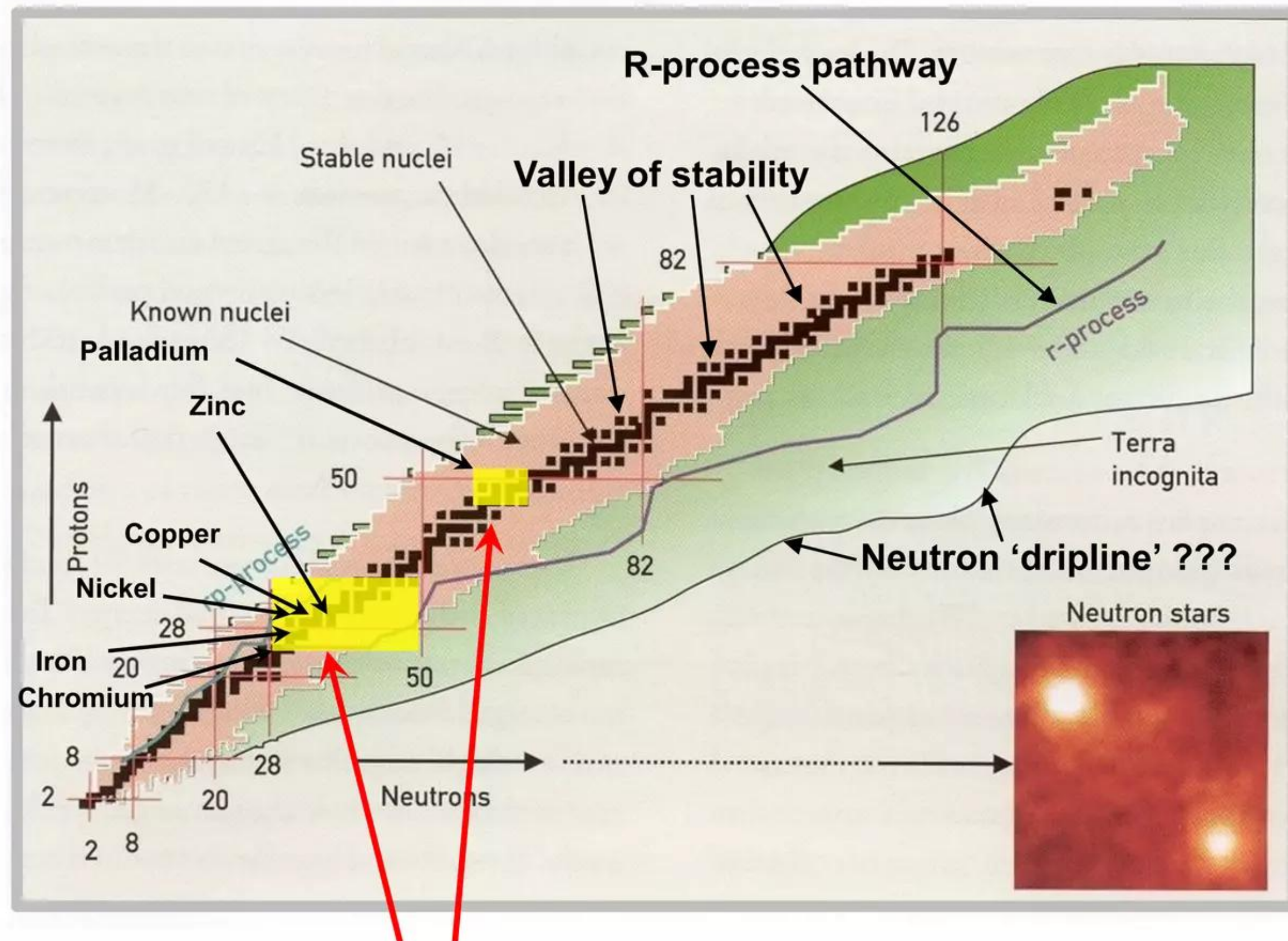
W-L optical model superimposed on Miley's ca.1996 data

Solar abundance data reflects the integrated cumulative results of stellar nuclear transmutation processes operating in super-hot plasmas across distances of AUs to light years and time spans of up to billions of years. By contrast, Miley's condensed matter LENR transmutations occurred in a volume of less than a liter over several weeks at comparatively low temperature and pressures.

Location of Ni/Fe/Cr-seed LENR Networks in Isotopic Space

Map of Isotopic Nuclear Landscape

The neutron-capture so-called “r-process” (see path on chart) that astrophysicists believe occurs mainly in stellar supernova explosions is thought to produce ~half of the nuclei heavier than Iron (Fe). It operates in the neutron-rich region of the nuclear landscape to the right of the valley of stability to beta⁻ decay. Extremely neutron-rich isotopes have a much wider variety of available decay channels in addition to ‘simple’ β^- .



While they differ from stellar environments in many important aspects, LENR systems can produce large fluxes of a wide variety of extremely neutron-rich nuclei from low to very high values of A. Thus, they may someday be able to provide nuclear physics with a new and exciting, much lower-cost experimental tool for exploring the far reaches of the nuclear landscape and boundaries of nuclear stability. This possibility deserves further careful study.

In this presentation, we will apply W-L theory and examine model LENR Ni/Fe/Cr-seed nucleosynthetic networks operating in the *approximate* yellow rectangular regions from the valley of stability (small black squares) out thru very neutron-rich, beta⁻ decay isotopic regions that lie to right of valley of stability near Chromium (Cr), Iron (Fe), Nickel (Ni), Copper (Cu), Zinc (Zn) and also in another context, Palladium (Pd)

Cr/Fe/Ni-seed ULM Neutron Catalyzed Network Pathways

THE PERIODIC TABLE

Major vector of LENR Cr/Fe/Ni-seed nucleosynthetic pathways discussed herein indicated by red arrow

'Seeds' of Iron (Fe), Nickel (Ni), and Chromium (Cr) are all present

Mostly end-up at Copper (Cu) and Zinc (Zn)

1 IA	2 IIA											13 IIIA	14 IVA	15 VA	16 VIA	17 VIIA	18 VIIIA	
H 1 1.008 Hydrogen												B 5 10.81 Boron	C 6 12.01 Carbon	N 7 14.01 Nitrogen	O 8 16.00 Oxygen	F 9 19.00 Fluorine	Ne 10 20.18 Neon	
Li 3 6.94 Lithium	Be 4 9.01 Beryllium											Al 13 26.98 Aluminum	Si 14 28.09 Silicon	P 15 30.97 Phosphorus	S 16 32.07 Sulfur	Cl 17 35.45 Chlorine	Ar 18 39.95 Argon	
Na 11 22.99 Sodium	Mg 12 24.31 Magnesium	3 IIIB	4 IVB	5 VB	6 VIB	7 VIIB	8 VIII	9 VIII	10 VIII	11 IB	12 IIB							
K 19 39.10 Potassium	Ca 20 40.08 Calcium	Sc 21 44.96 Scandium	Ti 22 47.88 Titanium	V 23 50.94 Vanadium	Cr 24 52.00 Chromium	Mn 25 54.94 Manganese	Fe 26 55.85 Iron	Co 27 58.93 Cobalt	Ni 28 58.69 Nickel	Cu 29 63.55 Copper	Zn 30 65.39 Zinc	Ga 31 69.72 Gallium	Ge 32 72.61 Germanium	As 33 74.92 Arsenic	Se 34 78.96 Selenium	Br 35 79.90 Bromine	Kr 36 83.80 Krypton	
Rb 37 85.47 Rubidium	Sr 38 87.62 Strontium	Y 39 88.91 Yttrium	Zr 40 91.22 Zirconium	Nb 41 92.91 Niobium	Mo 42 95.94 Molybdenum	Tc 43 (97.9) Technetium	Ru 44 101.07 Ruthenium	Rh 45 102.91 Rhodium	Pd 46 106.42 Palladium	Ag 47 107.87 Silver	Cd 48 112.41 Cadmium	In 49 114.82 Indium	Sn 50 118.71 Tin	Sb 51 121.76 Antimony	Te 52 127.60 Tellurium	I 53 126.90 Iodine	Xe 54 131.29 Xenon	
Cs 55 132.91 Cesium	Ba 56 137.33 Barium	La 57 138.91 Lanthanum	Hf 72 178.49 Hafnium	Ta 73 180.95 Tantalum	W 74 183.85 Tungsten	Re 75 186.21 Rhenium	Os 76 190.2 Osmium	Ir 77 192.22 Iridium	Pt 78 195.08 Platinum	Au 79 196.97 Gold	Hg 80 200.59 Mercury	Tl 81 204.38 Thallium	Pb 82 207.2 Lead	Bi 83 208.98 Bismuth	Po 84 (209) Polonium	At 85 (210) Astatine	Rn 86 (222) Radon	
Fr 87 223.02 Francium	Ra 88 226.03 Radium	Ac 89 227.03 Actinium	Rf 104 (261) Rutherfordium	Db 105 (262) Dubnium	Sg 106 (263) Seaborgium	Bh 107 (262) Bohrium	Hs 108 108 Hassium	Mt 109 109 Meitnerium	Unnamed Discovery 110	Unnamed Discovery 111	Unnamed Discovery 112		Unnamed Discovery 114		Unnamed Discovery 116		Unnamed Discovery 118 1999	
ALKALI METALS		ALKALI EARTH METALS																NOBLE GASES

LANTHANIDES

ACTINIDES

Ce 58 140.12 Cerium	Pr 59 140.91 Praseodymium	Nd 60 144.24 Neodymium	Pm 61 (145) Promethium	Sm 62 150.36 Samarium	Eu 63 152.97 Europium	Gd 64 157.25 Gadolinium	Tb 65 158.93 Terbium	Dy 66 162.50 Dysprosium	Ho 67 164.93 Holmium	Er 68 167.26 Erbium	Tm 69 168.93 Thulium	Yb 70 173.04 Ytterbium	Lu 71 174.97 Lutetium
Th 90 232.04 Thorium	Pa 91 231.04 Protactinium	U 92 238.03 Uranium	Np 93 237.05 Neptunium	Pu 94 (240) Plutonium	Am 95 243.06 Americium	Cm 96 (247) Curium	Bk 97 (248) Berkelium	Cf 98 (251) Californium	Es 99 252.08 Einsteinium	Fm 100 257.10 Fermium	Md 101 (257) Mendelevium	No 102 259.10 Nobelium	Lr 103 262.11 Lawrencium

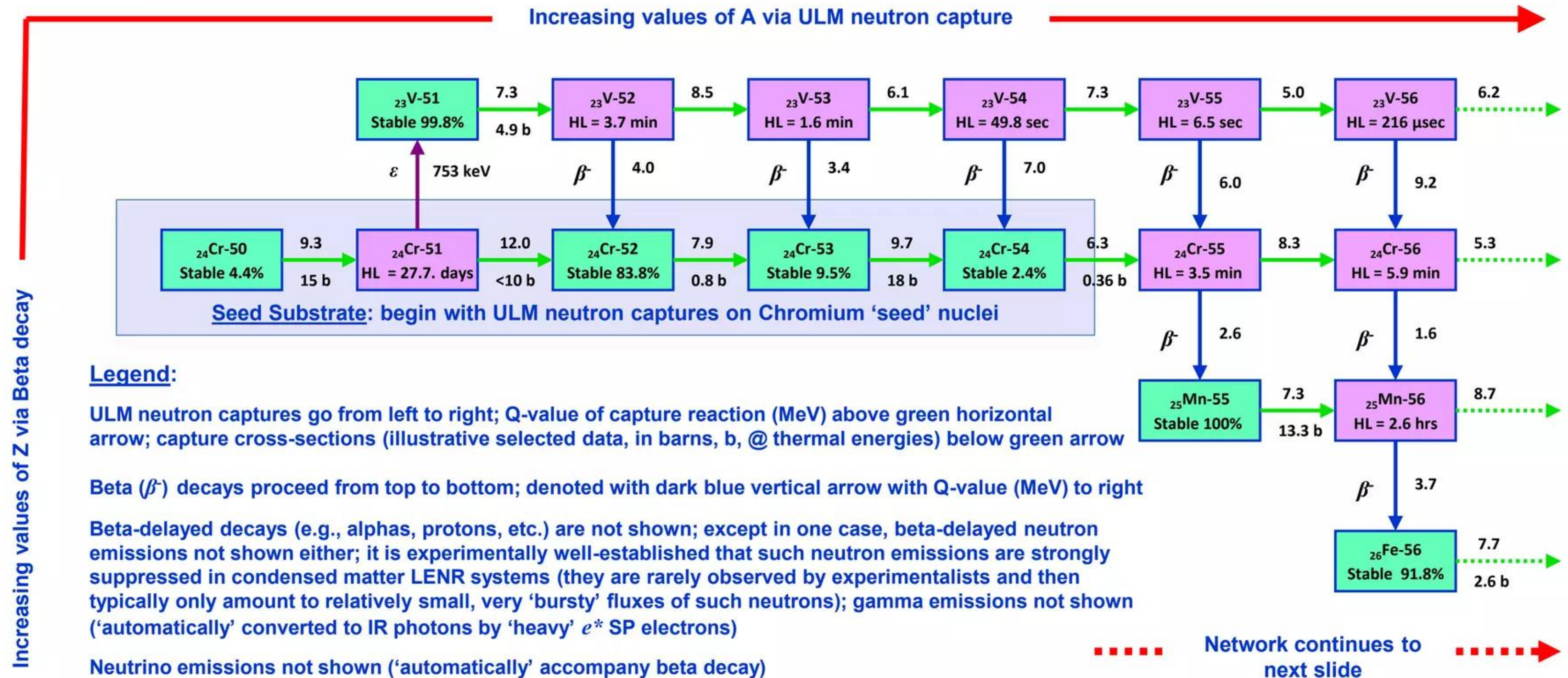
SPECIALTY
PRODUCTS

www.hmpublishing.com

© Hayden-McNeil Specialty Products

LENR W-L ULM neutron capture on Cr 'seeds,' neutron-rich isotope production, and decays

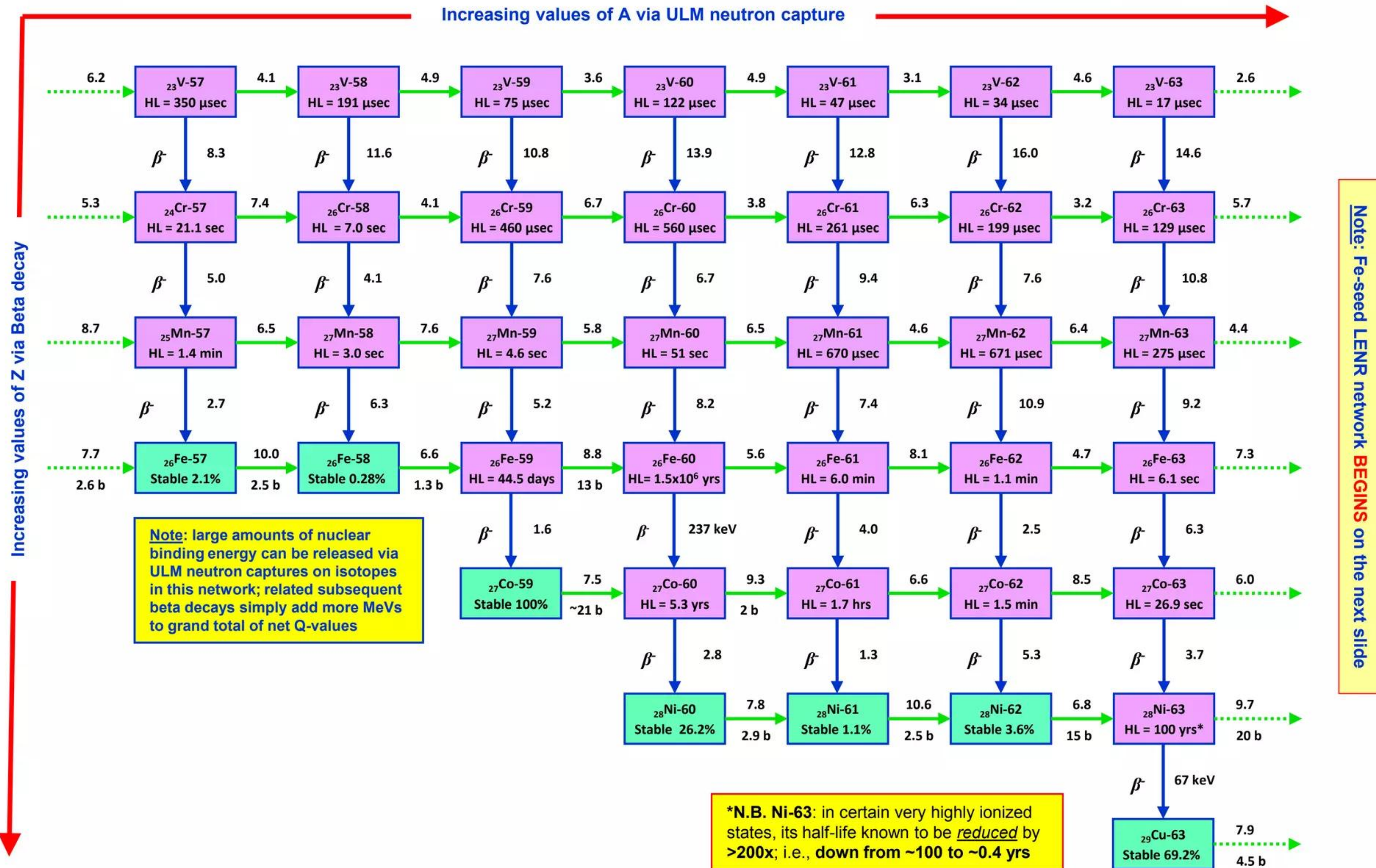
Stable 'target' seed nuclei on or very near LENR nuclear-active Chromium surfaces: Cr-50, Cr-52, Cr-53,, and Cr-54



LENR W-L ULM neutron capture on Cr 'seeds,' neutron-rich isotope production, and decays

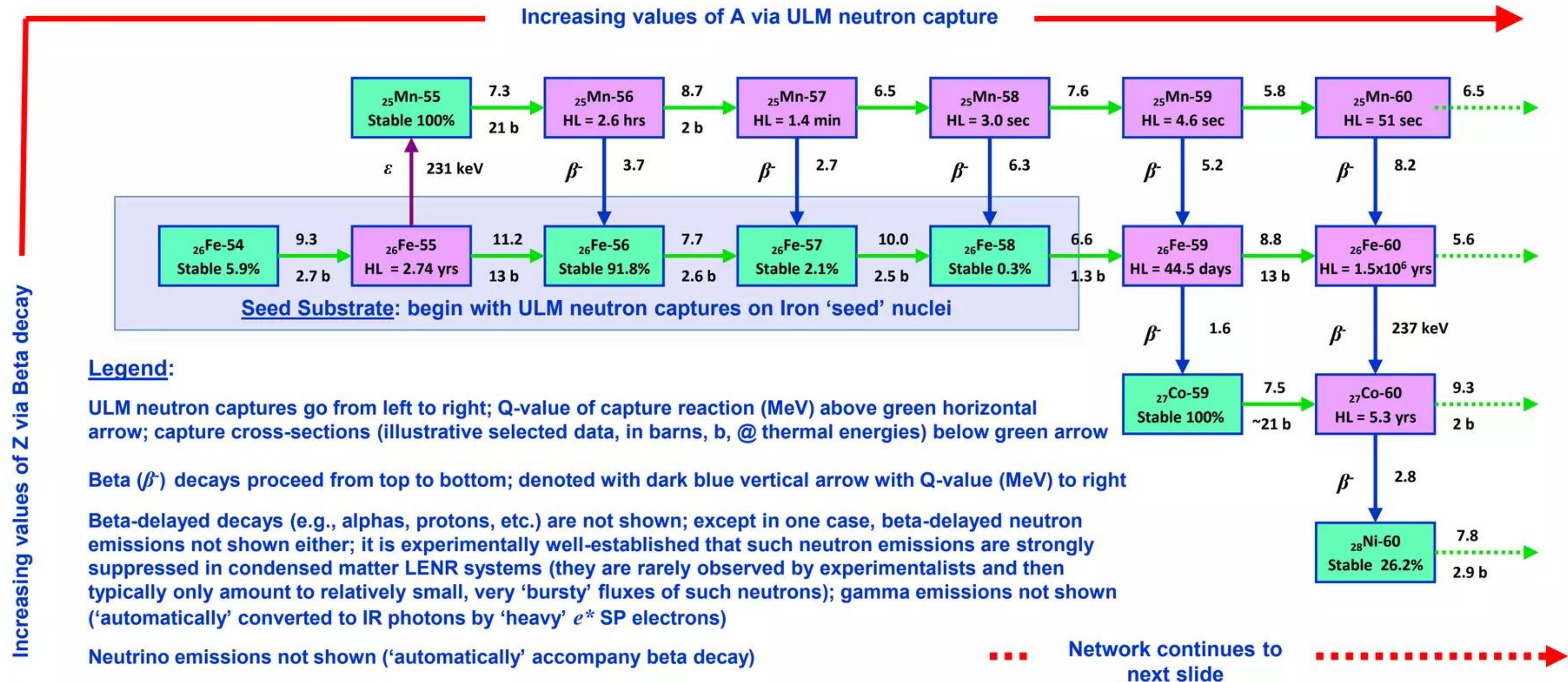
Stable 'target' seed nuclei on or very near LENR nuclear-active Chromium surfaces: Cr-50, Cr-52, Cr-53, and Cr-54

Increasing values of A via ULM neutron capture



LENR W-L ULM neutron capture on Fe 'seeds,' neutron-rich isotope production, and decays

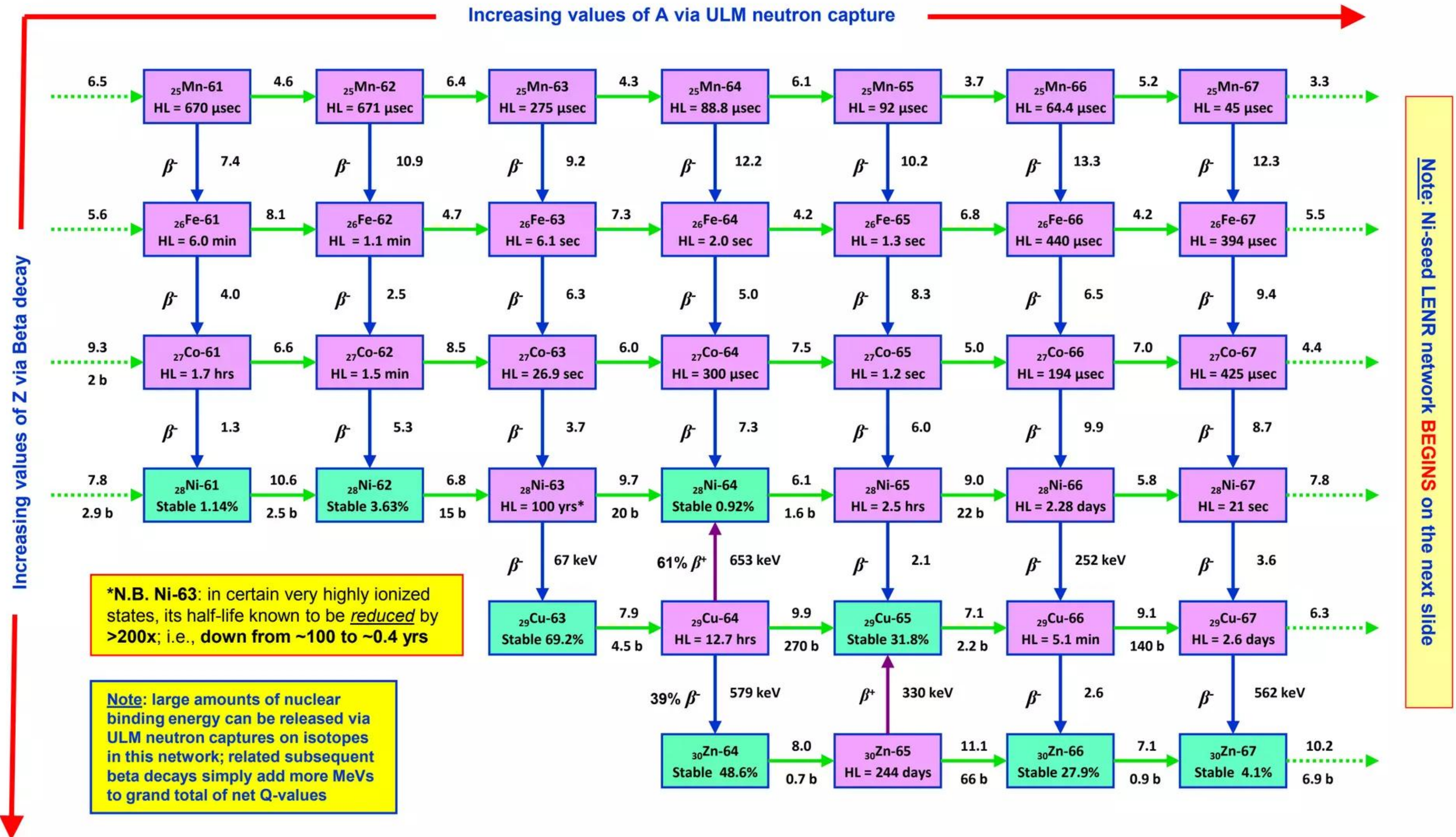
Stable 'target' seed nuclei on or very near LENR nuclear-active Nickel surfaces: Fe-54, Fe-56, Fe-57, and Fe-58



N.B: in some cases, Q-values for ULM neutron capture reactions are significantly larger than Q-values for 'competing' beta decay reactions. Also, neutron capture processes are much, much faster (~picoseconds) than most beta decays; if ULM neutron fluxes (rates) are high enough, neutron-rich isotopes of a given element can build-up (move along same row to right on the above chart) >>> faster than beta decays can transmute them to different chemical elements (e.g., move downward to other rows on chart)

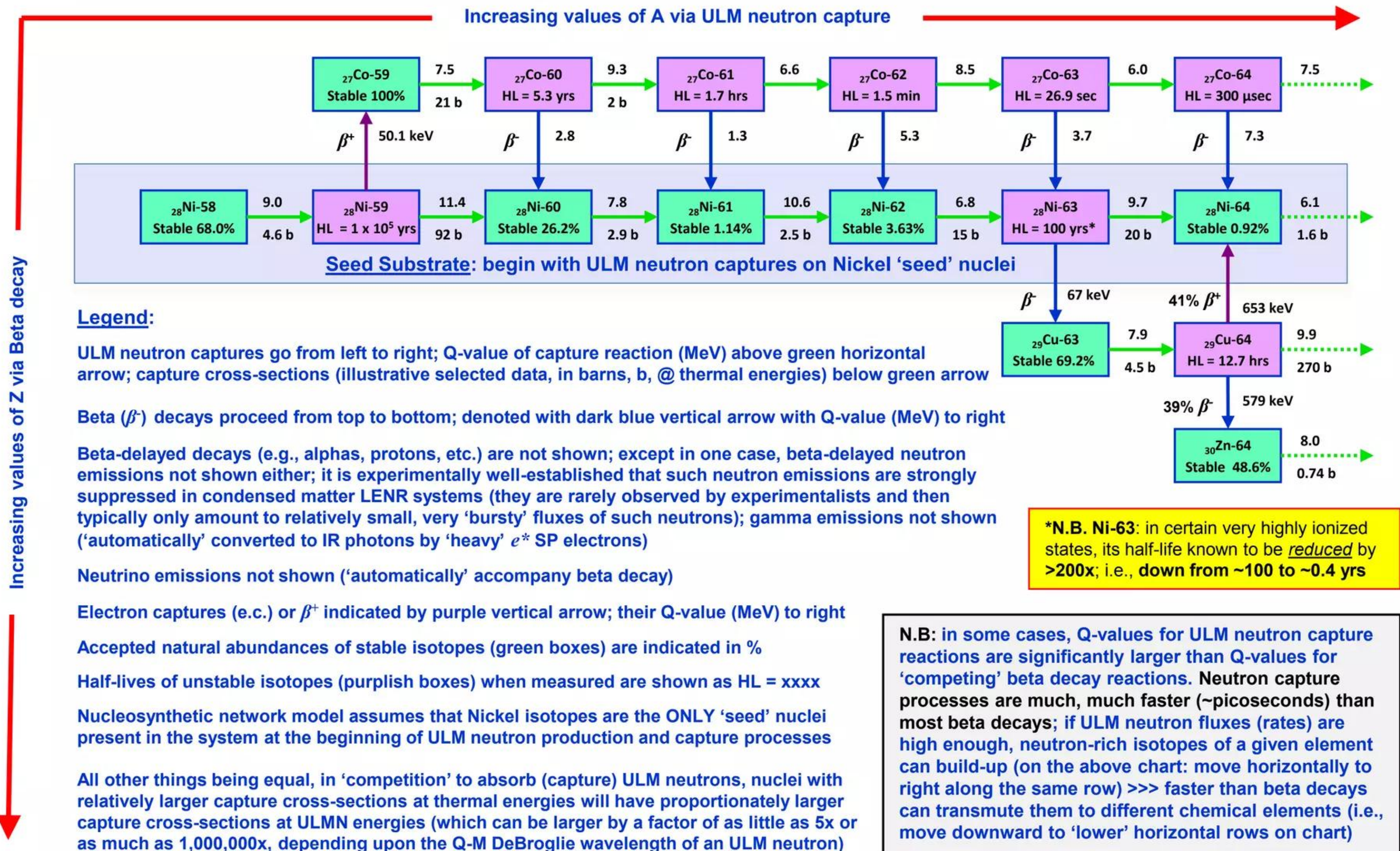
LENR W-L ULM neutron capture on Fe 'seeds,' neutron-rich isotope production, and decays

Stable 'target' seed nuclei on or very near LENR nuclear-active Nickel surfaces: Fe-54, Fe-56, Fe-57, and Fe-58

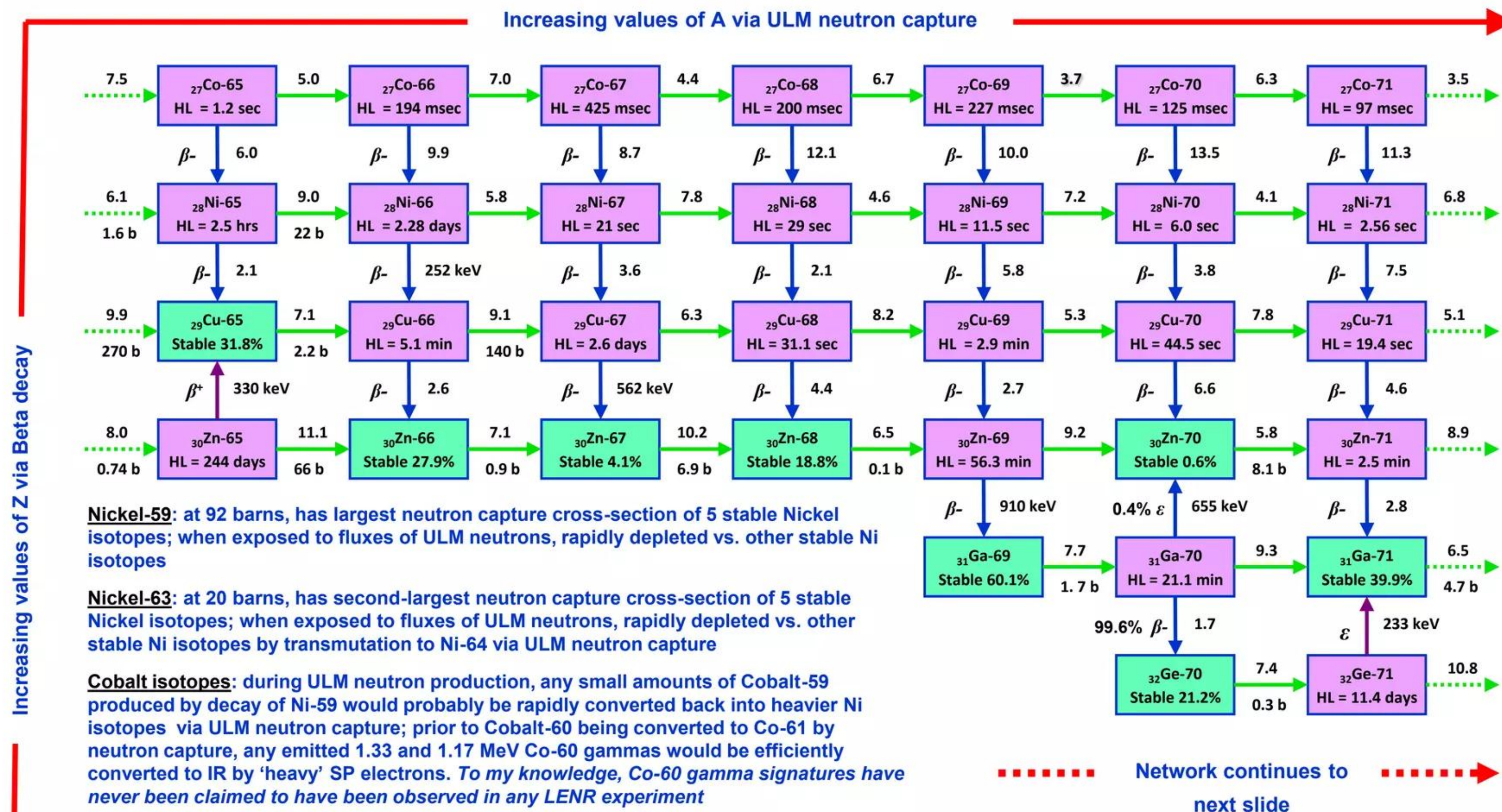


LENR W-L ULM neutron capture on Ni 'seeds,' neutron-rich isotope production, and decays

Stable 'target' seed nuclei on or very near LENR nuclear-active Nickel surfaces: Ni-58, Ni-60, Ni-61, Ni-62, and Ni-64



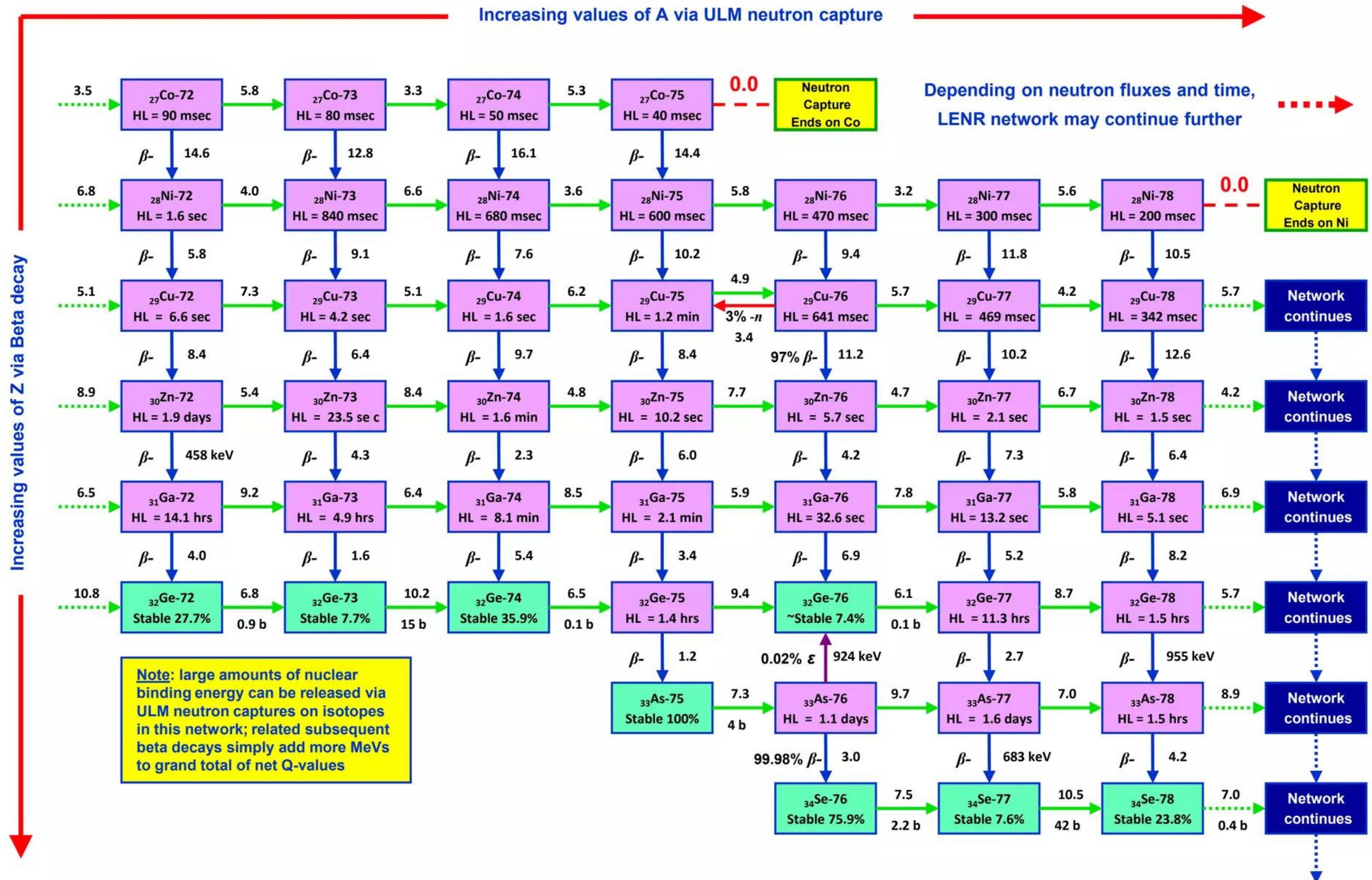
LENR W-L ULM neutron capture on Ni 'seeds,' neutron-rich isotope production, and decays



Predicted accumulation of stable isotopes at masses A~ 63 - 66: a narrow-width stable isotope abundance peak at around these masses is predicted by the W-L optical model (see previous Slides); model also implies that production of stable isotopes should fall-off relatively rapidly just beyond Copper and Zinc, assuming all other things being equal

Values of A and Z reached by Ni-seed nucleosynthetic networks in experiments depend on overall rates of ULM neutron production (which in turn depend upon the nature of the input energy) and time: the summation across all local neutron fluxes in micron-scale surface regions and their total duration in time (neutron dose history per unit of area) will determine exactly how far a given experiment can proceed into the labyrinth of our above-described Ni-seed network. In gas-phase LENR experiments in which energy is inputted into SP electrons solely through a combination of pressure and temperature, local ULMN fluxes would likely be modest (in comparison to experiments with additional high-current electrical input) and it might likely be difficult for the network to go very far beyond Zinc during a relatively short period of time (say, a few weeks). At the other extreme, electrolytic LENR experiments can sometimes trigger large bursts of ULM neutron production: in one such result, Mizuno went from K to Fe in 2 minutes (Lattice June 25, 2009, SlideShare)

LENR W-L ULM neutron capture on Ni 'seeds,' neutron-rich isotope production, and decays



Commercializing a Next-Generation Source of Safe Nuclear Energy

Discussion of W-L networks and experimental data

Cores of stars, fission reactors, and supernovae not required

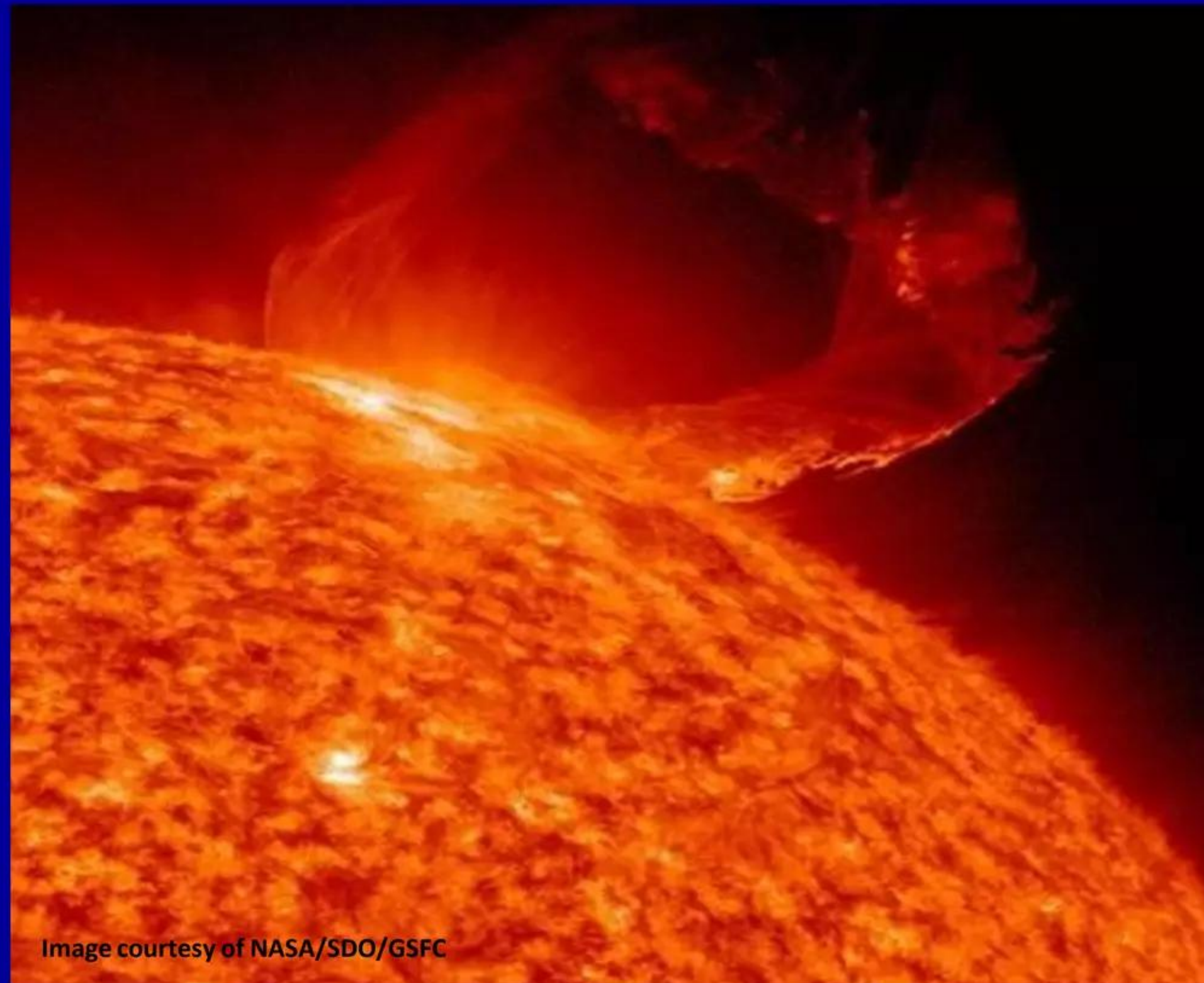
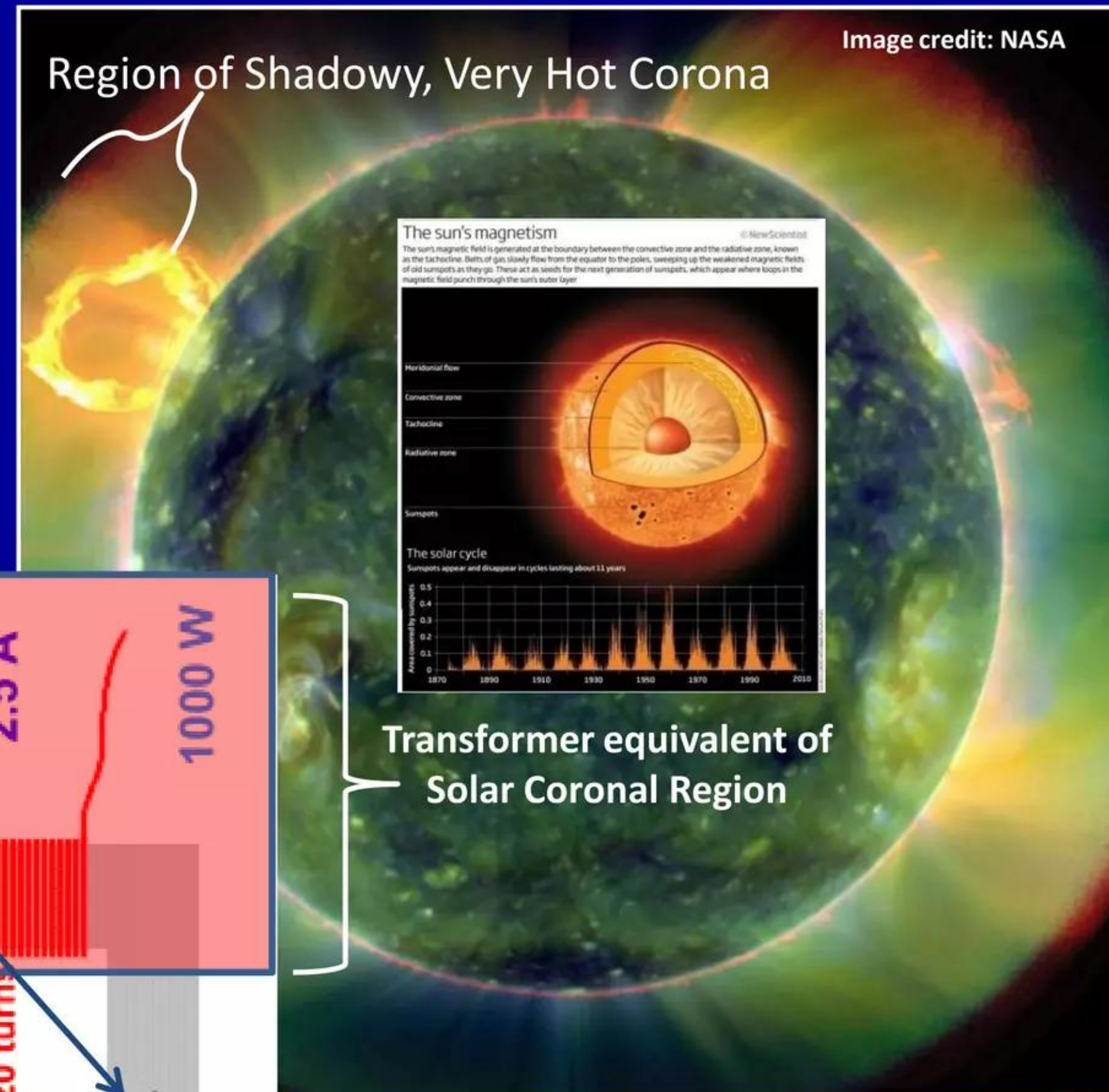
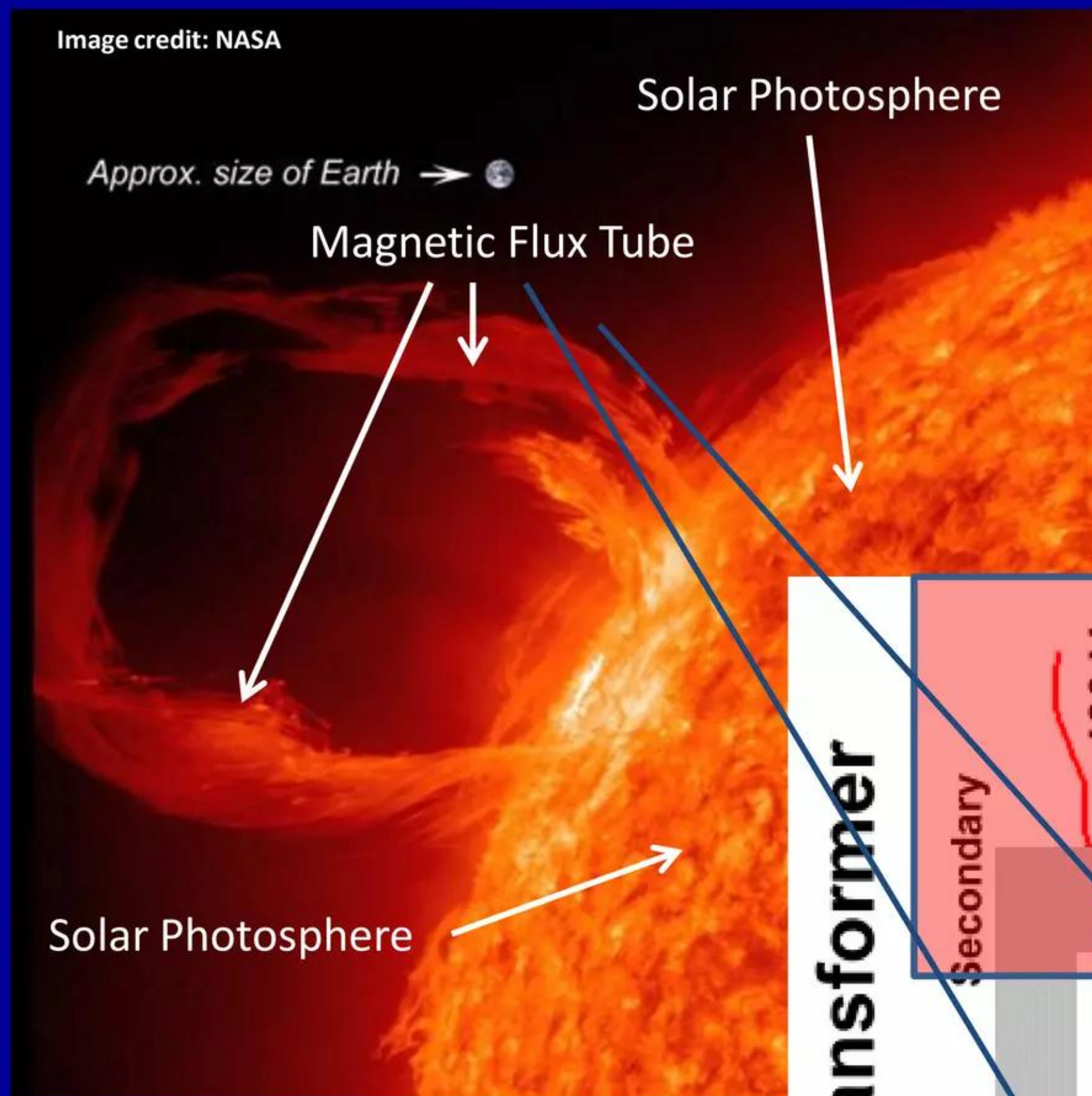


Image courtesy of NASA/SDO/GSFC

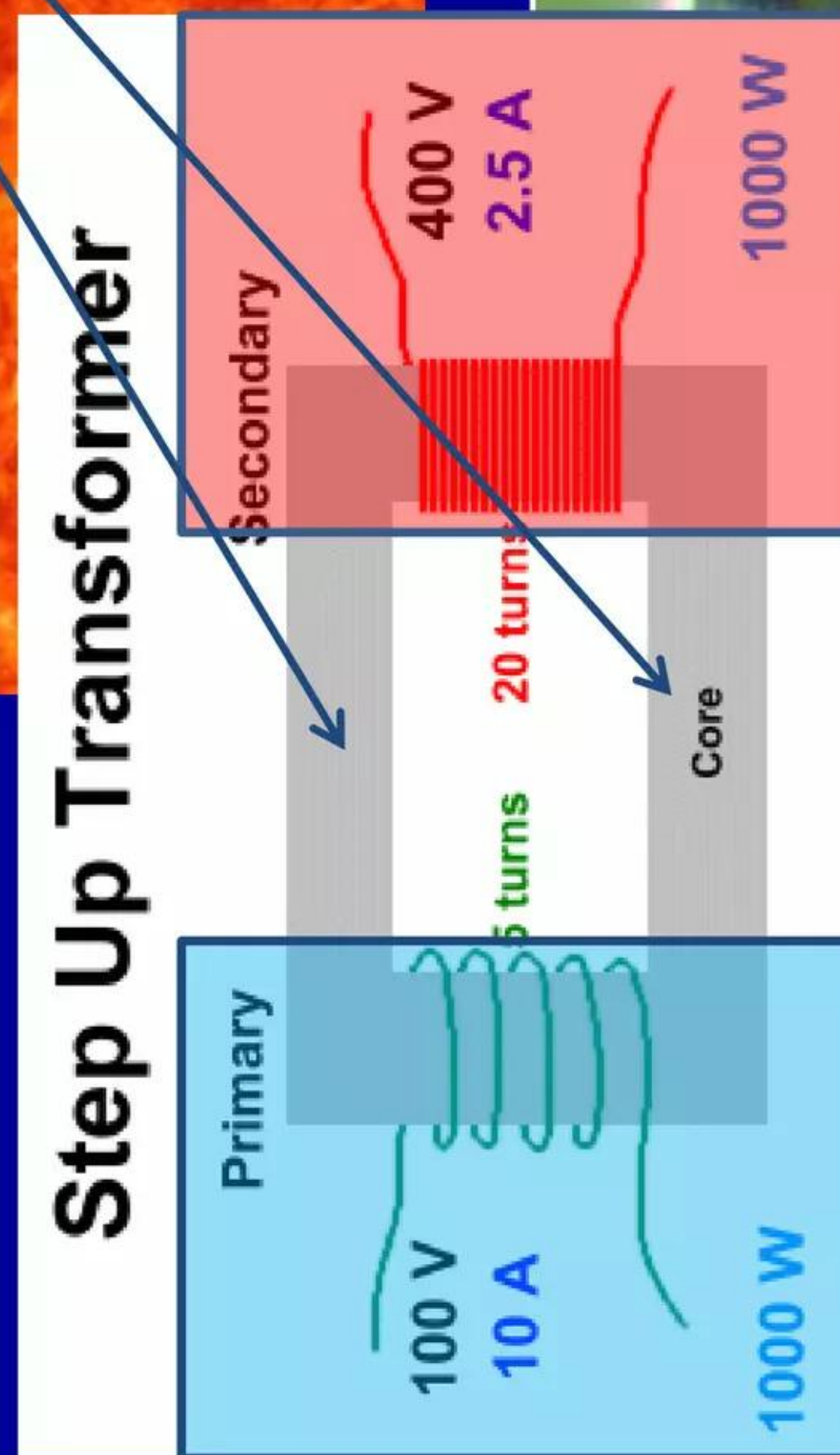
March 19, 2011 – photo of major eruption on the surface of the Sun

Magnetic-regime LENRs can occur in stellar photosphere and corona



“High Energy Particles in the Solar Corona”
- Widom, Srivastava, and Larsen (April 2008)

Abstract: collective Ampere law interactions producing magnetic flux tubes piercing through sunspots into and then out of the solar corona allow for low energy nuclear reactions in a steady state and high energy particle reactions if a magnetic flux tube explodes in a violent event such as a solar flare. Filamentous flux tubes themselves are vortices of Ampere currents circulating around in a tornado fashion in a roughly cylindrical geometry. The magnetic field lines are parallel to and largely confined within the core of the vortex. The vortices may thereby be viewed as long current carrying coils surrounding magnetic flux and subject to inductive Faraday and Ampere laws. These laws set the energy scales of (i) low energy solar nuclear reactions which may regularly occur and (ii) high energy electro-weak interactions which occur when magnetic flux coils explode into violent episodic events such as solar flares or coronal mass ejections.



Transformer equivalent of Solar Coronal Region



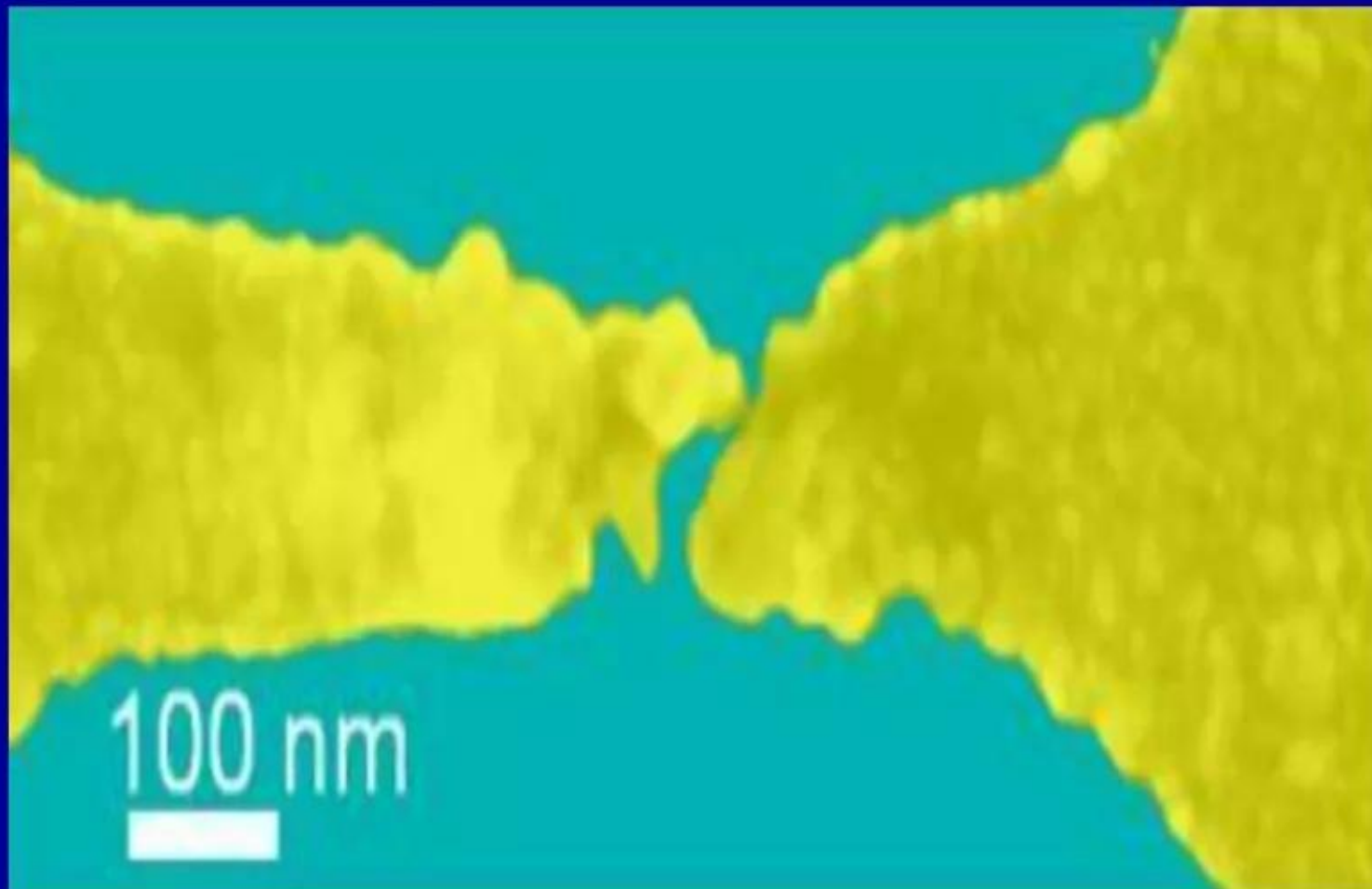
Electric utility transformers

Commercializing a Next-Generation Source of Safe Nuclear Energy

LENR-active surfaces: complex interactions

Time-varying E-M, chemical, and nuclear processes operate together

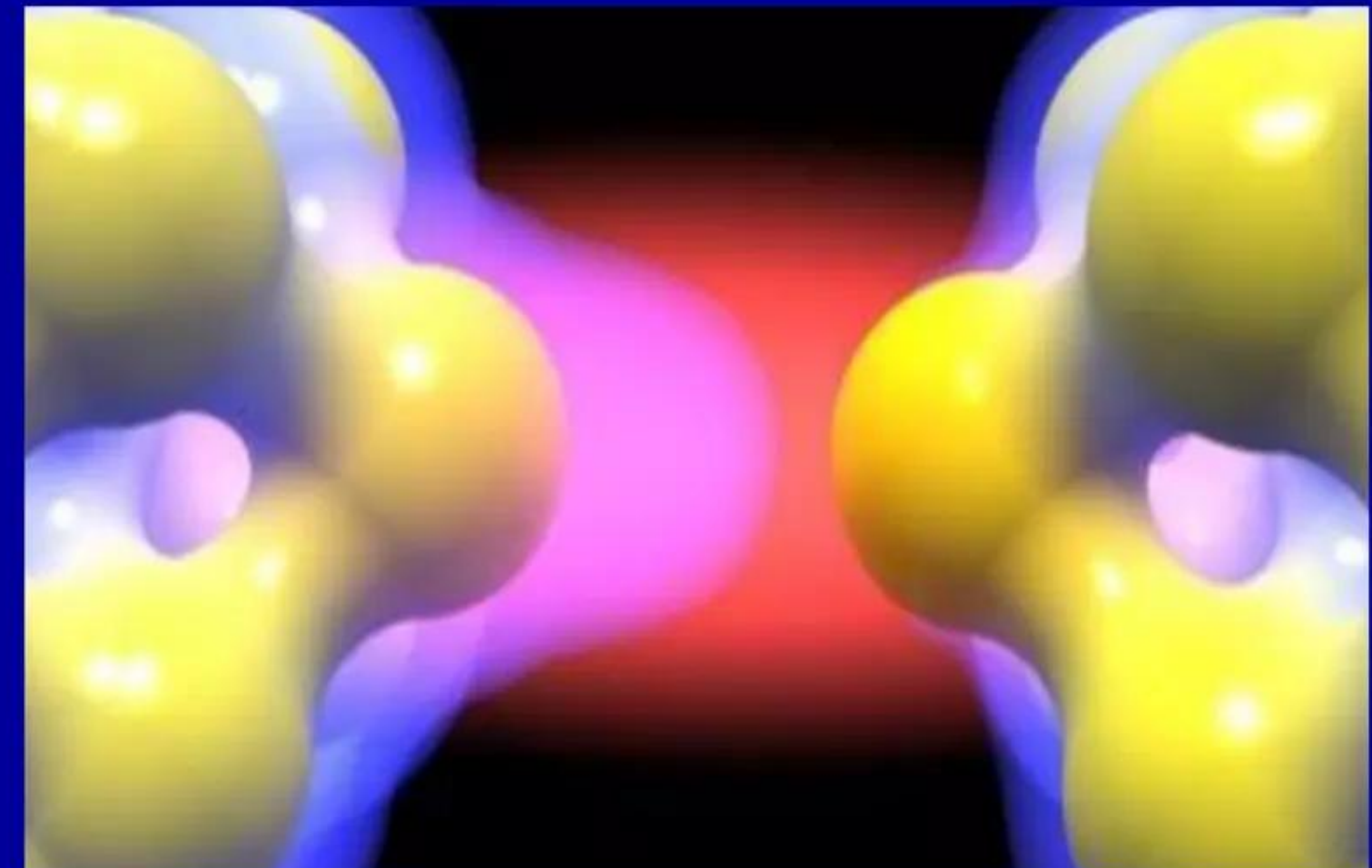
Artist's rendering (right) shows how surface plasmons on the surface of a pair of nanoscale gold (Au) nanotips (SEM image to left) concentrate incident light from a commercial laser, amplifying it locally by a factor of 1,000x



Credit: Natelson Lab/Rice University

Reference for two above images: “Optical rectification and field enhancement in a plasmonic nanogap,” D. Ward et al., *Nature Nanotechnology* 5 pp. 732–736 (2010)

“Metal nanostructures act as powerful optical antennas because collective modes ... are excited when light strikes the surface ... [their] plasmons can have evanescent electromagnetic fields ... orders of magnitude larger than ... incident electromagnetic field ... largest field enhancements ... occur in nanogaps between ... nanostructures.”



Credit: Natelson Lab/Rice University

Similarly: “Extraordinary all-dielectric light enhancement over large volumes,” R. Sainidou et al., *NANO Letters* 10 pp. 4450–4455 (2010)

“ ... allow us to produce arbitrarily large optical field enhancement using all dielectric structures ... measure the enhancement relative to the intensity of the incident light. ... if absorption losses are suppressed, resonant cavities can pile up light energy to create extremely intense fields ... no upper bound to the intensity enhancement factor that these structures can achieve ... [certain factors] limit it to around 4 orders of magnitude in practice.”

LENR-active surfaces: very complex with many parallel processes

- ✓ LENR ‘hot spots’ create intense local heating and variety of surface features such as ‘craters’; over time, LENR-active surfaces experience major micron-scale changes in nanostructures/composition
- ✓ On LENR-active substrate surfaces, there are a myriad of different complex, nanometer- to micron-scale electromagnetic, chemical, and nuclear processes *operating in parallel*. LENRs involve interactions between surface plasmons, E-M fields, and many different types of nanostructures with varied geometries, surface locations relative to each other, and chemical/isotopic compositions
- ✓ To greater or lesser degrees, many of these very complex, time-varying surface interactions are electromagnetically coupled on many different physical length-scales: E-M resonances important!
- ✓ Surface plasmons and their interactions with nanostructures/nanoparticles enable physics regime that permits LENRs to occur in condensed matter systems under relatively mild *macroscopic* conditions (cores of stars, fission reactors, or supernovas are not required). In concert with many-body, collective Q-M effects, SPs also function as two-way ‘transducers,’ effectively interconnecting the otherwise rather distant realms of chemical and nuclear energies
- ✓ *Please be aware that a wide variety of complex, interrelated E-M phenomena may be occurring simultaneously in parallel in different nm to μ -scale local regions on a given surface.* For example, some regions may be absorbing E-M energy locally, while others nearby can be emitting energy (e.g., as energetic electrons, photons, other charged particles, etc.). At the same time, energy can be transferred from regions of resonant absorption or ‘capture’ to other regions in which emission or ‘consumption’ is taking place: e.g., photon or electron emission, and/or LENRs in which [E-M field energy] $+ e \rightarrow e^* + p^+ \rightarrow n_{ulm} + \nu$ --- in LENRs, electrons and protons (particles) are truly consumed!

Interactions: resonant E-M cavities, E-M fields, SPs, and nanostructures

Large E-field enhancements occur near nanoparticles:

Pucci et al.: “If metal structures are exposed to electromagnetic radiation, modes of collective charge carrier motion, called plasmons, can be excited ... Surface plasmons can propagate along a distance of several tens of micrometers on the surface of a film.”

“In the case of one nanoparticle, the surface plasmon is confined to the three dimensions of the nanostructure and it is then called localized surface plasmon (LSP). In this situation, the LSP resonance depends on the metallic nature (effect of the metal permittivity) and on the geometry (effect of the confinement of the electron cloud) of the nanostructure.”

“If the smallest dimension of the particle is much larger than the skin depth of the electromagnetic radiation in the metal, also real metal wires can be estimated as perfect conductors. For ideal metal objects it is assumed that the light does not penetrate into the particle. This means an infinitely large negative dielectric function. Then, antenna-like resonances occur if the length L of an infinitely thin wire matches with multiples of the wavelength λ .”

“Electromagnetic scattering of perfect conducting antennas with D smaller than the wavelength and L in the range of the wavelength is discussed in classical antenna scattering theory ... It is a frequently used approximation to consider a metal nanowire as an ideal antenna. This approach has been proposed also for the modeling of nanowires in the visible spectral range ...”

“... field is enhanced at the tip of the nanowire when the excitation wavelength corresponds to an antenna mode ... the end of the nanowires in a relatively sharp and abrupt surface is a perfect candidate to host a lightning rod effect ...”

“... for metallic wires larger than several hundred nanometers. The increasing size of the nanoantennas makes the resonances to appear at wavelengths that present larger negative values of the dielectric function, i.e. for wavelengths well in the mid infrared portion of the spectrum in the case of micron-sized wires. It is actually this extension of the resonant behavior to micron-sized antennas what makes these structures optimal candidates for surface enhanced Raman spectroscopy (SERS) and surface-enhanced infrared absorption spectroscopy (SEIRA).”

Reference:

“Electromagnetic nanowire resonances for field-enhanced spectroscopy,” Chapt. 8 in “One-Dimensional Nanostructures,” Pucci et al., Series: Lecture Notes in Nanoscale Science and Technology, V. 3, Wang, Zhiming M. (Ed.), Springer 2008 178-181

Lattice Comments:

- In addition to optical frequencies, surface plasmons (SPs) in condensed matter systems often have some of their absorption and emission bands located in the infrared (IR) portion of the E-M energy spectrum
- Walls of gas-phase metallic reaction vessels intrinsically have SPs present on their outer and inner surfaces; they can radiate IR electromagnetic energy into the interior space, i.e., open cavity
- Metallic surface nanostructures and various types of nanoparticles located inside such reaction vessels also have SPs present on their outer surfaces and interior interfaces, e.g. metal/oxide or metal/gas
- Nanostructures and nanoparticles found inside metallic reaction vessels can absorb IR radiated from vessel walls if their absorption bands fall into the same spectral range as IR radiation emitted from the walls
- When this occurs, volume of space enclosed in a reaction vessel effectively becomes a resonant E-M cavity: two-way energy transfers via E-M fields
- Think of nanostructures and nanoparticles inside reaction vessels as IR ‘nanoantennas’ with ‘send’ and ‘receive’ channels; walls also contain E-M antennas with complementary ‘send’ and ‘receive’ channels --- complex two-way interplay between all of them

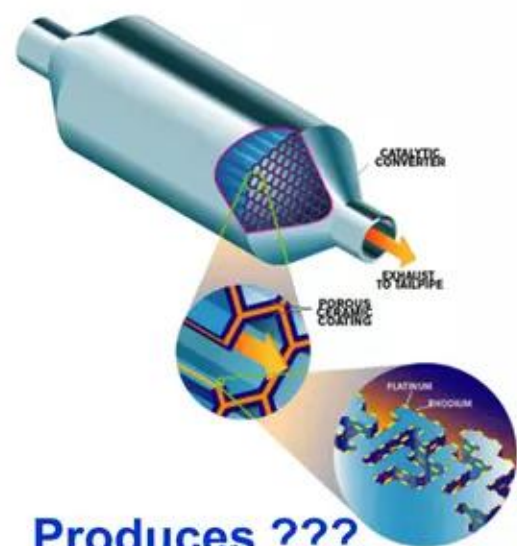
Resonant electromagnetic cavities occur inside steel reaction vessels

BMW auto catalytic converter:



End view: metal honeycomb

Below: heated and operating



Produces ???

Chemical and nuclear reactions occur in parallel

A common factor amongst these different types of, mainly stainless, steel reaction vessels is that, on some length scales, resonant electromagnetic (E-M) cavities exist inside of all of them. They also typically contain hydrogen isotopes in some chemical form. That, coupled with metallic 'catalysts' (e.g., Ni, Pd) and/or aromatic rings working together with thermal energy (temperature), and/or pressure, and time, can under exactly the right conditions produce detectable LENR transmutation products, e.g., ^{13}C , ^{15}N and 'new' elements, e.g., ^4He , ^{14}N , etc. in parallel with a variety of prosaic chemical reactions

Photo of a 'battery' of modern steel coking ovens in Australia



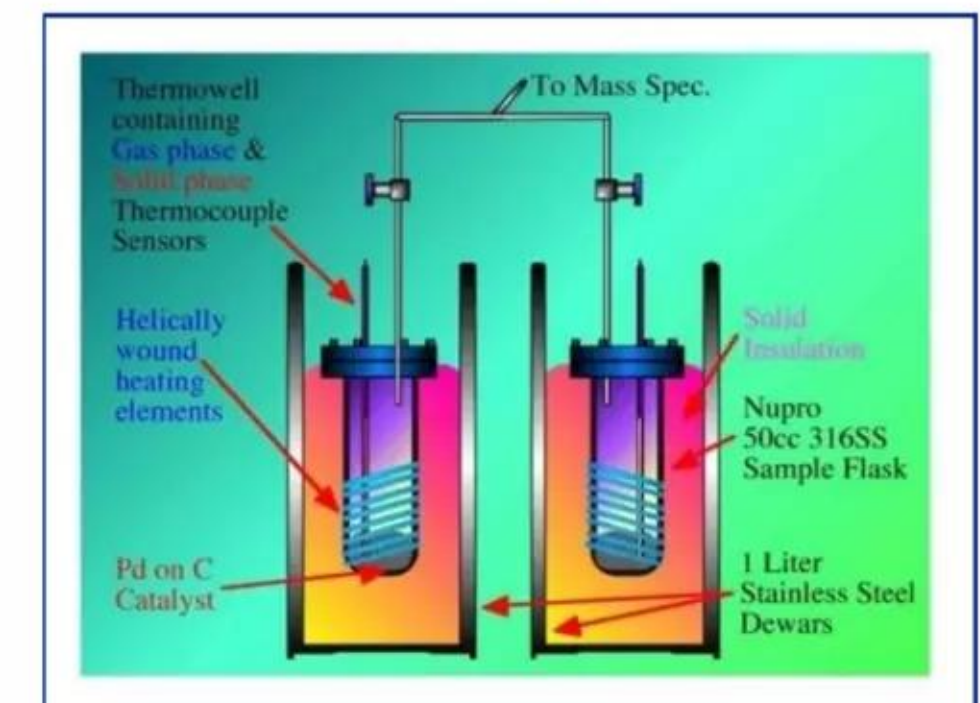
2002 IAEA study: coking ovens at S. African steel plant produced $\gg +\delta^{15}\text{N}$

Hokkaido Univ. 2008 - LENR reactor vessels:



Mizuno produced $\gg +\delta^{13}\text{C}$ and $^{14}\text{N}_2$ from $^{12-13}\text{C}_{14}\text{H}_{10}$ with Platinum (Pt)

SRI 1999 - Repeated Les Case LENR Experiment with D_2 gas:



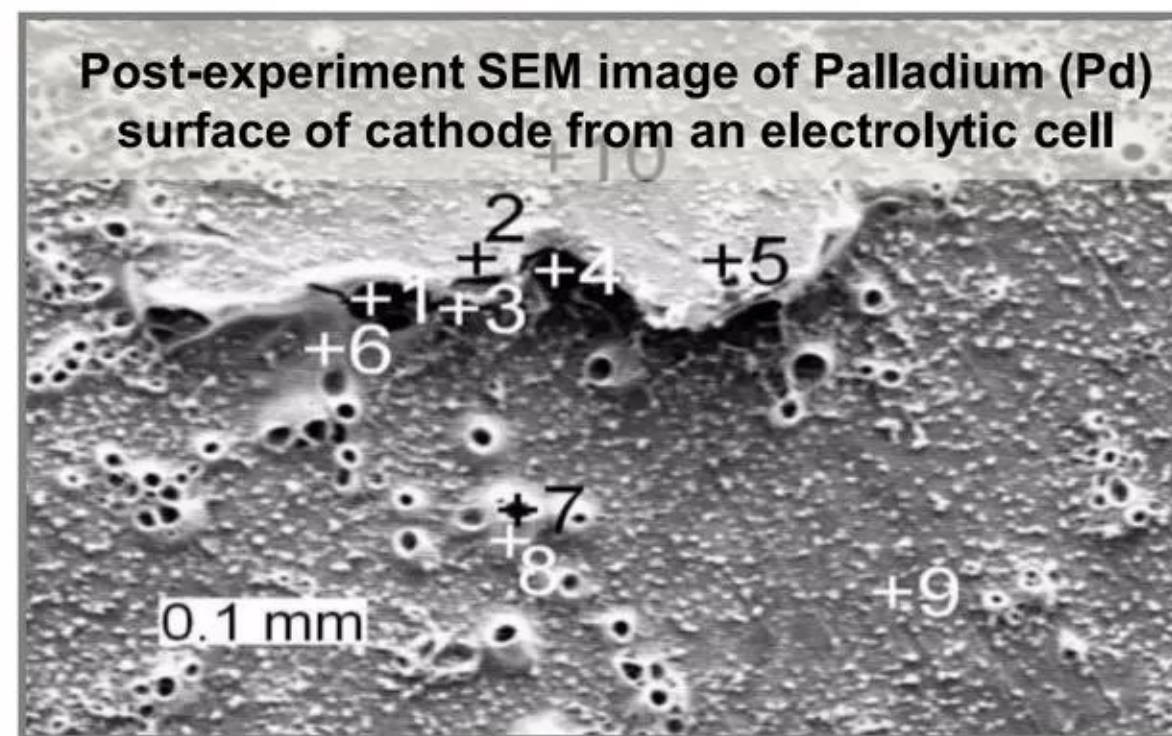
McKubre produced ^4He from $^2\text{D}_2$ and $^{12-13}\text{C}$ with Palladium (Pd)

For experimental results to make sense, one must know starting points

✓ When utilizing W-L theory and model LENR transmutation networks to help explain observed experimental data, please note that:

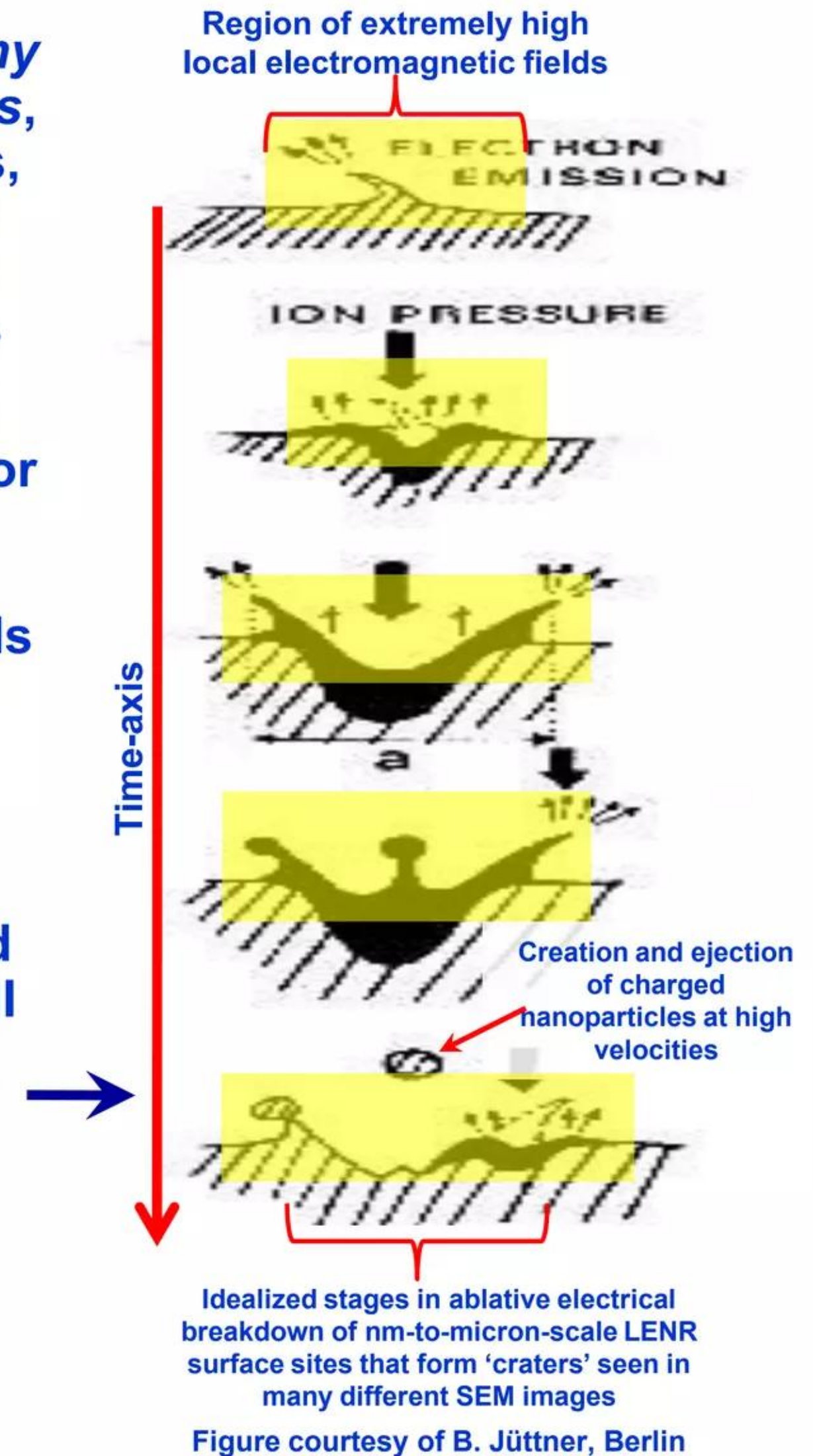
- Literally ANY element or isotope present inside LENR experimental apparatus that has an opportunity to somehow move into very close physical proximity to surfaces or nanoparticles on which ULM neutrons are being produced can potentially 'compete' with other nuclei (located within the same nm-to-micron-scale domains of spatially extended ULM neutron Q-M wave functions) to capture locally produced ULMNs
- Thus, some observations of transmutation products may appear oddly mystifying until one determines *exactly what elements/isotopes were initially present inside the apparatus when an experiment began*. In many cases, materials located inside such experiments are very poorly characterized; thus 'starting points' for ULMN captures on 'seed' nuclei may be quite unclear

LENR-active surface sites ('hot spots') are not permanent entities. In experimental systems with sufficient input energy, they will form spontaneously, 'light-up' for 10 to several hundred nanoseconds, and then suddenly 'die.' Over time, endless cycles of 'birth', nuclear energy release, and 'death' are repeated over and over again at many thousands of different, randomly scattered nm-to micron-sized locations found on a given surface. When LENRs are occurring, these tiny patches become temporary 'hot spots' -- their temperatures may reach 4,000 - 6,000° K or even higher. That value is roughly as hot as the surface temperature of the Sun and high enough to melt and/or even flash boil essentially all metals, including tungsten (b.p. = 5,666°C). For a brief period, a tiny dense 'ball' of very hot, highly ionized plasma is created. Such intense local heating events commonly produce numerous explosive melting features and/or 'craters' that are often observed in post-experiment surface SEM images such as for example (credit: Zhang & Dash, 2007):



Gas-phase LENR systems: wall interactions can be very significant

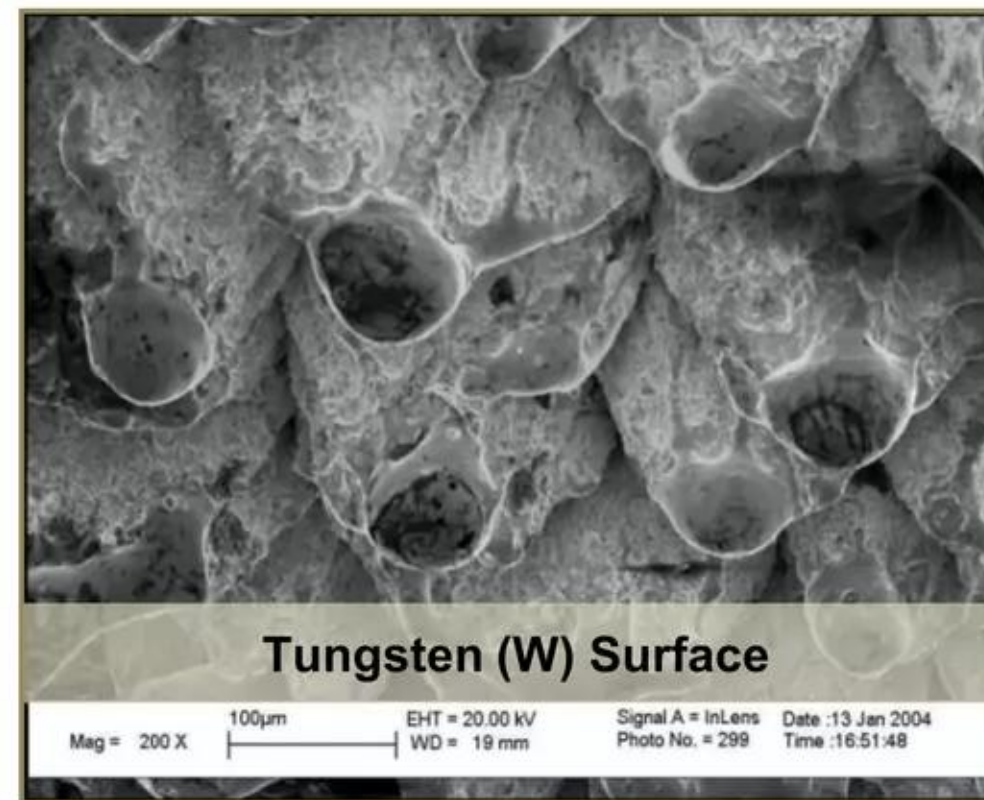
- ✓ In gas-phase LENR systems, *especially if they contain tiny 'target fuel' nanoparticles or volatile aromatic compounds*, e.g., benzene or polycyclic aromatic hydrocarbons (PAHs, e.g., Phenanthrene), it is virtually a certainty that walls of reaction vessels will come into intimate physical contact with introduced nanoparticles and/or aromatic molecules
- ✓ Contact can occur via gravity or gaseous turbulence that swirls tiny nanoparticles around inside reaction vessels or by condensation of organic residues on walls. Once in close proximity, chemical reactions and/or LENRs can readily occur at points of interfacial contact between walls and introduced nanoparticles and/or organic molecules
- ✓ In the case of LENRs, atomic nuclei comprising wall materials at or near a mutual point of brief contact will have an opportunity to 'compete' with nuclei in nearby nanoparticles or aromatic molecules to capture produced ULM neutrons. If wall nuclei capture neutrons, LENRs will then occur in a local 'patch,' resulting in surface-altering 'cratering' processes; one of which is illustrated to right
- ✓ Therefore, in such systems wall nuclei atoms can potentially also become 'seeds' in LENR transmutation networks; LENRs occurring in or near walls can cause significant amounts of wall materials to ablate into the local gas in the form of newly created nanoparticles



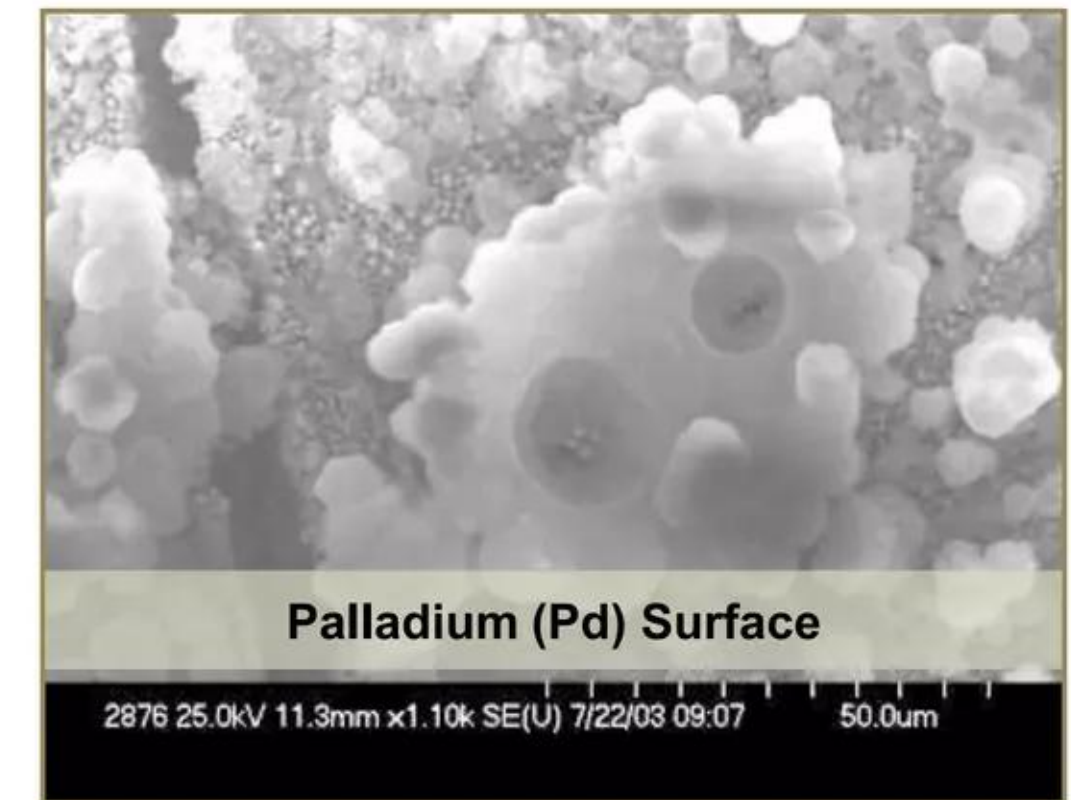
SEM images illustrate LENR 'flash melting' and cratering on surfaces



Credit: Y. Toriabe et al.



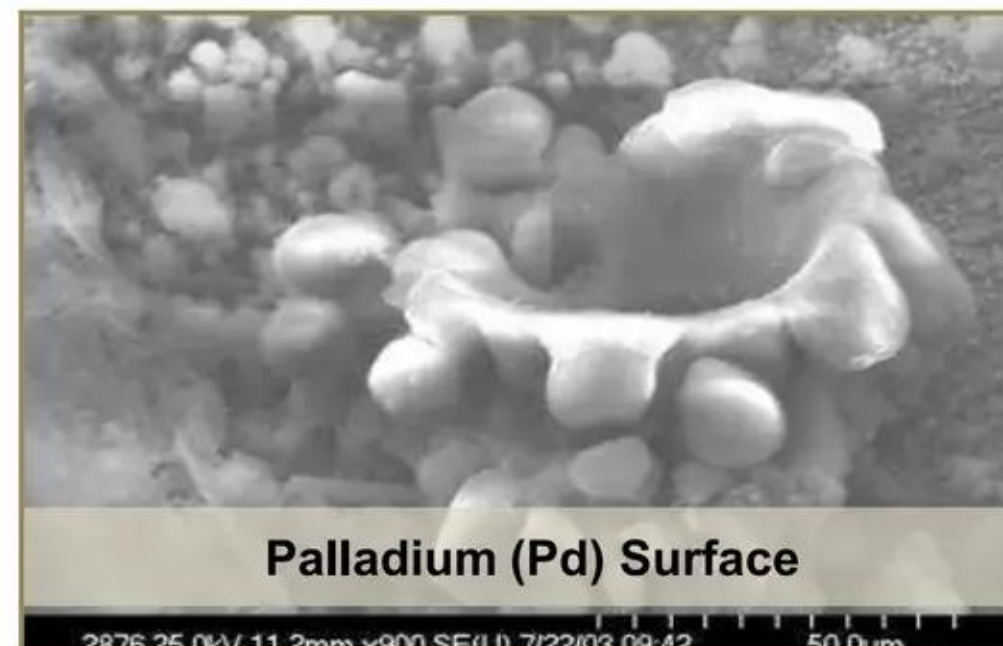
Credit: Cirillo & Iorio



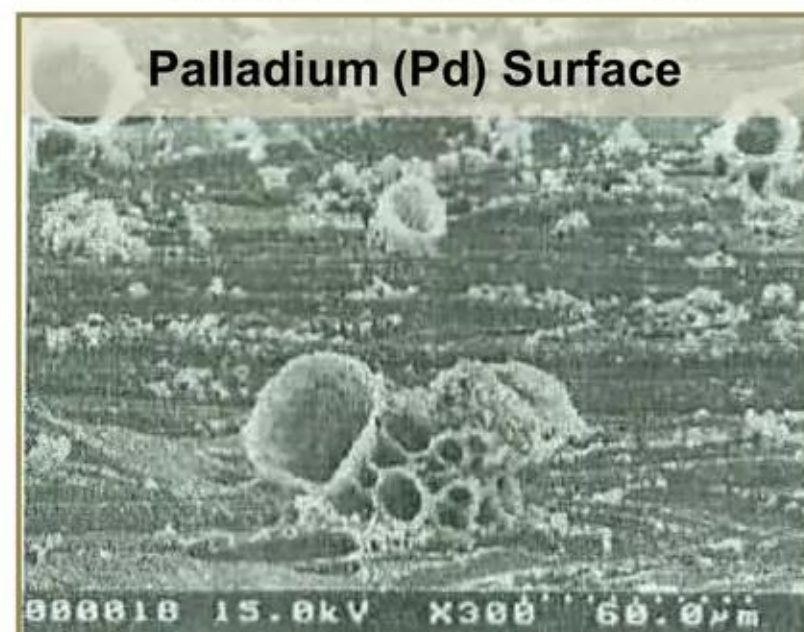
Credit: P. Boss et al.



Credit: Y. Toriabe et al.



Credit: P. Boss et al.



Credit: Y. Toriabe et al.



Credit: P. Boss et al.



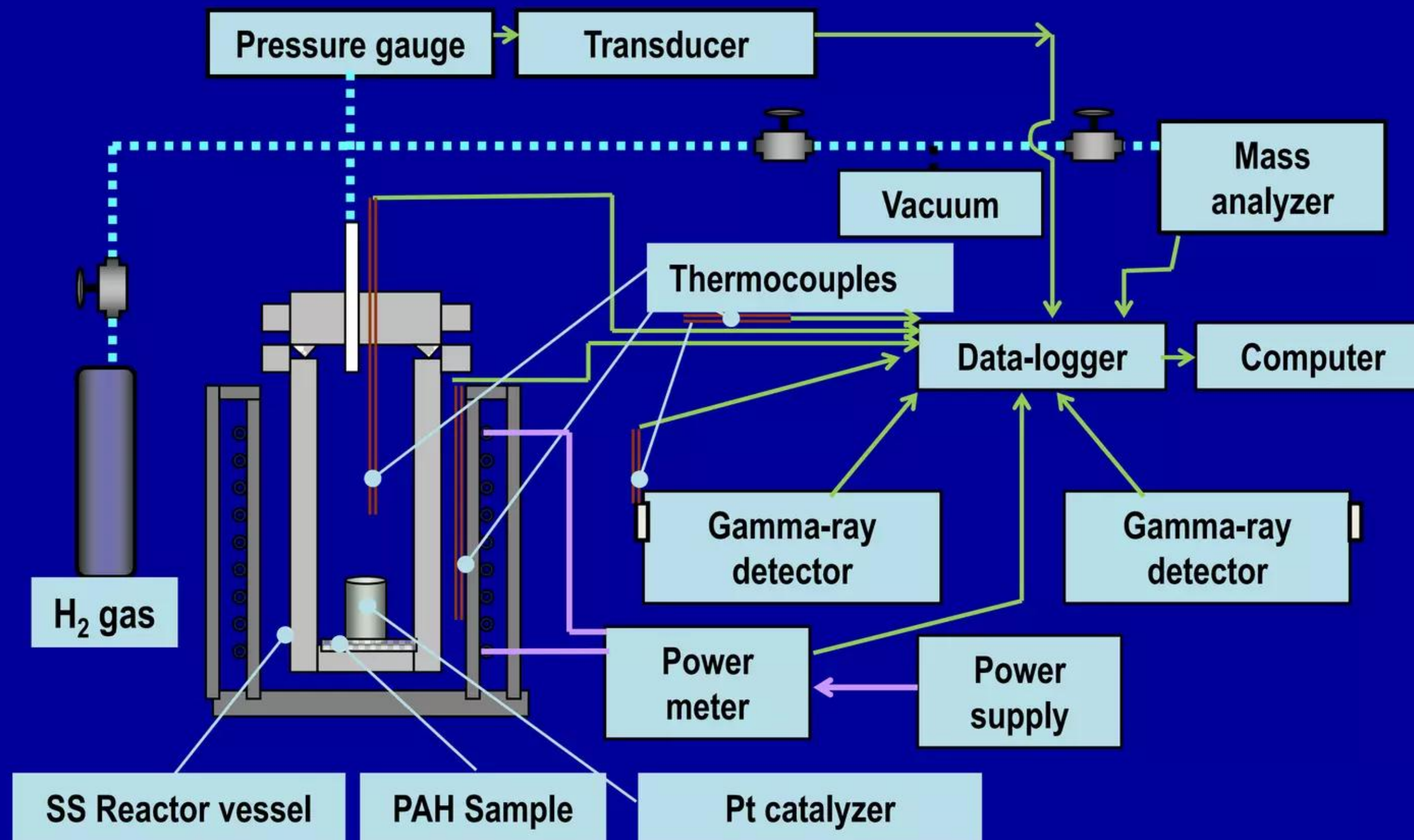
Credit: Energetics Technologies Ltd.

Note: besides the examples shown here, nanostructures created by LENRs display an extremely varied array of different morphologies and can range in size from just several nanometers all the way up to ~100 microns or more

Commercializing a Next-Generation Source of Safe Nuclear Energy

Gas-phase LENR systems with metallic vessels

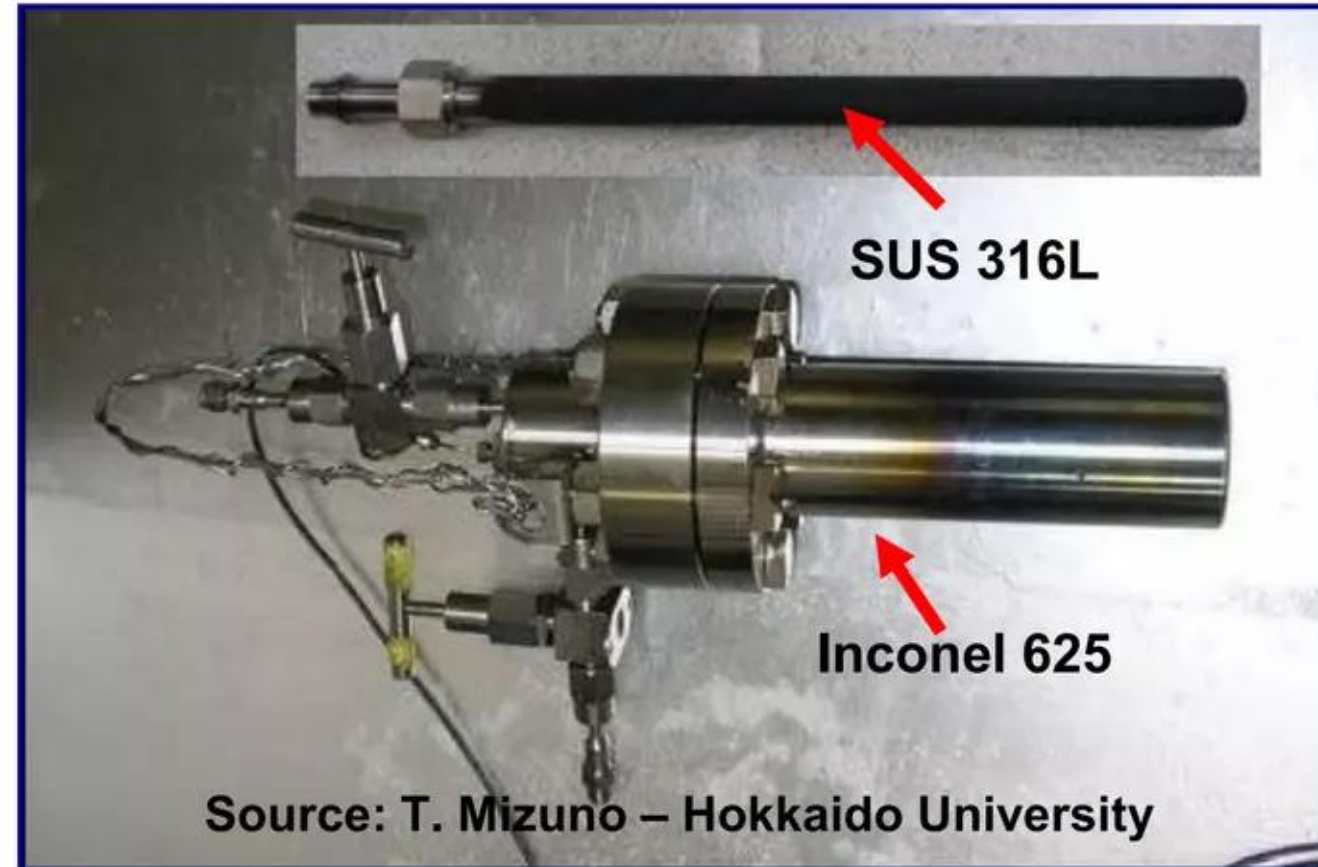
Schematic diagram of Mizuno PAH experiment with SS reactor vessel



Note: graphic adapted from T. Mizuno's 2009 ICCF-15 LENR conference presentation

Reaction vessels for gas-phase experiments often stainless steel Tolerate substantial heat, gas pressures, and chemicals for long periods

Mizuno's H₂ gas/Phenanthrene/Pt SS reactor vessels



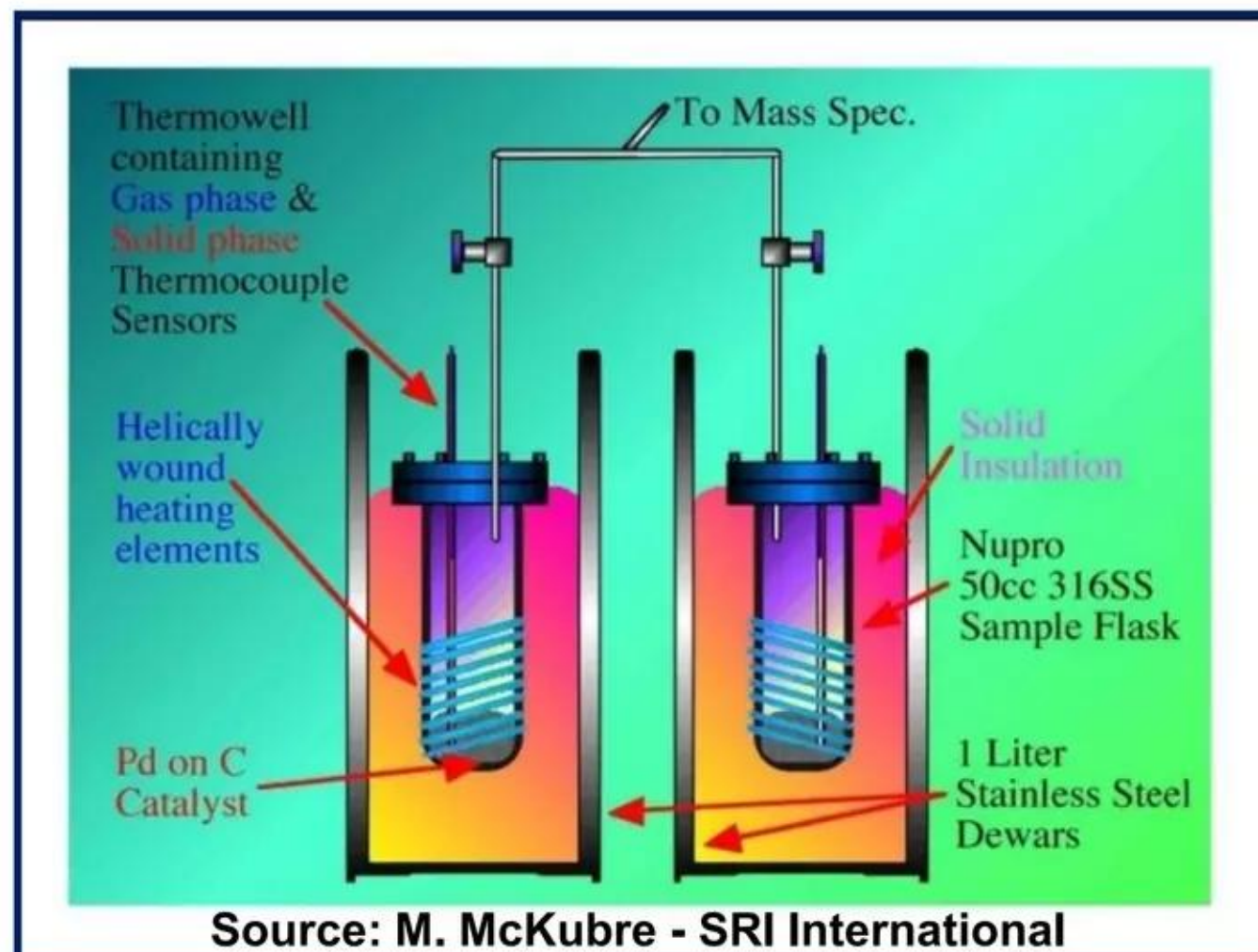
Composition of stainless steels (SS) commonly used in laboratory experiments:

Inconel 625: family of austenitic nickel-chromium (Ni-Cr) based superalloys that are typically used in high temperature applications. Forms passive oxidized layer upon heating that resists corrosion. Inconel 625 contains approximately: 58% Ni; 20 – 23% Cr; 5% Fe; as well as 8 - 10% Mo; 3.15 – 4.15% Nb; 1% Co; 0.5% Mn; 0.4% Al; 0.4% Ti; 0.5% Si; 0.1% C; 0.015% S; and 0.015% P

SUS 316L: family of standard, molybdenum-bearing austenitic stainless steels (Fe). Grade 316L is a low-carbon version that is immune to grain boundary carbide precipitation. This grade of stainless Fe contains maximum of approximately: 0.03% C; 2.0% Mn; 0.75% Si; 0.045% P; 0.03% S; 18% Cr; 3% Mo; 14% Ni; and 0.10%N

Note: as good practice, ALL materials found inside experimental reactor vessels should be very well-characterized from an isotopic and compositional standpoint. This is *extremely* important when assessing results of sensitive mass spectroscopy techniques that are used to detect and measure a wide variety of nuclear transmutation products that may be produced in different LENR experiments

Schematic: McKubre's D₂ gas/C/Pd SS reactor vessels



Composition of stainless steel varies: always contains at least 12% Cr

What Is Stainless Steel and Why Is it Stainless?

In 1913, English metallurgist Harry Brearly, working on a project to improve rifle barrels, accidentally discovered that adding chromium to low carbon steel gives it stain resistance. In addition to iron, carbon, and chromium, modern stainless steel may also contain other elements, such as nickel, niobium, molybdenum, and titanium. Nickel, molybdenum, niobium, and chromium enhance the corrosion resistance of stainless steel. It is the addition of a minimum of 12% chromium to the steel that makes it resist rust, or stain 'less' than other types of steel.

Types of Stainless Steel:

“The three main types of stainless steels are austenitic, ferritic, and martensitic. These three types of steels are identified by their microstructure or predominant crystal phase.”

Austenitic:

“Austenitic steels have austenite as their primary phase (face centered cubic crystal). These are alloys containing chromium and nickel (sometimes manganese and nitrogen), structured around the Type 302 composition of iron, 18% chromium, and 8% nickel. Austenitic steels are not hardenable by heat treatment. The most familiar stainless steel is probably Type 304, sometimes called T304 or simply 304. Type 304 surgical stainless steel is an austenitic steel containing 18-20% chromium and 8-10% nickel.”

Ferritic:

“Ferritic steels have ferrite (body centered cubic crystal) as their main phase. These steels contain iron and chromium, based on the Type 430 composition of 17% chromium. Ferritic steel is less ductile than austenitic steel and is not hardenable by heat treatment.”

Martensitic:

“The characteristic orthorhombic martensite microstructure was first observed by German microscopist Adolf Martens around 1890. Martensitic steels are low carbon steels built around the Type 410 composition of iron, 12% chromium, and 0.12% carbon. They may be tempered and hardened. Martensite gives steel great hardness, but it also reduces its toughness and makes it brittle, so few steels are fully hardened.”

Above definitions quoted directly from: “*Why is Stainless Steel Stainless? What It Is and How It Works*”

Anne Marie Helmenstine at source URL = <http://chemistry.about.com/cs/metalsandalloys/a/aa071201a.htm>

Discussion: results of earlier Italian gas-phase H₂/Ni experiments - I

- ✓ First conceived in mid-1989 by Francesco Piantelli, then of the University of Siena, about 1990 a small group of Italian “cold fusion” scientists broke with common practice (vast majority of researchers in field at that time used ‘classic’ Pons-Fleischmann glass aqueous electrolytic cells with Pt anode, Pd cathodes, and Li salts in D₂O) and began new LENR experiments using stainless steel reactor vessels, Nickel (Ni) metal rods or planar bars, H₂ gas, with only modest gas pressures and initial resistance heating for triggering
- ✓ Reported many remarkable results from long series of mostly Italian Ni/H₂ gas experiments conducted and published from 1990 to the present:
 - Although reproducibility was very spotty, *very large* amounts of measured heat (up to as much as ~900 megajoules) were produced during certain experiments over relatively long periods of time (months)
 - System-startup energy inputs were modest H₂ pressures (mbar up to ~1 bar) with initial heat provided by an electrical resistance heater (Pt heating wire coiled around long axis of ferromagnetic Ni cylinder, or planar Ni bars, attached to three equidistant ceramic support rods)
 - Experiments exhibiting very large heat production did not produce any large, readily detectible fluxes of ‘hard’ (defined as photon energies of ~1 MeV and higher) gamma radiation; no large fluxes of energetic MeV neutrons were detected nor significant production of any long-lived radioactive isotopes --- *anomalously free of dangerous radiation*
 - Results showed evidence of positive thermal feedback from 420-720° K. If correct, it suggests walls of SS reaction vessels may be behaving as resonant E-M radiation cavities; thus, LENRs may turn ‘on-and-off’ as Nickel surface nanostructures move in and out of resonance with spectral peaks of temperature-dependent emitted cavity radiation

Please note:

"Anomalous Heat Production in Ni-H Systems," Focardi S., Habel R., and Piantelli F., *Nuovo Cimento*, 107A pp. 163-167 (1994) – peer reviewed

Much of this interesting technical history was recounted in some detail in two well written news articles published by science journalist Steven Krivit in *New Energy Times* Issue #29, July 10, 2008, as follows:

Source URL =

<http://www.newenergytimes.com/v2/news/2008/NET29-8dd54geg.shtml#pf>

Article 12. “Deuterium and Palladium not required”

Article 13. “Piantelli-Focardi publication and replication path”

Contains comprehensive list of references to various technical publications by different members of this group of Italian researchers; in some cases, hyperlinks to free downloadable papers are provided

Key point: roots of the gas-phase Ni/H₂ line of LENR experimentation began in Italy roughly 20 years ago

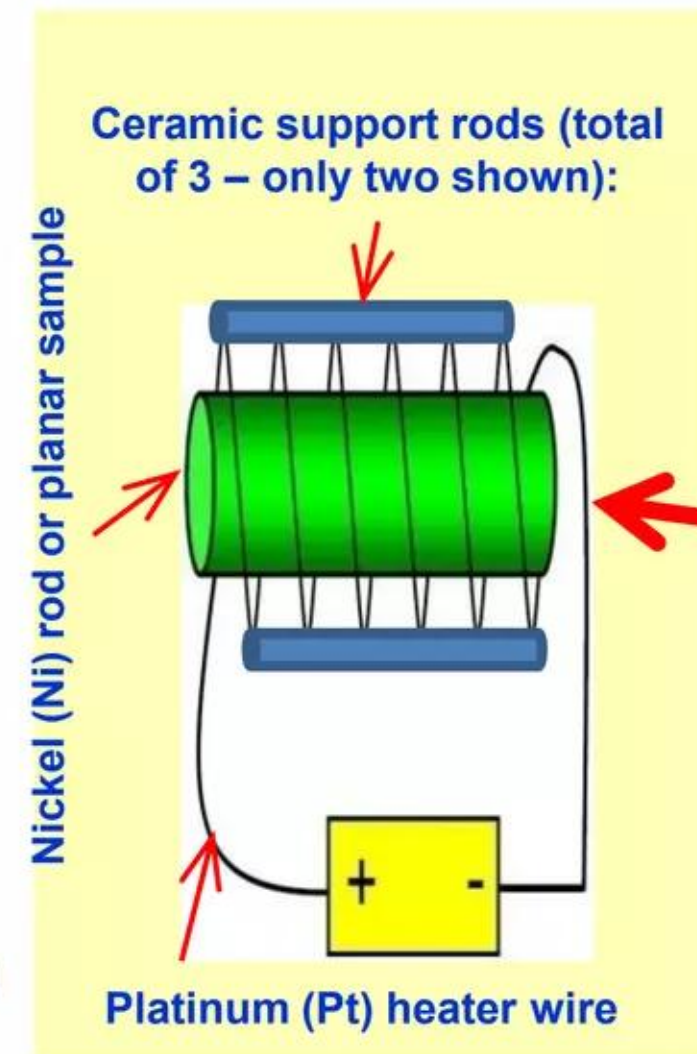
Discussion: results of earlier Italian gas-phase H_2/Ni experiments – II

Selected illustrative examples of experimental apparatus

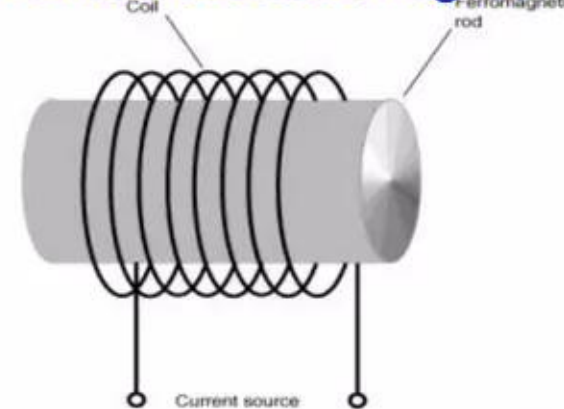


Ca. 1992 Piantelli-Focardi Ni-H Cell
(photo credit: S. B. Krivit)

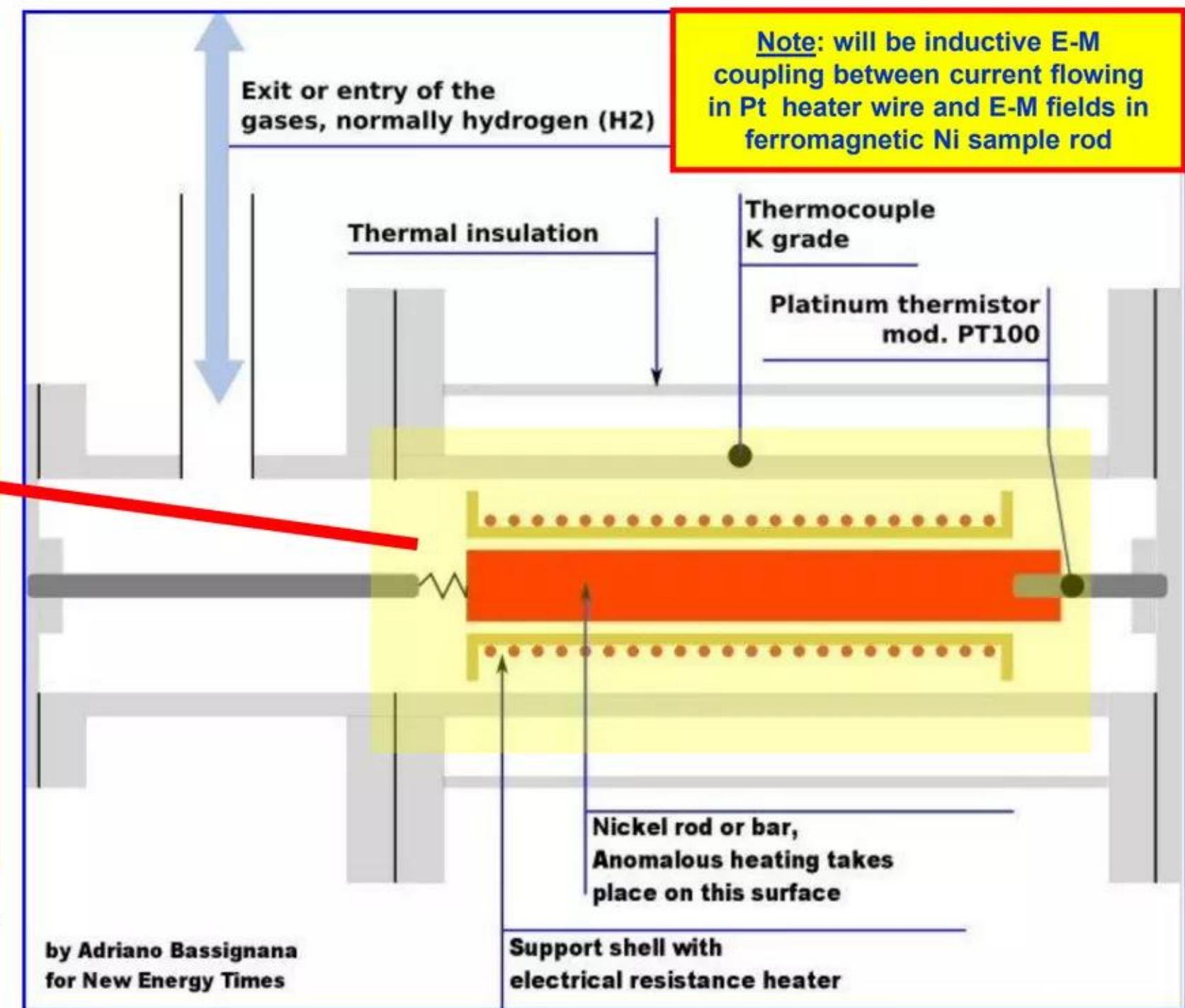
Schematic of electrical resistance heater:



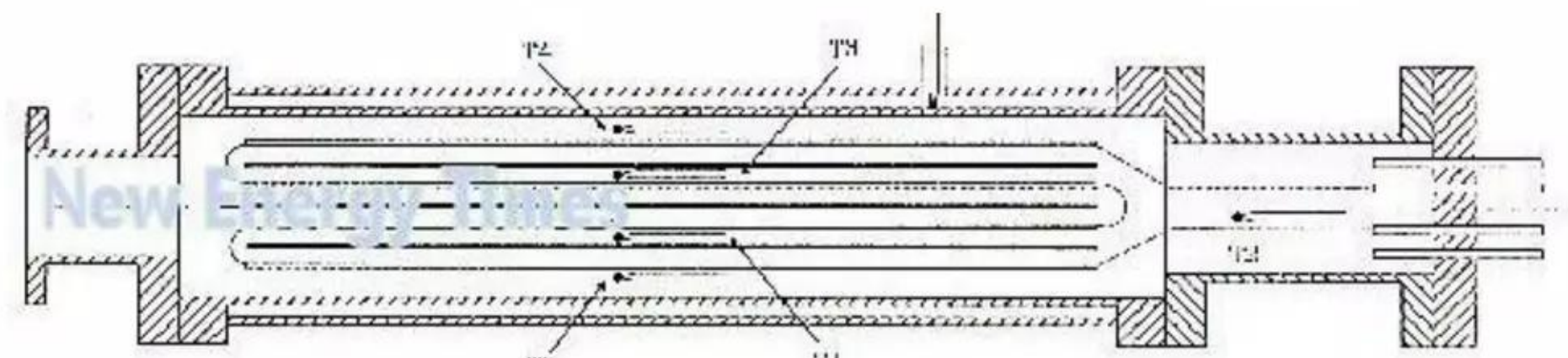
Schematic of electromagnet



Ca. 1992 Piantelli-Focardi Ni-H Cell (photo credit: S. B. Krivit)



Conceptual diagram of Piantelli-Focardi-type Ni-H Cell



Engineering drawing of Piantelli-Focardi-type Ni-H Cell

Discussion: results of earlier Italian gas-phase H₂/Ni experiments – III

Large admixtures of Deuterium (D₂) can ‘kill’ heat production in Ni/H₂ systems

“Piantelli has some very interesting things to say about deuterium. *New Energy Times* asked him whether he had ever tried using deuterium instead of normal hydrogen. Yes, he said, but if you put the deuterium inside a hydrogen-based experiment, it stops the reaction instantly. Piantelli said that, if he uses just normal hydrogen with very high purity, which may have a trace amount of deuterium, it works fine. But if he injects even just 2 percent or 3 percent of deuterium with respect to the hydrogen, it stops the experiment, kills it. Whether Piantelli had ever tried pure deuterium, rather than pure hydrogen, was not clear.”

“This is the strangest information; researchers who are accustomed to working in the deuterium/palladium system say almost the same thing - but the opposite: If you allow any normal hydrogen into the system, you will never get excess heat. It's quite a paradox. For years, the deuterium/palladium researchers have said that the proof that normal hydrogen can't make excess heat is that, time after time, normal hydrogen poisons the excess heat effect in deuterium-based systems. Even the emotive language in their descriptions – ‘poisons,’ ‘kills’—has a similar ring.”

Source of quote: S. B. Krivit in Article 12. “Deuterium and Palladium not required,” *New Energy Times* Issue #29, July 10, 2008



Ca. 2007 Piantelli-Focardi Ni-H Cell (photo credit: S.B. Krivit)

Negative effect of large Hydrogen isotope admixtures fully explained by the Widom-Larsen theory of LENRs:

“(iii) However, one seeks to have either nearly pure proton or nearly pure deuterium systems, since only the isotopically pure systems will easily support the required coherent collective oscillations.”

In other words, because their masses differ greatly, substantial admixtures of different hydrogen isotopes will destroy Q-M coherence in the many-body, collectively oscillating surface ‘patches’ of protons, deuterons or tritons that are necessary to produce ULM neutrons in condensed mater LENR systems

Reference: “Ultra Low Momentum Neutron Catalyzed Nuclear Reactions on Metallic Hydride Surfaces,” *European Physical Journal C – Particles and Fields* 46, pp. 107 (March 2006) A. Widom and L. Larsen

Discussion: results of earlier Italian gas-phase H₂/Ni experiments – IV

Large fluxes of dangerous ‘hard’ gammas not observed in these systems - 1

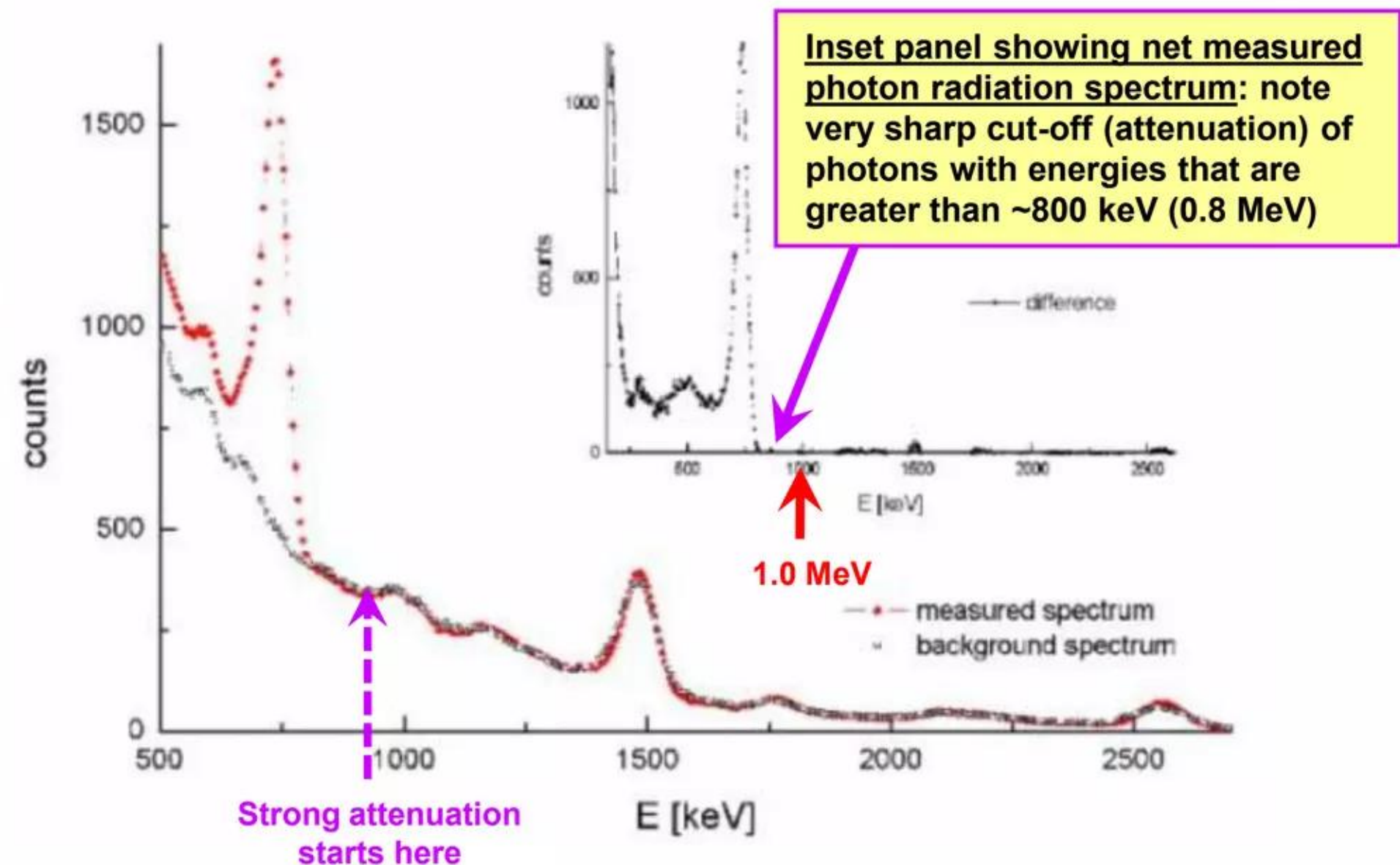
Comments:

In Fig. 7 to the right, the inset panel at the upper right shows the net measured photon radiation spectrum; that is, it represents the radiation spectrum measured during LENR experiments by Campari et al. (2004) from which the known laboratory background radiation spectrum has been subtracted. This reported net radiation spectral data shows substantial attenuation of energetic photons above ~ 800 KeV. Given that nuclear processes were probably occurring in the experimental system during gamma-ray measurements (likely LENR transmutation products were detected in post-experiment EDAX spectral analyses of Nickel surfaces), this is an anomalous, surprising result. Under normal circumstances, nontrivial fluxes of >MeV-energy photons (‘hard’ gammas) would be expected

Assuming that the underlying measurements by Campari et al. are correct as reported (2004), this anomalous data is explained by the Widom-Larsen theory of LENRs.

Specifically, in condensed matter LENR systems, gammas produced by nuclear processes in energy range of 0.5 – 1.0 MeV all the way up through ~10 MeV are efficiently absorbed by heavy-mass electrons and directly converted into much lower-energy infrared (IR) photons with a somewhat variable, poorly understood ‘soft’ X-ray ‘tail’

Reference: “Absorption of Nuclear Gamma Radiation by Heavy Electrons on Metallic Hydride Surfaces,” A. Widom and L. Larsen http://arxiv.org/PS_cache/cond-mat/pdf/0509/0509269v1.pdf (Sept 2005)



Source of the above graph: Figure 7 in "Overview of H-Ni Systems: Old Experiments and New Setup," Campari, E., Focardi, S., Gabbani, V., Montalbano, V., Piantelli, F., and Veronesi, S., 5th Asti Workshop on Anomalies in Hydrogen-Deuterium-Loaded Metals, Asti, Italy (2004) free copy online at www.lenr-canr.org

Also please see Lattice’s 6th issued patent:

US #7,893,414 issued February 22, 2011

“Apparatus and Method for Absorption of Incident Gamma Radiation and its Conversion to Outgoing Radiation at Less Penetrating, Lower Energies and Frequencies”

Inventors: Lewis Larsen and Allan Widom

Clean electronic copy of issued patent at source URL =

<http://www.slideshare.net/lewisglarsen/us-patent-7893414-b2>

Discussion: results of earlier Italian gas-phase H_2/Ni experiments – V

Large fluxes of dangerous ‘hard’ gammas not observed in these systems - 2

Full reference:

“Evidence of electromagnetic radiation from Ni-H systems”
S. Focardi, V. Gabbani, E. Campari, V. Montalbano, F. Piantelli, and S. Veronesi, CONDENSED MATTER NUCLEAR SCIENCE pp. 70 – 80,
Proceedings of the 11th International Conference on Cold Fusion
Marseilles, France, 31 October - 5 November 2004
edited by Jean-Paul Biberian (Université de la Méditerranée, France), World Scientific Publishing 2006
DOI No: 10.1142/9789812774354_0034

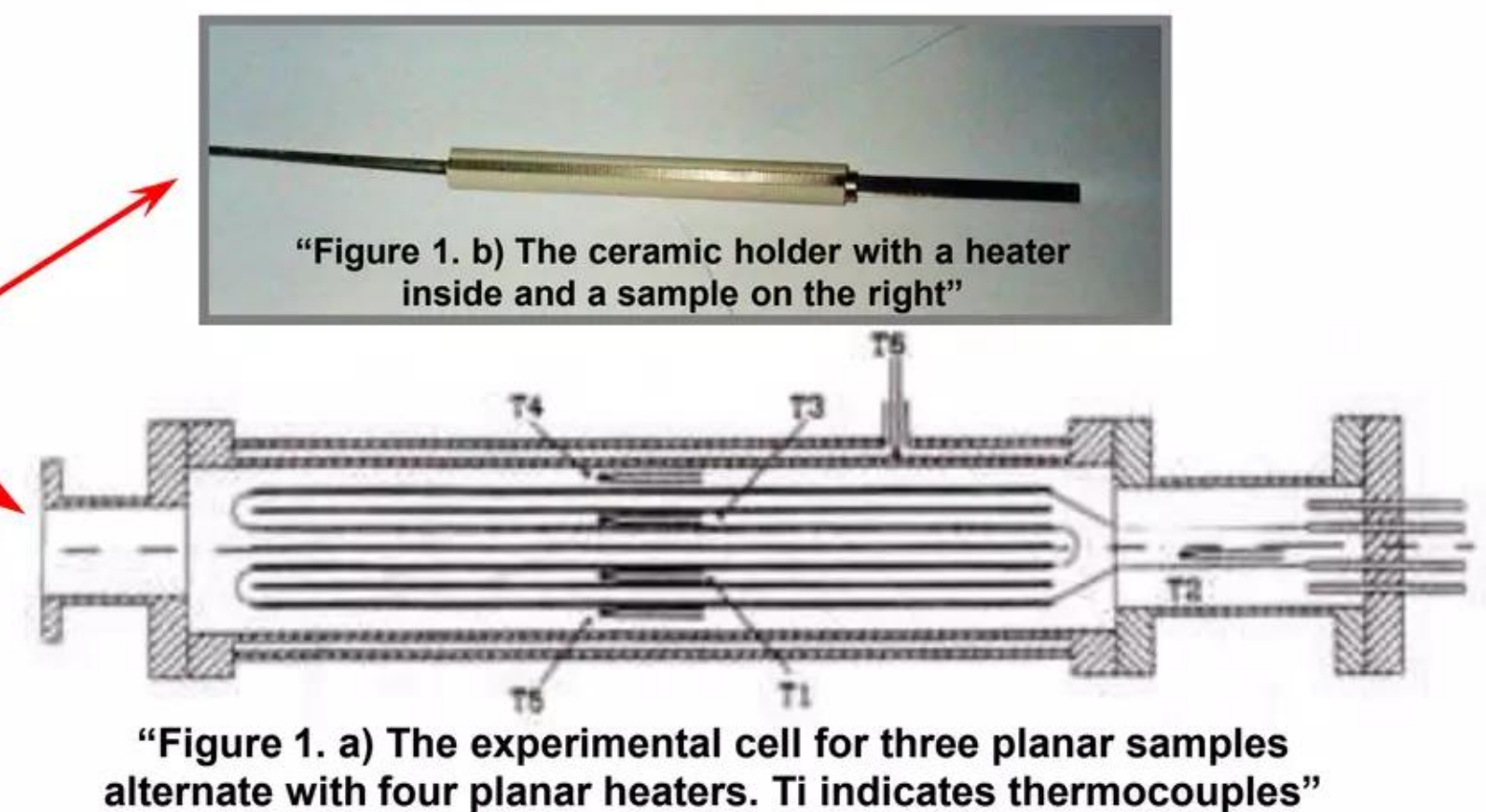
Source URL (free public copy of conference paper on LENR-CANR.org;
this may differ slightly from final version published by World Scientific in
2006) = <http://www.lenr-canr.org/acrobat/FocardiSevidenceof.pdf>

Selected highlights of the experiments:

- This conference paper reports results of three experiments
- Stainless steel used in reaction vessel identified as AISI 304 with standard composition: Iron (Fe) 66 – 74%; Chromium (Cr) 18 – 20%; Nickel (8 – 10.5%); Manganese (Mn) max 2%; Silicon (Si) max 1%; Carbon (C) max .08%; Phosphorus (P) max .045%; and Sulfur (S) max 1% --- CF35 vacuum flanges generally made from Type 316L stainless
- Nickel samples were stated to be “99.5% pure” Ni
- Resistance heater inside reaction vessel was very different design compared to what was used in otherwise similar experiments discussed in the previous slide (Campari et al., Asti 2004). Instead of a Pt heater coil helically wound around the Ni sample; quoting, “ ... The heater consists of four plate coils, each made from a small NiCr slab of analogous dimensions, connected in series and held in a ceramic cylinder with the Ni samples in alternating positions.”

Selected highlights of the experiments (continued):

- Duration of a given experiment ranged up to 85 days (#1)
- Substantial amounts of excess heat (total of 25 MJ over period of 35 days) were measured during a later phase of Experiment #1; no excess heat seen in Expts. #2 and #3
- In their conclusions about Experiment #1, Focardi et al. suggested that post-experiment “new elements” Cr and Mn widely observed across surface of reacted Ni sample with SEM-EDAX were LENR transmutation products. That may or may not be true, because ablation from vessel walls (Cr 18 -20%; Mn max 2%) and resistance heater surfaces (NiCr alloy) could have easily deposited nanoparticles on surface of 99.5% pure Ni sample. *That said, please note that large amounts of nuclear binding energy can be released simply as a result of ULM neutron captures on stable Ni isotopes*
- Chronology and discussion of key events that occurred in Experiment #1 is presented on next slide



Discussion: results of earlier Italian gas-phase H_2/Ni experiments – VI

Large fluxes of dangerous ‘hard’ gammas not observed in these systems - 3

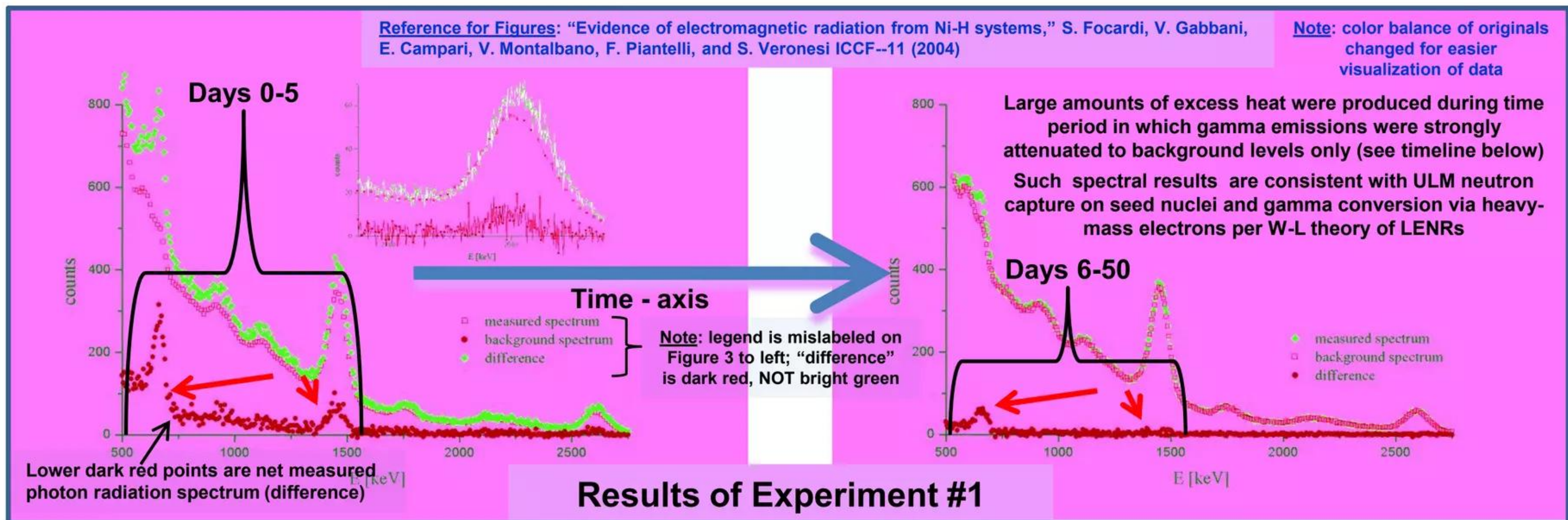


Fig. 3 (left) and Fig.4 (above right) were copied from pp. 3 of Focardi et al. (ICCF-11 in 2004) and annotated by Lattice as shown above

Quoting: “Figure 3. First experiment: background and measured spectra, at the beginning of gamma measurements, obtained with the NaI(Tl) detector placed in front. The background spectrum is a mean of 90 acquisition (live time 12000 s) while the measured one is a mean of 6 acquisitions. The lower curve is the difference between measured and background spectrum.”

Quoting: “Figure 4. First experiment: background and measured spectra 45 days after the beginning of gamma measurements, the measured spectrum is a mean of 18 acquisitions. The lower curve is the difference between measured and background spectra.”

Timeline and Commentary on Key Events that occurred during Experiment #1

Days into expt.	Focardi et al. remark in their paper	Key event	Lattice comments about key events
Day 0 to Day 5	5 days into degassing phase, net measured photon spectrum changed from spectrum of Fig. 3 to what is shown in Fig. 4	Abrupt decrease in gamma spectrum	Heavy SP electrons begin appearing; fields not yet high enough to make large fluxes of ULM neutrons
Day 6 thru Day 50	Day 19 inject H_2 gas - no change in spectrum; on Day 50 “difference” goes to zero; then <u>only</u> see background radiation	Spectrum changes to <u>background only</u>	Bigger population of ‘heavy’ SP electrons at larger masses; hit threshold for producing ULM neutrons
Day 51 thru Day 85	Quoting: “Later on the cell produced excess power (maximum 25 W ...) for about 35 days ...”	Total of 25 MJ heat prod. over ~35 days	ULM N captures on seed elements, then various decays; gammas converted to IR by heavy electrons

Discussion: results of earlier Italian gas-phase H_2/Ni experiments – VII W-L LENR Ni/Fe/Cr ‘seed’ networks and transmutation data of Campari et al.

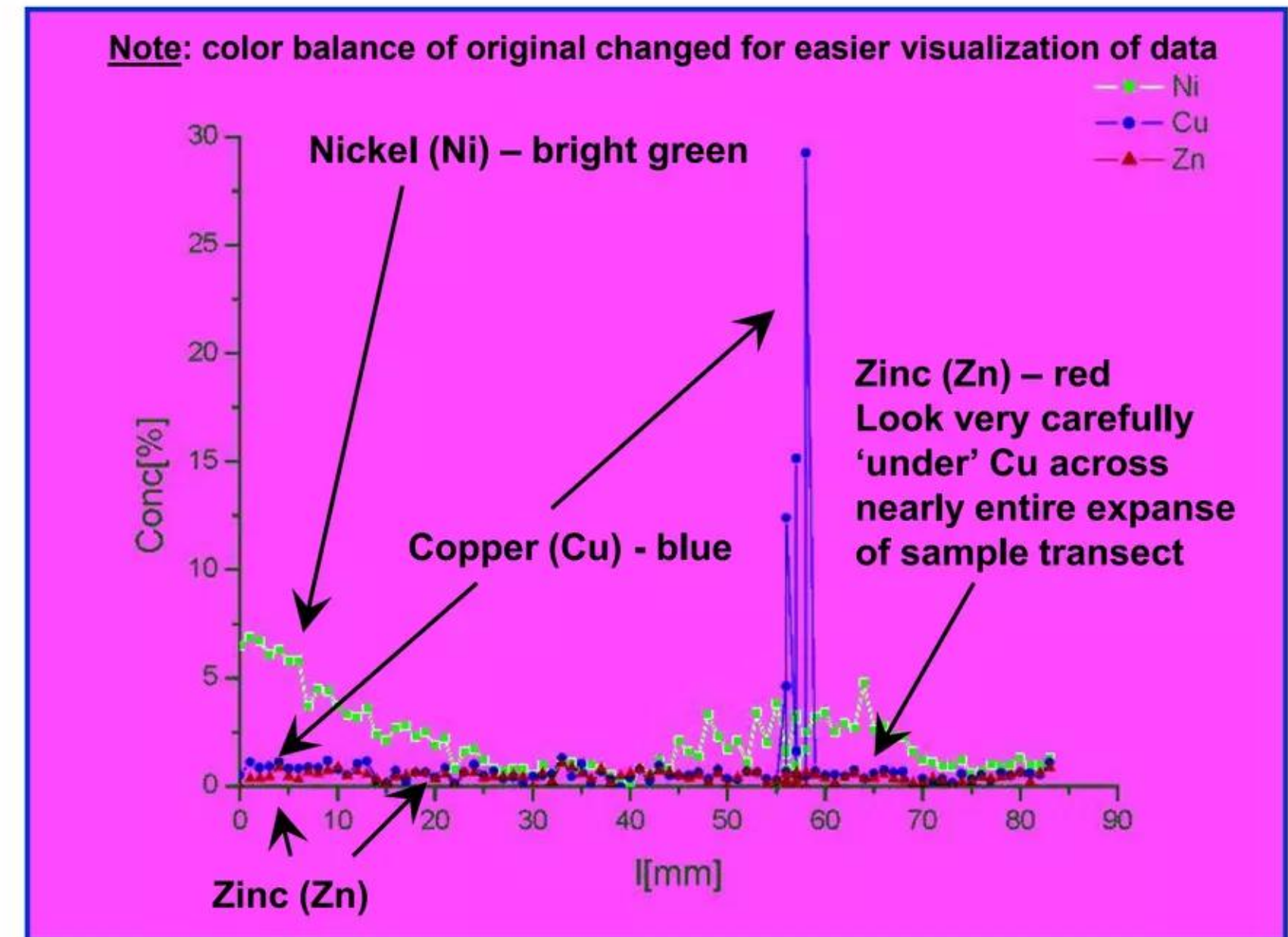
Reference (for details see Slide #4):

“Surface analysis of hydrogen-loaded nickel alloys,” E. Campari et al., ICCF-11 Conference, Marseilles, France (November 2004)

Selected highlights of the experiments:

- Stainless steel reaction vessel with integrated Pt resistance heater as previously described
- Sample was 9 cm Nickel-alloy rod of composition: Ni (7.6%), Cr (20.6%), Fe (70.4%), and Mn (1.4%)
- Temperature range: 400 – 700° K
- Range of H_2 gas pressure: 100 to 1,000 mbar
- Sample analysis technique: SEM-EDX which determines elements present on surface; can't resolve individual isotopes like ICP-MS or NAA

Comments: Zinc and Copper not initially present in either ‘blank’ sample or vessel walls. Unless these were contaminants, Zn and Cu are probably LENR transmutation products; consistent with W-L neutron capture Ni/Fe/Cr ‘seed’ networks illustrated in Slides #19 – 25 of this presentation



Source of adapted graph: Campari et al. (2004) Figure on pp. 6
“Fig. 10 Spatial distribution of Ni and Cu on the sample surface”

Quoting directly from their paper: “In Fig. 10, a quantity of Cu is measured in a narrow zone of the sample. Moreover, in a wide region of the sample, nickel is absent from the surface.”

“In contrast, the elemental analysis of the sample rod (Fig. 7) are very different from the *blank rod analysis*, and they are very different from one region to the next along the sample. This is why a systematic investigation along the sample was performed. We obtained the elemental distribution along the rod.”

Discussion: results of earlier Italian gas-phase H_2/Ni experiments – VIII Cu isotopes: results from Ni-seed aqueous LENR electrolytic experiment

Reference: “Analysis of Ni-hydride thin film after surface plasmons generation by laser technique,” V. Violante et al., Condensed Matter Nuclear Science – Proceedings of the 10th International Conference on Cold Fusion (ICCF-10 2003), eds. P. Hagelstein and S. Chubb, pp. 421-434, World Scientific 2006 ISBN# 981-256-564-7 Source URL to free copy = <http://www.lenr-canr.org/acrobat/ViolanteVanalysisof.pdf>

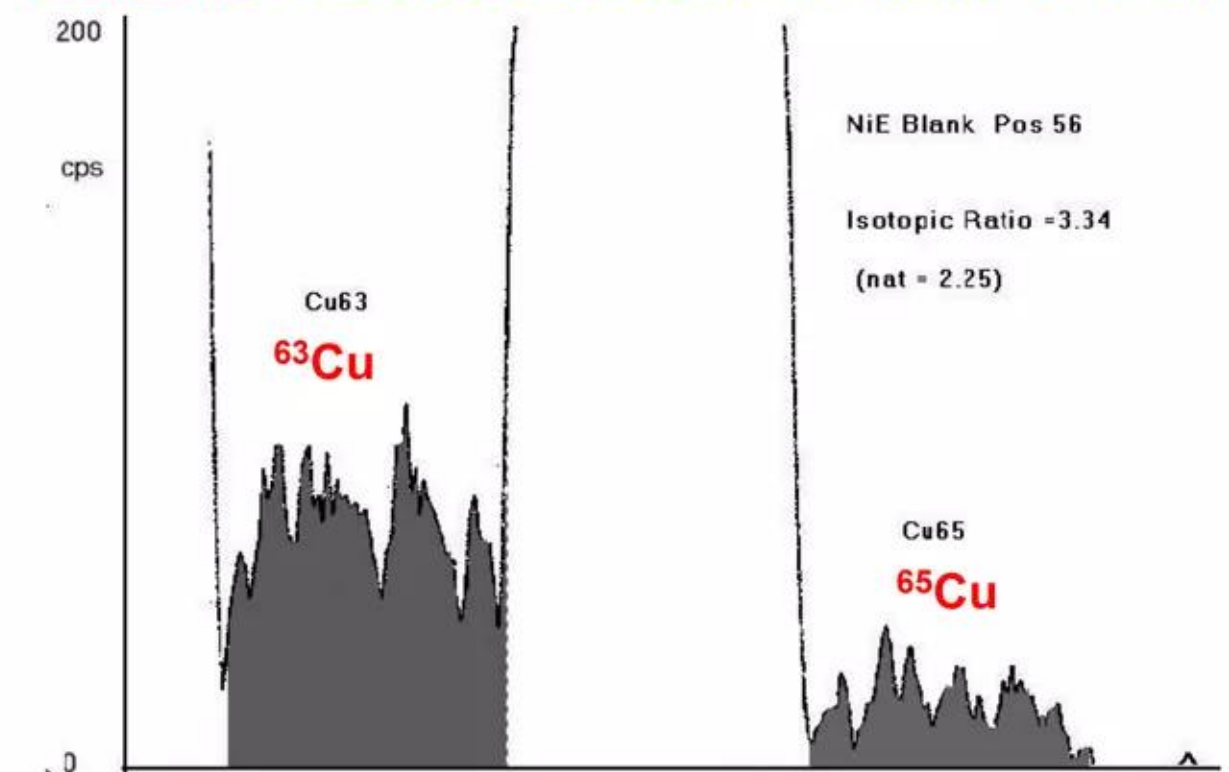
Key highlights of the experiment:

- Fabricated two sputtered thin-film pure Nickel ‘target’ samples; “black” sample was loaded with hydrogen (made NiH) in electrolytic cell; “blank” sample was not put into the electrolytic cell (not loaded)
- Aqueous H_2O 1 M Li_2SO_4 P&F-type electrolytic cell; thin-film Nickel (Ni) cathode; [Platinum pt anode?]; loaded “black” Ni ‘target’ cathode with Hydrogen for 40 minutes at currents ranging from 10-30 mA and then removed it from the aqueous electrolyte bath
- Irradiated both samples with He-Ne laser (632 nm beam) for 3 hours
- After laser irradiation, analyzed Cu isotopes present on surface in “blank” and “black” Ni samples with SIMS; results shown in Figs. 12 and 13 to right: abundance of ^{63}Cu went down; ^{65}Cu went way up
- Suggested surface plasmons might have important role in LENRs

Comments: the observed dramatic isotopic shift (^{63}Cu goes down; ^{65}Cu goes up in an experiment) is readily explained by ULM neutron capture on ^{63}Cu ‘seed’ according to W-L theory of LENRs; if data is correct, only other possible explanation is magically efficient isotopic “fractionation” process

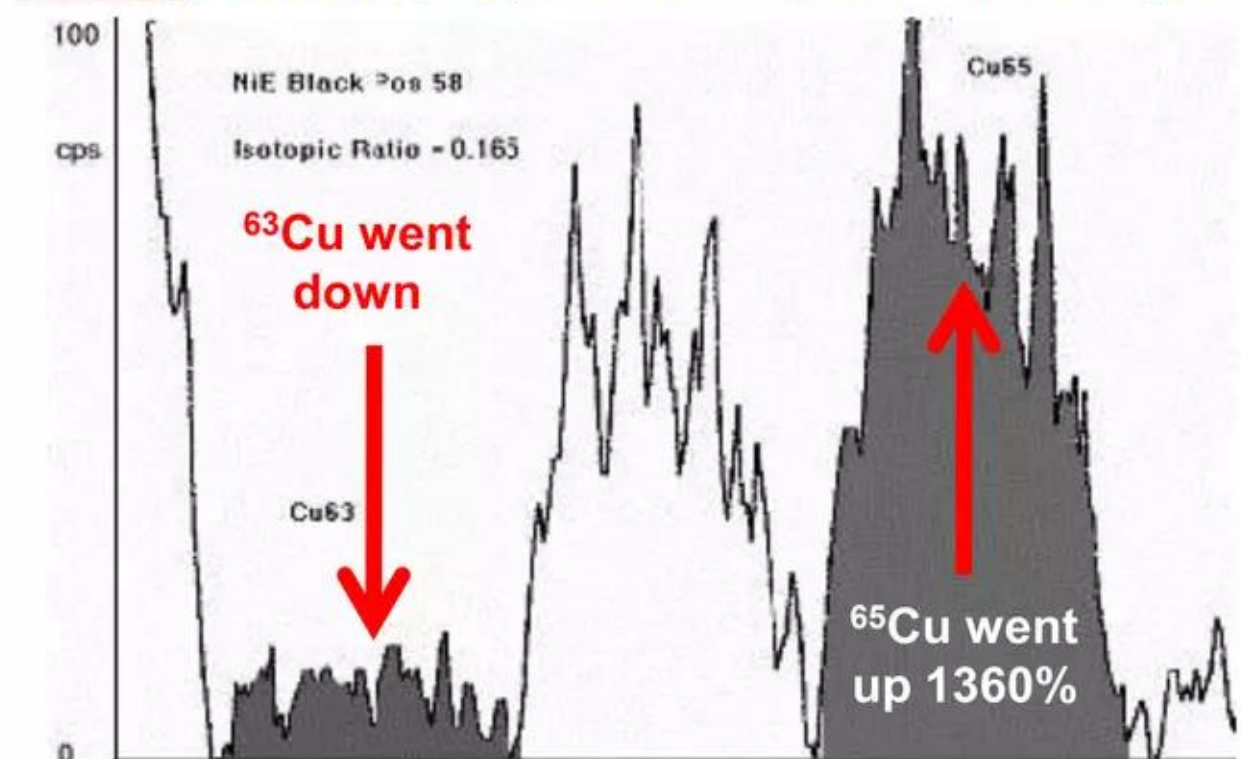
Note: we have been informed that Violante et al. have openly questioned their own claims for reasons that we find dubious. Readers are urged to review the relevant publications and then judge whether such concerns are plausible

BEFORE: Cu isotopes present in “blank” Ni sample



Quoting: “Figure 12. Blank of NiE, ^{63}Cu results to be more abundant of ^{65}Cu , the difference with the natural isotopic ratio is due to the small signal on mass 65. The sample was undergone to laser excitation of plasmons-polaritons for 3 hr”

AFTER: Cu isotopes present in “black” NiH sample



Quoting: “Figure 13. Black of NiE, after 40 min electrolysis + 3 hr of plasmons-polaritons excitation by laser. Isotopic ratio is changed of 1360%”

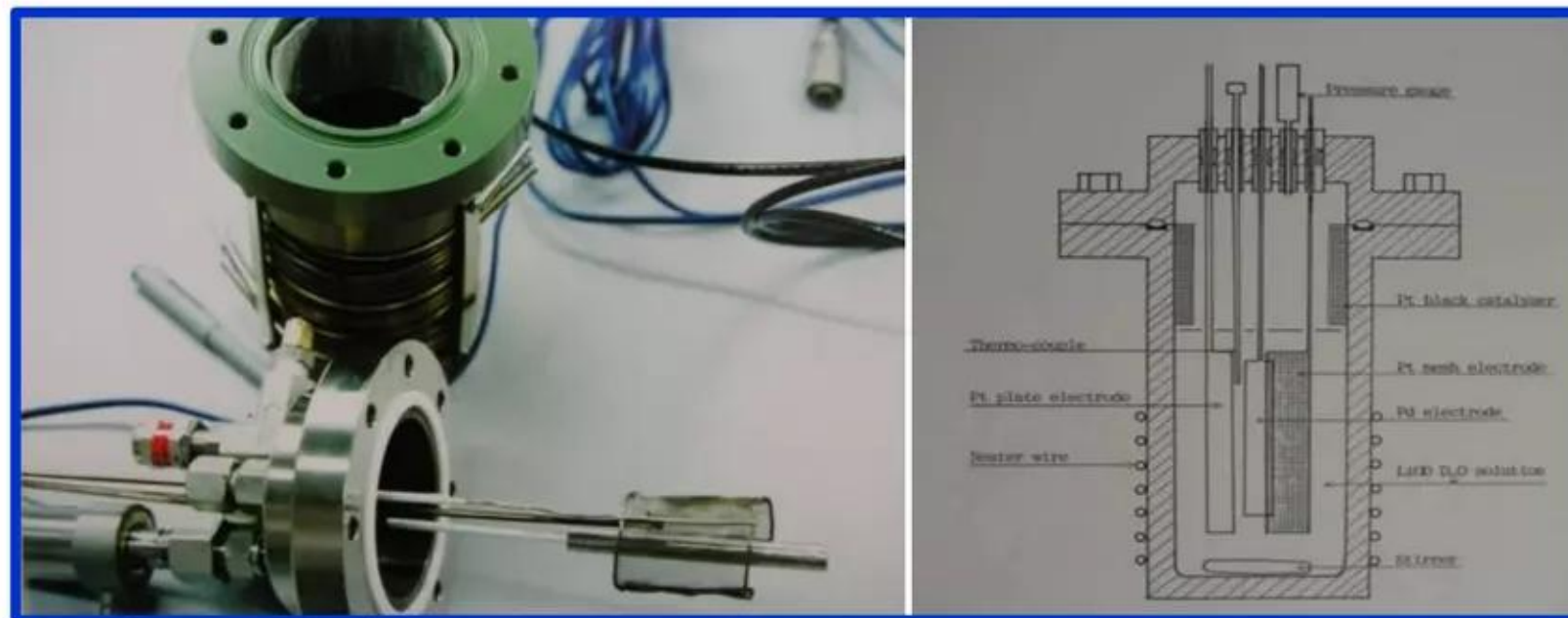
Discussion: results of earlier Italian gas-phase H_2/Ni experiments – IX

Cr isotopic results: aqueous D_2O LENR electrolytic cell similar to Miley's (H_2O)

Reference: “Isotopic changes of elements caused by various conditions of electrolysis,” T. Mizuno and H. Kozima, American Chemical Society, March 2009

Abstract of Mizuno & Kozima's 2009 ACS presentation:

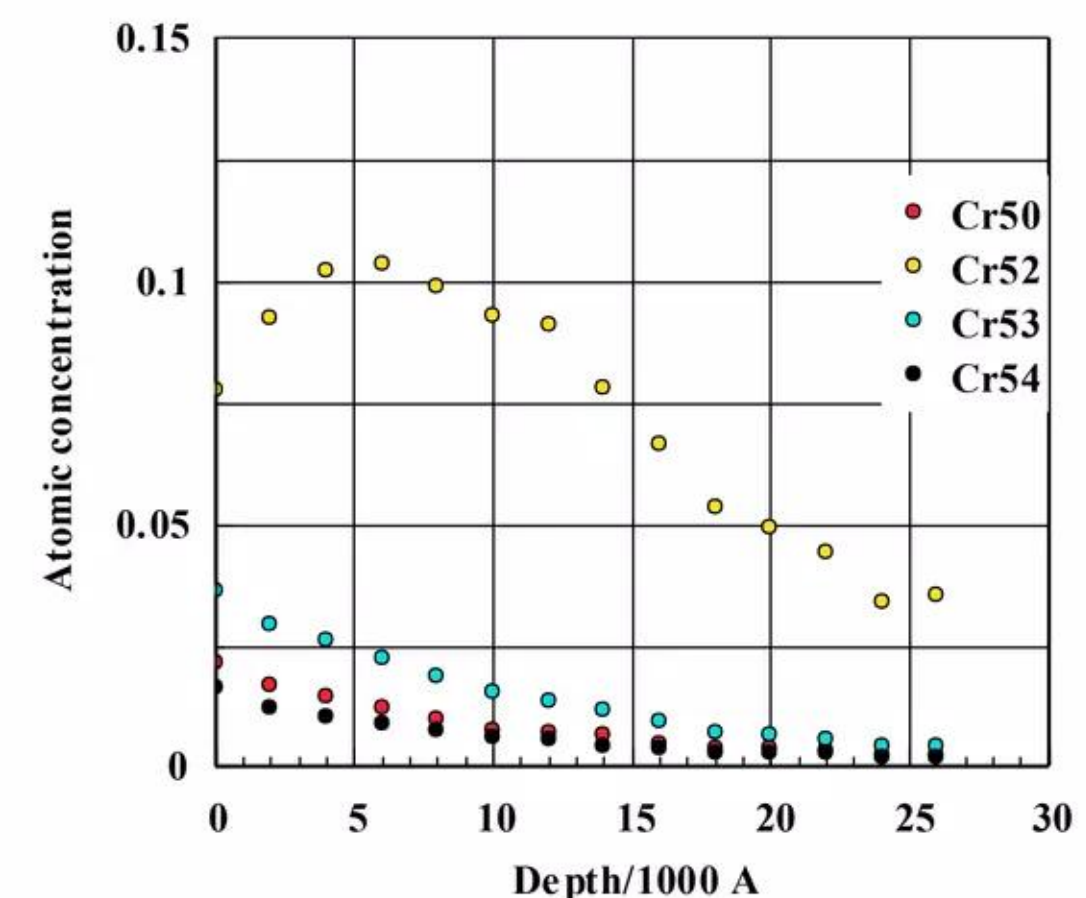
Quoting directly from it: “The appearance of elements on palladium electrodes after electrolysis in various conditions were confirmed by several analytic methods. Mass numbers as high as 208 corresponding to elements ranging from hydrogen to lead were found, and the isotopic distributions of many of these elements were radically different from the naturally occurring ones. Changes in element distribution and in their isotopic abundances took place during electrolysis in both heavy and light water, whether or not excess energy was generated. If the transmutation mechanism can be understood, it may then be possible to control the reaction, and perhaps produce macroscopic quantities of rare elements by this method. In the distant future, industrial scale production of rare elements might become possible, and this would help alleviate material shortages worldwide.”



Quoting directly: “All electrolysis was performed in a closed cell made from a stainless steel cylinder. The cell has an inner Teflon cell made with 1-mm thick wall and 1 cm thick upper cap; the inner height and diameter are 20 cm and 7 cm, the volume is 770 cm³. Before electrolysis electrolyte were pre-electrolyzed using another Pt mesh electrode. After that the Pt electrode was removed and the palladium rod sample was connected to the electrical terminal. Electrolysis experiments were performed with the current density of 0.2 A/cm² for 20 days at 105°C.”

Quoting from their comments about Chromium transmutation products observed in a Pd/ D_2O electrolytic cell :

“Much Cr was detected on the Pd surface [that] generated excess heat. The quantity of Cr exceeded that of impurities in the electrolysis system. Depth profile of Cr concentration in the sample is shown in left figure. Here, you can see change of each isotopes. And the view of depth distribution for their isotope ratios are seen in right figure. You can recognize very large isotope change at the sample surface.”

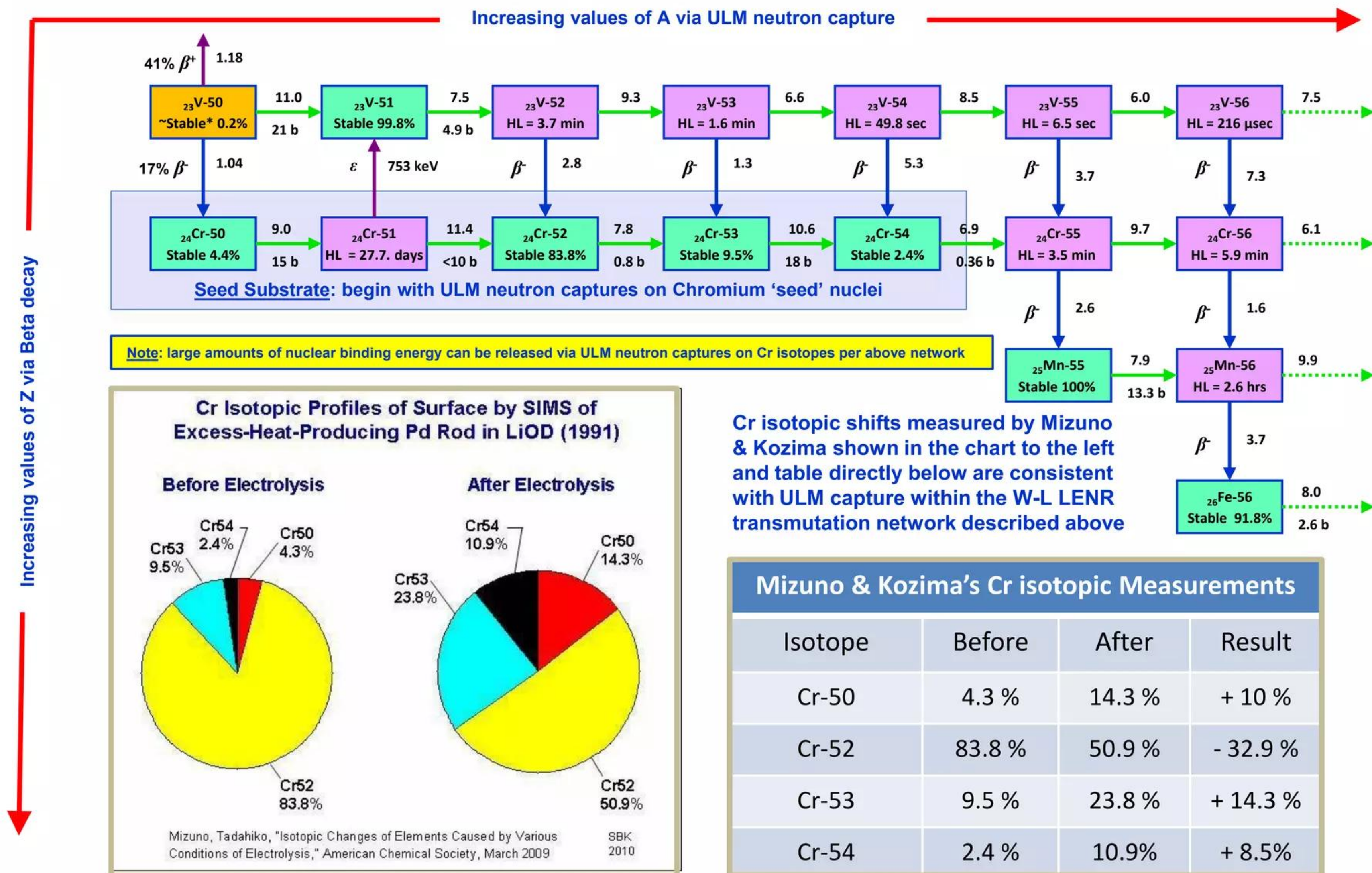


Quoting: “Depth profile of Cr concentration in the sample is shown [above] ... you can see change of each isotopes ... [and] can recognize very large isotope change at the sample surface ... concentrations except for ⁵²Cr decreased exponentially with depth.”

Note: Mizuno & Kozima's exp. results for Chromium (Cr) presented on next slide

LENR W-L ULM neutron capture on Cr 'seeds,' neutron-rich isotope production, and decays

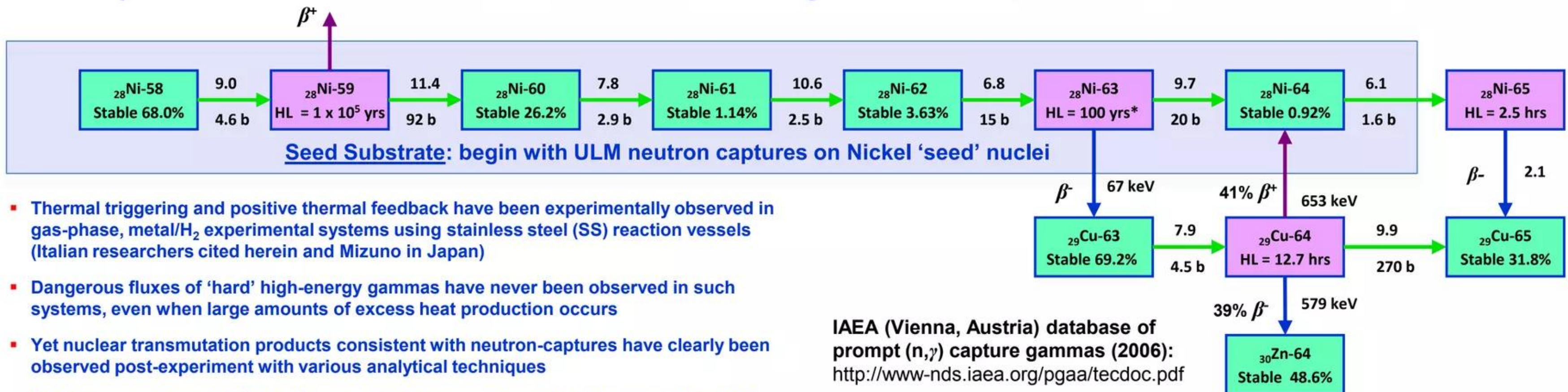
Stable 'target' seed nuclei on or very near LENR nuclear-active Chromium surfaces: Cr-50, Cr-52, Cr-53,, and Cr-54



Source: Mizuno & Kozima, ACS meeting, March 2009

Discussion: results of earlier Italian gas-phase H_2/Ni experiments – X

Likely mechanism and favorable energetics for positive thermal feedback



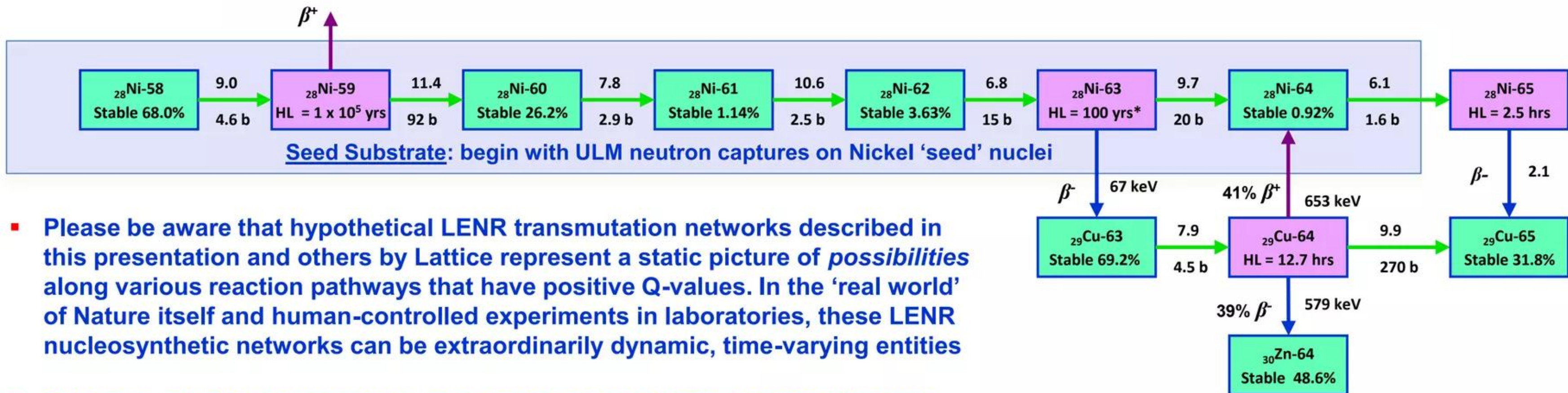
IAEA (Vienna, Austria) database of prompt (n, γ) capture gammas (2006):
<http://www-nds.iaea.org/pgaa/tecdoc.pdf>

Summary of energetics for one possible Ni-seed LENR network pathway

Isotope Capturing ULM Neutron or Beta decaying	Capture Q-value in ~MeV (all +)	Some of its Hrd. Gamma Lines* (MeV)	'Cost' to Produce ULM Neutrons	Net Q-value
Ni-58	9.0	8.1, 8.5, 8.9	0.78 MeV	8.22
Ni-59	11.4	Not in IAEA	0.78 MeV	10.62
Ni-60	7.8	7.5, 7.8	0.78 MeV	7.02
Ni-61	10.6	Not in IAEA	0.78 MeV	9.82
Ni-62	6.8	6.3, 6.8	0.78 MeV	6.02
Ni-63	9.7	Not in IAEA	0.78 MeV	8.92
Ni-64	6.1	6.0	0.78 MeV	5.32
Ni-65 (decay)	2.1	1.5	~1 (*neutrino)	~1.1*
Totals (MeV)	63.5	NA	6.46	57.04
Gain = (net total Q-value for entire pathway) divided by (total cost) = 8.83				

- Thermal triggering and positive thermal feedback have been experimentally observed in gas-phase, metal/ H_2 experimental systems using stainless steel (SS) reaction vessels (Italian researchers cited herein and Mizuno in Japan)
- Dangerous fluxes of 'hard' high-energy gammas have never been observed in such systems, even when large amounts of excess heat production occurs
- Yet nuclear transmutation products consistent with neutron-captures have clearly been observed post-experiment with various analytical techniques
- W-L theory explains all of this; it turns-out that conversion of 'hard' gammas into IR by heavy electrons is also crucial to providing a plausible mechanism for positive thermal feedback: it hinges on the idea of stainless steel reaction vessels behaving as if they were resonant E-M cavities in the IR portion of the spectrum
- Please examine the network pathway shown to the right. Note that prompt gamma ray emission can comprise a substantial percentage of positive Q-values for the ULM neutron capture process; that being the case, energy associated with gamma emission can comprise vast majority of pathway's total net Q-value of 57.04 MeV and also the strongly positive total gain across the entire pathway of 8.83
- Now consider a stainless steel reaction vessel with a resonant IR E-M cavity inside it as a system. If neutron captures occurred inside the cavity per network pathway shown at right and gamma conversion by heavy electrons did NOT take place, the vast majority of released nuclear binding energy associated with 'hard' gammas would likely escape through the SS cavity walls (at the wall thicknesses used in laboratory systems) and would thus be 'lost' to the system proper. Without gamma conversion to IR, from the system's standpoint as a resonant IR cavity, net energy gain would likely be negative, not a strongly positive 8.83
- Unlike extremely penetrating 'hard' gammas, SS cavity walls are relatively opaque to IR radiation; moreover, with thermal conductivity of 12-45 W/(m·K) SS 'holds the heat in' much better than Copper at 401 W/(m·K). When gamma conversion to IR DOES occur, released nuclear binding energy in the form of IR tends to stay inside the cavity and is thus available to heat it up and, most importantly, to be absorbed by surface plasmons (found on cavity walls and objects inside the cavity) that can concentrate that energy and transport it to many-body surface 'patches' of collectively oscillating protons or deuterons which in turn can make more ULM neutrons. This 'virtuous circle' enables the possibility of a positive feedback loop between releases of nuclear binding energy, conversion of γ to IR, local energy retention, absorption of cavity IR by SPs on nanostructures, additional neutron production --- in a potentially self-sustaining cycle until the system exhausts its reactants

Comments about LENR transmutation network products and isotope ratios



- Please be aware that hypothetical LENR transmutation networks described in this presentation and others by Lattice represent a static picture of *possibilities* along various reaction pathways that have positive Q-values. In the 'real world' of Nature itself and human-controlled experiments in laboratories, these LENR nucleosynthetic networks can be extraordinarily dynamic, time-varying entities
- Pathways actually traversed in a given system can change dramatically over surprisingly short time-scales and on very small length-scales (nanometers to microns) in response to a myriad of different causative factors. Final product nucleosynthetic results observed in a given experiment run reflect a sum total across many parallel alternate reaction paths --- LENR network computer codes really need to be developed to better understand dynamics of such processes
- A frequent question in readers' minds is whether or not LENR networks typically produce final stable products with isotopic ratios that are roughly the *same* as the known natural abundances, or whether they would be more likely to differ? The straight answer to that question, as best we know today, is that sometimes they do, and sometimes they don't --- also, there is compelling evidence that some LENRs do occur outside laboratory settings in Nature
- For example, a series of aqueous electric arc experiments conducted at Texas A&M University and BARC (India) in the 1990s apparently transmuted Carbon into Iron (see Slides #46-56 in Lattice SlideShare technical overview dated Sept. 3, 2009, with file title, "Carbon-seed LENR networks"). In those experiments, measured isotopic ratios of the produced Iron did not differ significantly from natural abundances. On the other hand, there are many examples of LENR experiments in which product isotopic ratios differed greatly from natural ones

Let's take Copper (Cu) for example - see hypothetical W-L LENR network pathway above:

Given the long half-life and slow decay rate of Ni-63, one might reasonably expect that the network would produce Cu-65 at a much higher rate than Cu-63, hence the final elemental Copper isotopic ratio would probably shift in the direction of the heavier species. This is exactly what was observed by Violante et al. (ICCF-10, 2003, see Slide #45 herein)

On the other hand, it is well-known among astrophysicists that in certain very highly ionized states the half-life of Ni-63 can be *reduced* by >200x; i.e., it goes down from ~100 years to ~0.4 yrs. Could something like that ever happen in a condensed matter LENR system? Mostly likely not, but the little micron-scale LENR 'plasma balls' do get awfully hot, but not for a long enough period of time (~200 nanoseconds or less). That said, it would truly be extremely naïve to assume that LENR systems will not deal-out a few more big surprises along the way

Commercializing a Next-Generation Source of Safe Nuclear Energy

Pd-seed experiments consistent with ULMN capture

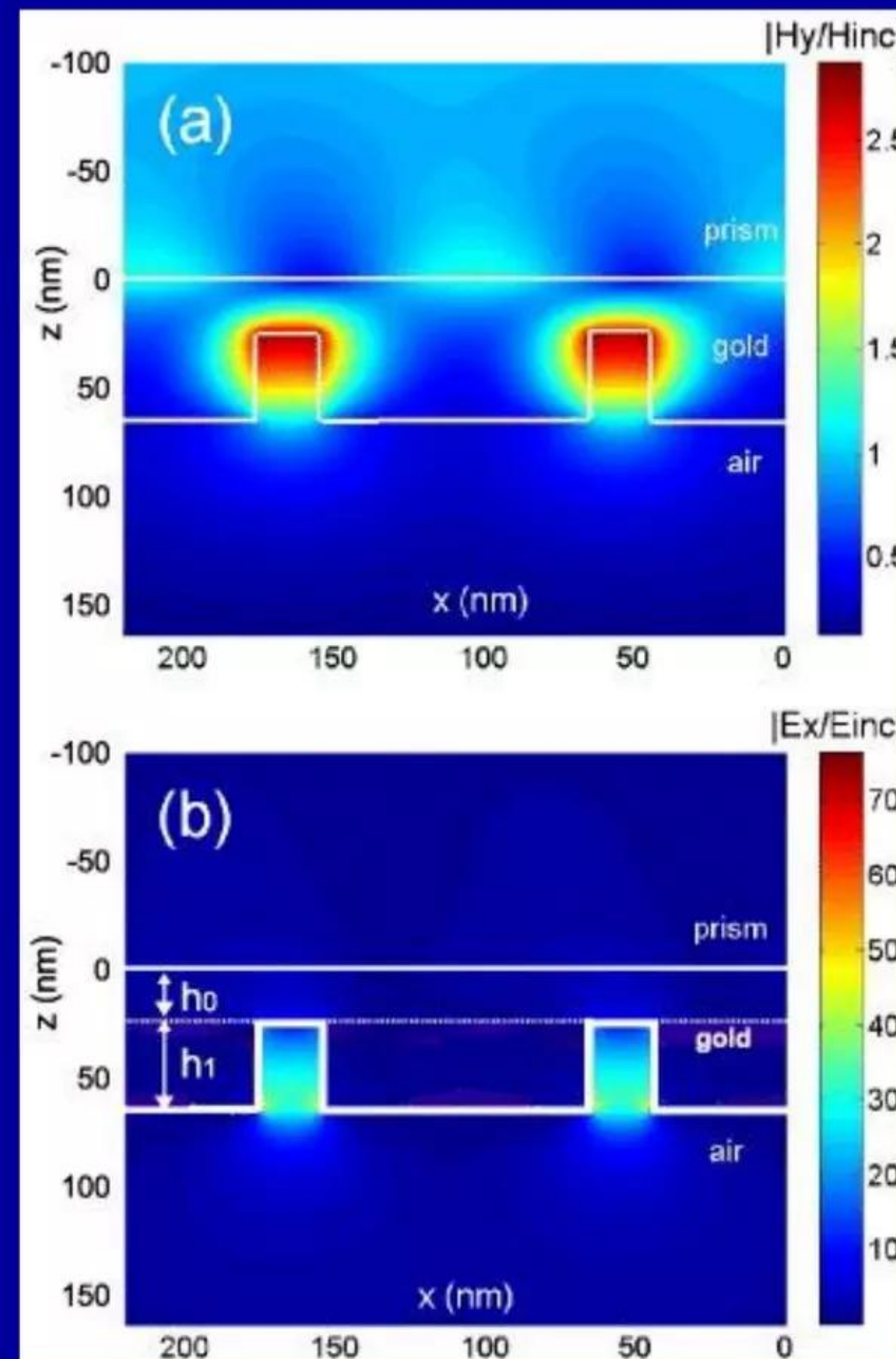
Surface plasmons can transport, concentrate, and store energy

Reference:

“Enhancing reactive energy through dark cavity plasmon modes”

J. Le Perchec

Europhysics Letters 92 DOI:
10.1209/0295-5075/92/67006 (2010)



Credit: J. Le Perchec

Abstract:

“We present an opto-geometrical configuration in which a metallic surface having nanometer-scale grooves can be forced to efficiently resonate without emitting radiation. The structure is excited from the backside, by an evanescent wave, which allows to inhibit light re-emission and to drastically modify the quality factor of the resonance mode. The energy balance of the system, especially the imaginary part of the complex Poynting vector flux, is theoretically analysed thanks to a modal method. It is shown how the generated hot spots (coherent cavity modes of electrostatic type) can store a great amount of unused reactive energy. This behaviour might thus inspire a novel use of such highly sensitive surfaces for chemical sensing.”

Pd-seed ULM Neutron Catalyzed Network Pathway

THE PERIODIC TABLE

Major vector of LENR Pd-seed nucleosynthetic pathway
discussed herein indicated by red arrow

'Seeds' of Palladium (Pd) are
present

In these experiments, mostly measure
Palladium isotopes (Pd) and Silver (Ag)

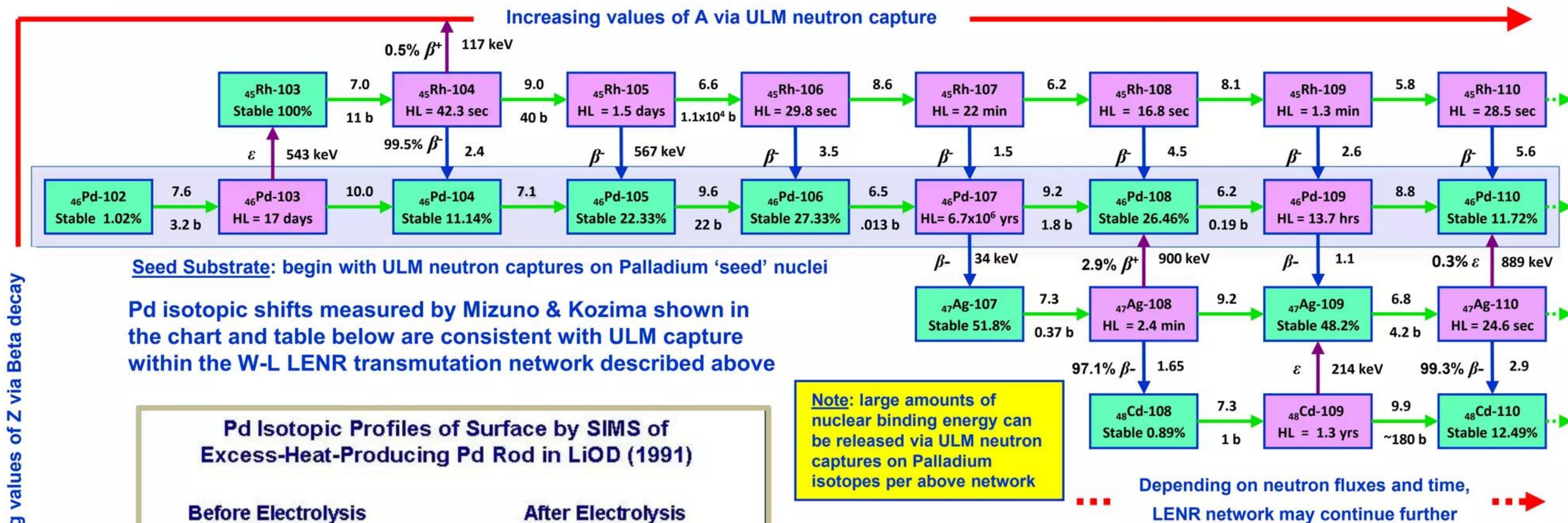
1 IA	2 IIA											13 IIIA	14 IVA	15 VA	16 VIA	17 VIIA	18 VIIIA	
H 1 1.008 Hydrogen												B 5 10.81 Boron	C 6 12.01 Carbon	N 7 14.01 Nitrogen	O 8 16.00 Oxygen	F 9 19.00 Fluorine	Ne 10 20.18 Neon	
Li 3 6.94 Lithium	Be 4 9.01 Beryllium											Al 13 26.98 Aluminum	Si 14 28.09 Silicon	P 15 30.97 Phosphorus	S 16 32.07 Sulfur	Cl 17 35.45 Chlorine	Ar 18 39.95 Argon	
Na 11 22.99 Sodium	Mg 12 24.31 Magnesium	3 IIIB	4 IVB	5 VB	6 VIB	7 VIIB	8 VIII	9 VIII	10 VIII	11 IB	12 IIB	Ga 31 69.72 Gallium	Ge 32 72.61 Germanium	As 33 74.92 Arsenic	Se 34 78.96 Selenium	Br 35 79.90 Bromine	Kr 36 83.80 Krypton	
K 19 39.10 Potassium	Ca 20 40.08 Calcium	Sc 21 44.96 Scandium	Ti 22 47.88 Titanium	V 23 50.94 Vanadium	Cr 24 52.00 Chromium	Mn 25 54.94 Manganese	Fe 26 55.85 Iron	Co 27 58.93 Cobalt	Ni 28 58.69 Nickel	Cu 29 63.55 Copper	Zn 30 65.39 Zinc	Cd 48 112.41 Cadmium	In 49 114.82 Indium	Sn 50 118.71 Tin	Sb 51 121.76 Antimony	Te 52 127.60 Tellurium	I 53 126.90 Iodine	Xe 54 131.29 Xenon
Rb 37 85.47 Rubidium	Sr 38 87.62 Strontium	Y 39 88.91 Yttrium	Zr 40 91.22 Zirconium	Nb 41 92.91 Niobium	Mo 42 95.94 Molybdenum	Tc 43 (97.9) Technetium	Ru 44 101.07 Ruthenium	Rh 45 101.07 Rhodium	Pd 46 106.42 Palladium	Ag 47 107.87 Silver	Cd 48 112.41 Cadmium	In 49 114.82 Indium	Sn 50 118.71 Tin	Sb 51 121.76 Antimony	Te 52 127.60 Tellurium	I 53 126.90 Iodine	Xe 54 131.29 Xenon	
Cs 55 132.91 Cesium	Ba 56 137.33 Barium	La 57 138.91 Lanthanum	Hf 72 178.49 Hafnium	Ta 73 180.95 Tantalum	W 74 183.85 Tungsten	Re 75 186.21 Rhenium	Os 76 190.2 Osmium	Ir 77 192.22 Iridium	Pt 78 195.08 Platinum	Au 79 196.97 Gold	Hg 80 200.59 Mercury	Tl 81 204.38 Thallium	Pb 82 207.2 Lead	Bi 83 208.98 Bismuth	Po 84 (209) Polonium	At 85 (210) Astatine	Rn 86 (222) Radon	
Fr 87 223.02 Francium	Ra 88 226.03 Radium	Ac 89 227.03 Actinium	Rf 104 (261) Rutherfordium	Db 105 (262) Dubnium	Sg 106 (263) Seaborgium	Bh 107 (262) Bohrium	Hs 108 (265) Hassium	Mt 109 (266) Meitnerium	Unlabeled Discovery 110 Nov. 1994 Unlabeled	Unlabeled Discovery 111 Nov. 1994 Unlabeled	Unlabeled Discovery 112 1996 Unlabeled	Unlabeled Discovery 113 Unlabeled	Unlabeled Discovery 114 1999 Unlabeled	Unlabeled Discovery 115 Unlabeled	Unlabeled Discovery 116 1999 Unlabeled	Unlabeled Discovery 117 Unlabeled	Unlabeled Discovery 118 1999 Unlabeled	
ALKALI METALS		ALKALI EARTH METALS												HALOGENS		NOBLE GASES		
LANTHANIDES		Ce 58 140.12 Cerium	Pr 59 140.91 Praseodymium	Nd 60 144.24 Neodymium	Pm 61 (145) Promethium	Sm 62 150.36 Samarium	Eu 63 152.07 Europium	Gd 64 157.25 Gadolinium	Tb 65 158.93 Terbium	Dy 66 162.50 Dysprosium	Ho 67 164.93 Holmium	Er 68 167.26 Erbium	Tm 69 168.93 Thulium	Yb 70 173.04 Ytterbium	Lu 71 174.97 Lutetium			
ACTINIDES		Th 90 232.04 Thorium	Pa 91 231.04 Protactinium	U 92 238.03 Uranium	Np 93 237.05 Neptunium	Pu 94 (240) Plutonium	Am 95 243.06 Americium	Cm 96 (247) Curium	Bk 97 (248) Berkelium	Cf 98 (251) Californium	Es 99 252.08 Einsteinium	Fm 100 257.10 Fermium	Md 101 (257) Mendelevium	No 102 259.10 Nobelium	Lr 103 262.11 Lawrencium			

HAYDEN
McNEIL
SPECIALTY
PRODUCTS

www.hmpublishing.com

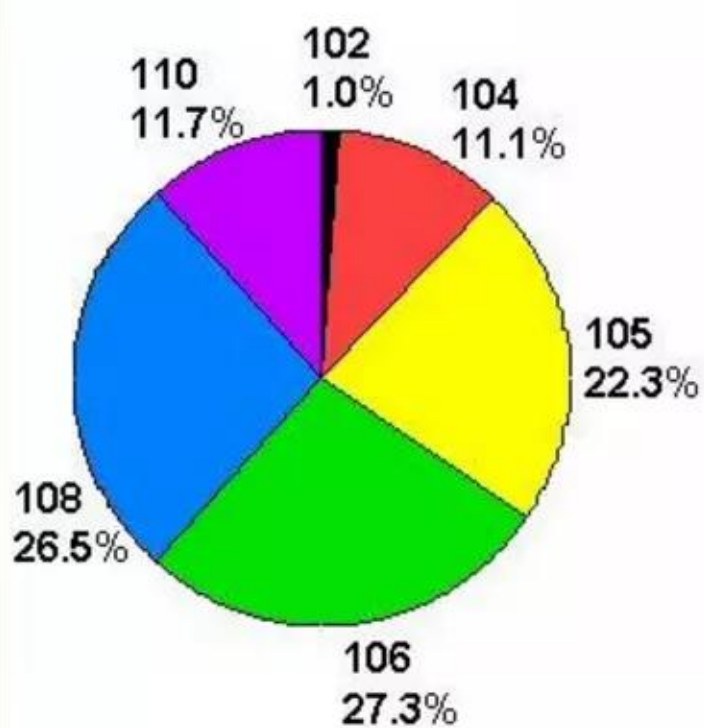
© Hayden-McNeil Specialty Products

LENR W-L ULM neutron capture on Pd 'seeds,' neutron-rich isotope production, and decays

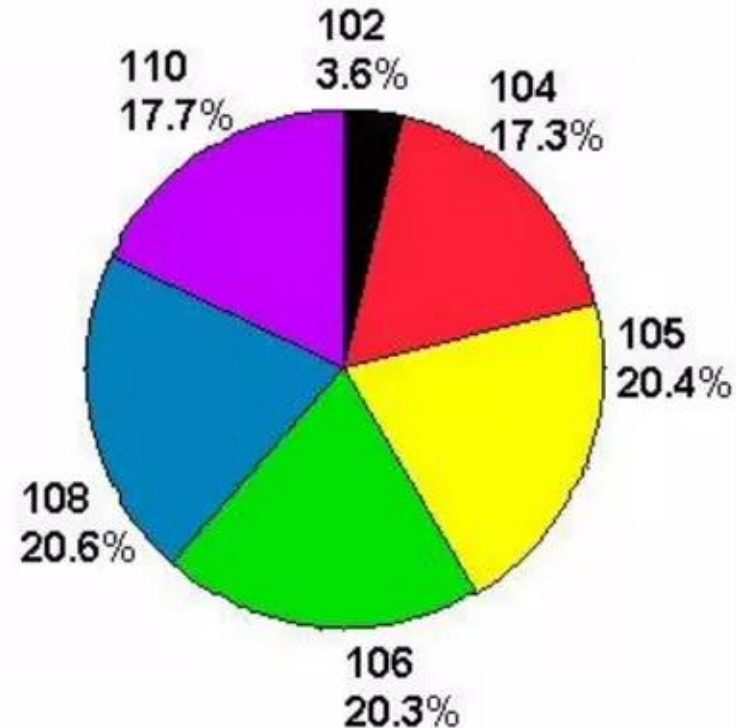


Pd Isotopic Profiles of Surface by SIMS of Excess-Heat-Producing Pd Rod in LiOD (1991)

Before Electrolysis



After Electrolysis



Mizuno, Tadahiko, "Isotopic Changes of Elements Caused by Various Conditions of Electrolysis," American Chemical Society, March 2009

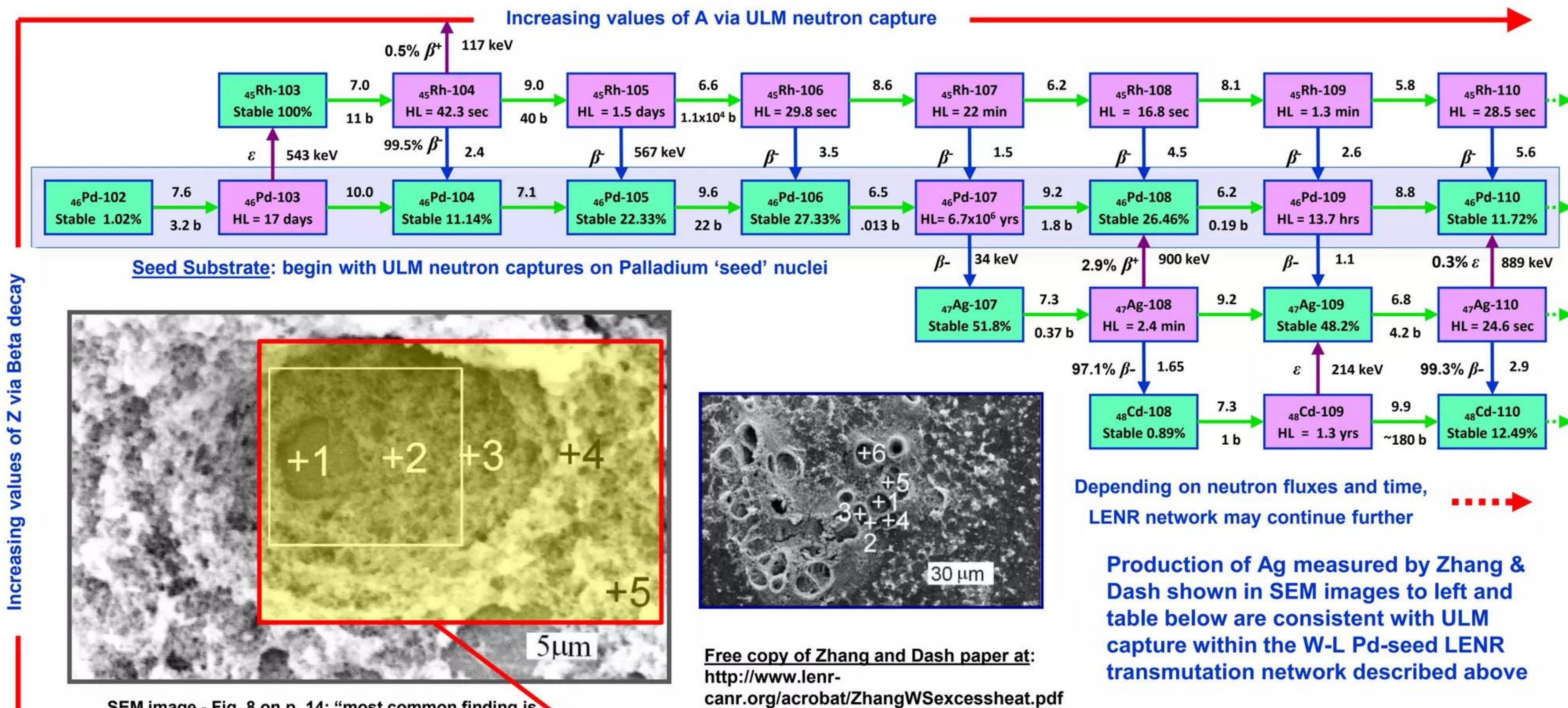
SBK 2010

Source: Mizuno & Kozima, ACS meeting, March 2009

Mizuno & Kozima's Pd Isotopic Measurements

Isotope	Before	After	Result
Pd-102	1.0 %	3.6 %	+ 2.6 %
Pd-104	11.1 %	17.3 %	+ 6.2%
Pd-105	22.3 %	20.4 %	- 1.9%
Pd-106	27.3%	20.3%	- 7.0 %
Pd-108	26.5 %	20.6 %	- 5.9%
Pd-110	11.7 %	17.7 %	+ 6.0%

LENR W-L ULM neutron capture on Pd 'seeds,' neutron-rich isotope production, and decays



SEM image - Fig. 8 on p. 14: "most common finding is that Ag occurs in craters"

Zhang and Dash: Table IX. Relative atomic percent concentrations of silver (Ag) in area and spots shown in Fig. 9

Spot #	wa*	area**	+1	+2	+3	+4	+5
Ag/(Pd+Ag)	1.2 +/- 0.5	5.6 +/- 0.4	6.8 +/- 0.4	5.6 +/- 0.3	6.3 +/- 0.4	3.6 +/- 0.6	1.2 +/- 0.5

*wa = whole entire area comprising image in Fig. 9

** area = delimited by the white square outlined in Fig. 9

Reference: "Excess heat reproducibility and evidence of anomalous elements after electrolysis in Pd/D₂O + H₂SO₄ electrolytic cells," W. Zhang and J. Dash, 13th International Conference on Condensed Matter Nuclear Science, Sochi, Russia (2007)

LENR transmutation products in catalytic converters of cars and trucks?

Palladium (Pd) - six stable isotopes: ^{102}Pd , ^{104}Pd , ^{105}Pd , ^{106}Pd , ^{108}Pd , ^{110}Pd - 1

- ✓ **Palladium is one of three principal metallic catalysts used in most converters: natural abundance ^{102}Pd = 1.02%; ^{104}Pd = 11.14%; ^{105}Pd = 22.33%; ^{106}Pd = 27.33%; ^{108}Pd = 26.46%; ^{110}Pd = 11.72%; ^{103}Pd - unstable, h.l. = 17 days, decays via electron capture to stable ^{103}Rh ; ^{107}Pd - unstable; h.l. = 6.7×10^6 yrs, β^- decays to stable ^{107}Ag ; and ^{109}Pd - unstable, h.l. = 13.7 hrs, β^- decays to stable ^{109}Ag ; ^{105}Pd also has very small cross-section for α -decay to ^{101}Ru on ULMN capture**
- ✓ **Comments: of six stable isotopes, ^{105}Pd has the largest neutron capture cross-section = ~22 barns (b) at thermal energies, then ^{102}Pd = ~3.2 b, and ^{107}Pd = ~1.8 b; other stable Pd isotopes have smaller capture cross-sections; ULMN c-s are 10^3 x - 10^6 x larger**
- ✓ **All other things being equal, at low rates of LENR ULM neutron production where only 1 - 2 neutrons are captured per 'lucky' Pd atom, there would be tendency to *deplete* ^{105}Pd , ^{102}Pd , and ^{107}Pd (if present) and enrich ^{106}Pd , ^{103}Pd (which then decays via e.c. to stable ^{103}Rh if ULM neutron is not captured fast enough) and ^{108}Pd . These tendencies are reflected in the natural abundances**
- ✓ **Please note: to our knowledge, no one has ever published a detailed and exhaustive analysis of all Palladium isotopes present inside a used catalytic converter; nor has there been such an analysis of Pd particles emitted in exhausts, either**

Emissions of small Pd, Pt, and Rh particles from vehicle exhausts are well known; please see:

A. Dubiella-Jackowska, Z. Polkowska, and J. Namiesnik, "Platinum Group elements: A challenge for environmental analytics," *Polish Journal of Environmental Studies* 16 pp. 329 - 345 (2007)

Free copy of this review paper online at:

<http://www.pjoes.com/pdf/16.3/329-345.pdf>

S. Rauch, H. Hemond, C. Barbante, M. Owari, G. Morrison, B. Peucker-Ehrenbrink, and U. Wass, "Importance of automobile exhaust emissions for the deposition of Platinum, Palladium, and Rhodium in the Northern Hemisphere," *Environmental Science & Technology* 39 pp. 8156 - 8162 (2005)

J. Whiteley, "Seasonal variability of Platinum, Palladium, and Rhodium (PGE) levels in road dusts and roadside soils of Perth, Western Australia," *Water, Air & Soil Pollution* 160 pp. 77 - 93 (2005)

S. Rauch, M. Lu, and G. Morrison, "Heterogeneity of Platinum Group metals in airborne particles," *Environmental Science & Technology* 35 pp. 595 - 599 (2000)

M. Moldovan, M. Milagros-Gomez, and M. A. Palacios, "Determination of Platinum, Rhodium, and Palladium in car exhaust fumes," *Journal of Analytical Atomic Spectrometry* 14 pp. 1163 - 1169 (1999)

LENR transmutation products in catalytic converters of cars and trucks?

Palladium (Pd) - six stable isotopes: ^{102}Pd , ^{104}Pd , ^{105}Pd , ^{106}Pd , ^{108}Pd , ^{110}Pd - 2

- ✓ Second point: we are presently unaware of any published work which provides a plausible explanation for effective chemical fractionation of Palladium or Platinum isotopes. That being the case, any significant isotopic shifts from natural abundances observed in well-used Pd or Pt from catalytic converters (and/or detection of traces of 'new' elements, e.g., Ag, Ru, Au, etc.) on interior working surfaces and/or in particles emitted from exhausts could potentially represent a telltale 'signature' of nuclear processes taking place, namely LENRs and ULM neutron-capture on Pd or Pt atoms inside catalytic converters
- ✓ Lattice comments: in that regard, a very interesting and perhaps important paper by Kanitsar et al. (2003) is cited at right. The purpose of this study was to measure, "... Pt, Pd, and Rh concentration levels ... in Viennese aerosol ... emitted from car catalysts."
- ✓ Of note is Fig. 1, where they plot values of $^{194}\text{Pt}/^{196}\text{Pt}$ vs. $^{195}\text{Pt}/^{196}\text{Pt}$ for field samples, which happen to fall along a straight line connecting an "isotopically enriched spike sample" (97.25% ^{196}Pt) with the x, y coordinate for the standard natural abundance ratios of these particular Pt isotopes. They then plot the same graph for Pd with $^{106}\text{Pd}/^{108}\text{Pd}$ vs. $^{105}\text{Pd}/^{108}\text{Pd}$ for field samples, which also fall neatly along a straight line connecting an "enriched spike sample" (98.25% ^{106}Pd) with the x, y coordinate for the standard natural abundance ratios of these Pd isotopes. Importantly, field samples are not distributed randomly along the lines, nor are they clustered close to the natural abundance values

In this interesting paper, Pd and Pt isotopes are analyzed in small particles emitted from vehicle exhausts:

K. Kanitsar, G. Koellensperger, S. Hann, A. Limbeck, H. Puxbaum, and S. G. Stinger, "Determination of Pt, Pd, and Rh by inductively coupled plasma sector field mass spectrometry (ICP-SFMS) in size-classified urban aerosol samples," *Journal of Analytical Atomic Spectrometry* 18 pp. 239 - 246 (2003)

Free copy available online at:

http://www.rsc.org/delivery/_ArticleLinking/DisplayArticleForFree.cfm?doi=b212218a&JournalCode=JA

Regarding Fig. 1 in Kanitsar et al. above, for comparison purposes see Fig. 2 in:

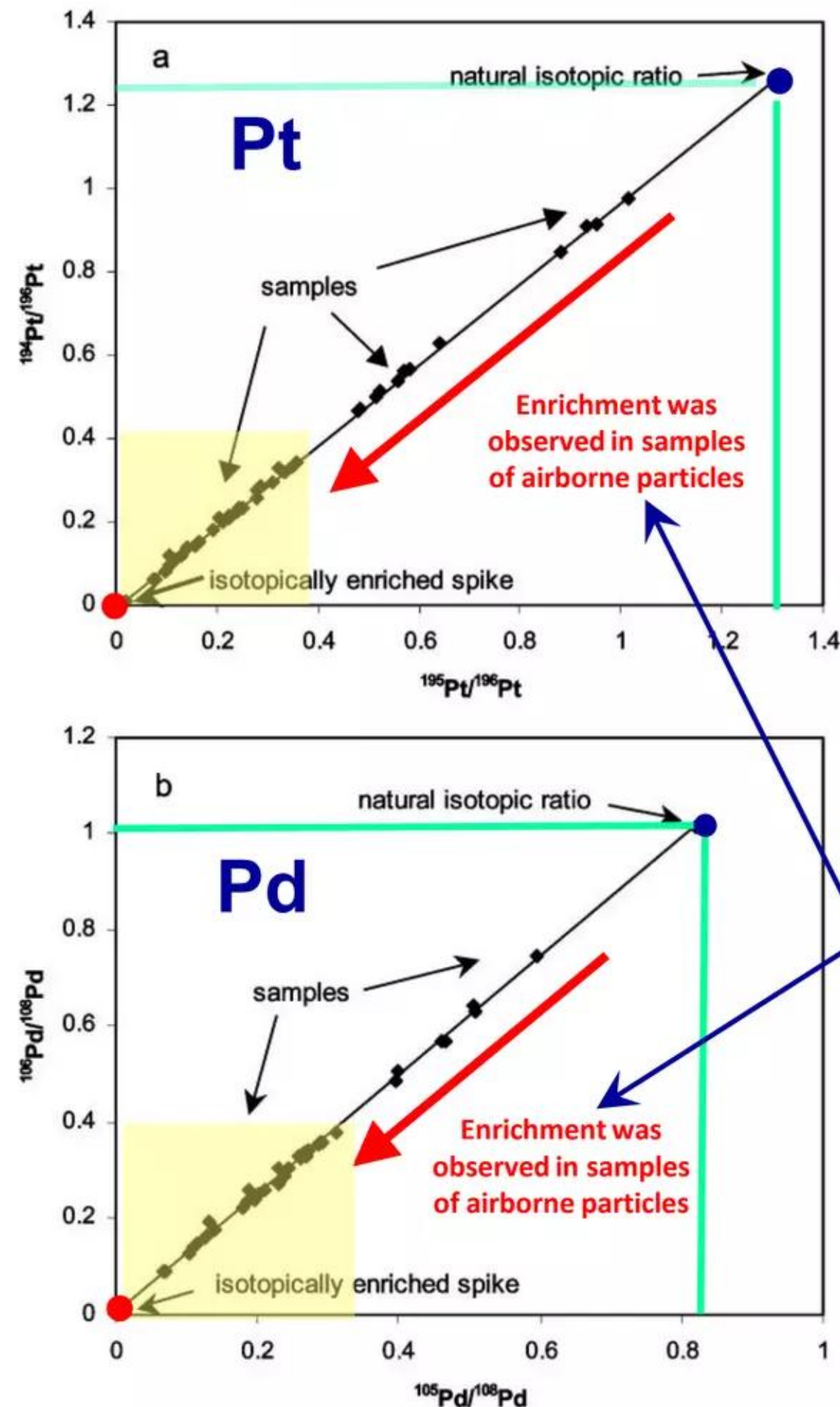
E. Rudolph, A. Limbeck, and S. Hann, "Novel matrix separation – on-line pre-concentration procedure for accurate quantification of palladium in environmental samples by isotope dilution inductively coupled plasma sector field mass spectrometry," *Journal of Analytical Atomic Spectrometry* 21 pp. 1287 - 1293 (2006)

Note: see Figs. 1 and 2 on the next slide

LENR transmutation products in catalytic converters of cars and trucks?

Palladium (Pd) - six stable isotopes: ^{102}Pd , ^{104}Pd , ^{105}Pd , ^{106}Pd , ^{108}Pd , ^{110}Pd - 3

Pt and Pd isotopic ratios observed in nature by Kanitsar et al.:



Note: green lines show x,y intercept of ratios of standard natural abundances

Region of enrichment highlighted in yellow

Pt "spike" was 97.25% ^{196}Pt from Russian Federation

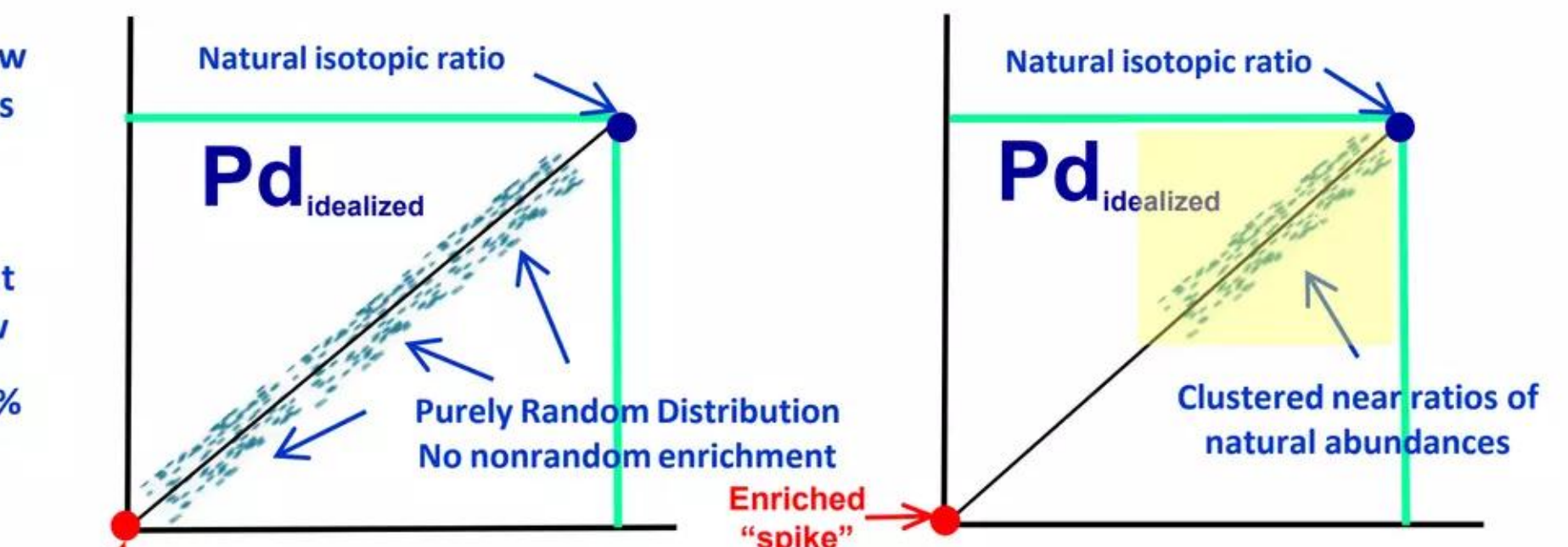
Pd "spike" was 98.25% ^{106}Pd from Russian Federation

Pt and Pd samples in adapted Fig. 1 to left show signs of enrichment

This data is consistent with what would be expected from ULM neutron capture per W-L theory of LENRs

Note: x and y axes are reversed for Pd on Fig. 1 to left versus Fig. 2 to right

Lattice - Larsen: two idealized examples:



Lattice - Larsen: two idealized examples (just above)

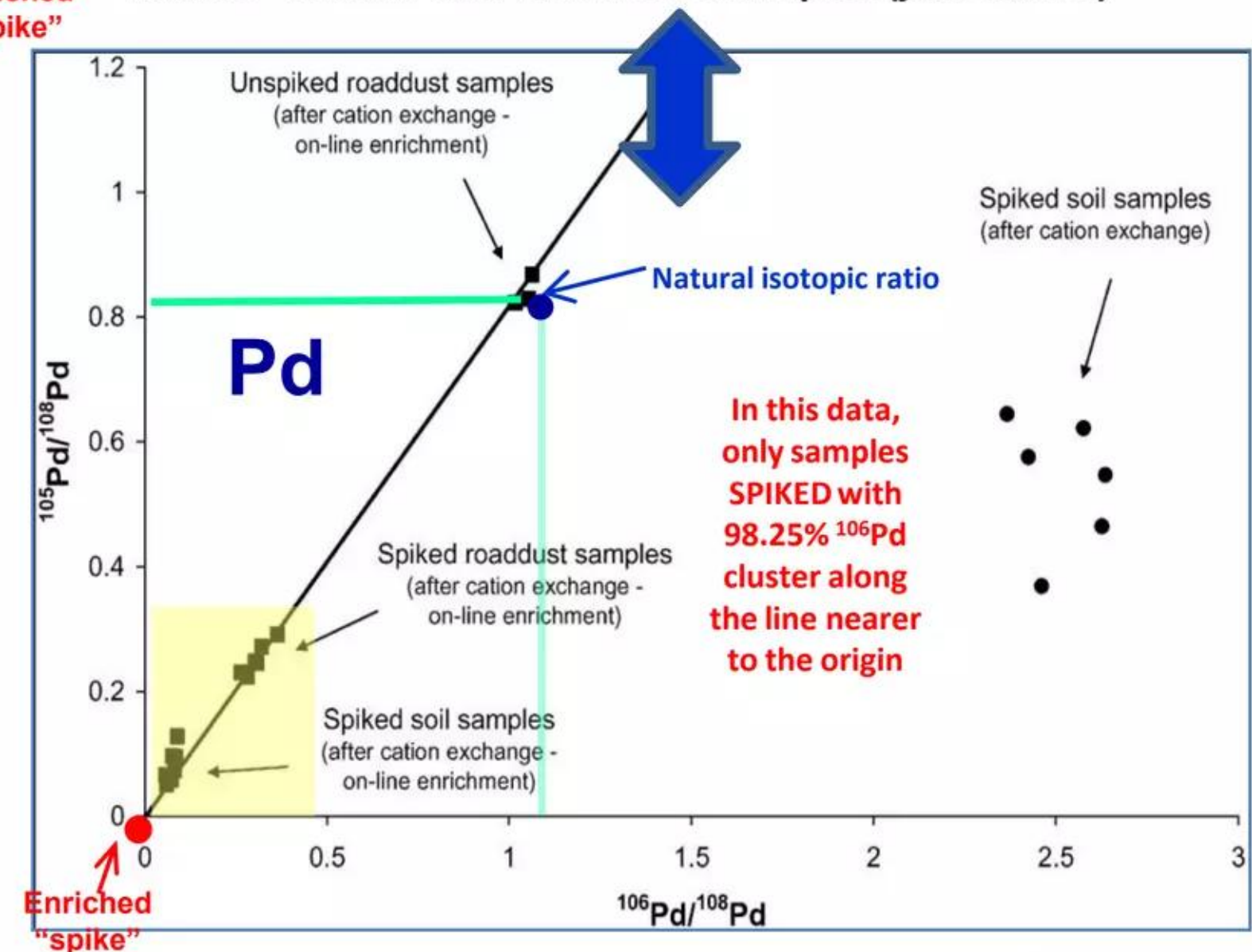


Fig.1 above was adapted from Kanitsar et al. (2003)

Fig.2 above was adapted from Rudolph et al. (2006)

LENR transmutation products in catalytic converters of cars and trucks?

Palladium (Pd) - six stable isotopes: ^{102}Pd , ^{104}Pd , ^{105}Pd , ^{106}Pd , ^{108}Pd , ^{110}Pd - 4

- ✓ **Discussion of previous slide:** presuming that we are not misinterpreting sample isotope data presented in Fig. 1 of Kanitsar et al. (2003), it appears that some nonrandom isotopic enrichment process took place in Pd and Pt found in small airborne particles emitted from vehicle exhausts
- ✓ **Please recall we said earlier that of the six stable isotopes, “ ^{105}Pd [22.33% nat. ab.] has the largest neutron capture cross-section of ~22 barns ... All other things being equal, at low rates of LENR ULM neutron production where only 1 - 2 neutrons are captured per Pd atom, there would be a tendency to *deplete* ^{105}Pd , ^{102}Pd and ... enrich ^{106}Pd ...” Such results would be predicted by W-L theory of LENRs**
- ✓ **Also recall we stated that we are unaware of any chemical fractionation theories that could plausibly explain significant isotopic shifts in Pd and Pt. That being the case, while perhaps some new novel chemical process might be proposed that could also explain such results, the data in Kanitsar et al. can be explained by a nuclear process, that is, ULM neutron-captures on Pd or Pt atoms in catalytic converters per W-L theory and networks such as those shown herein**

LENR Pd isotopic shifts reported by EPRI:

EPRI = the Electric Power Research Institute

"Trace elements added to Palladium by electrolysis in heavy water," EPRI Report # TP-108743 Technical Progress, November 1999

EPRI Project Managers: A. Machiels & T. Passell
Contract Investigators in the Dept. of Chemistry at University of Texas - Austin: B. Bush & J. Lagowski
EPRI public release date: October 22, 2009

Free copy of report available at EPRI website:

http://my.epri.com/portal/server.pt?Abstract_id=TP-108743

Lattice comments – probably a very high rate of ULM neutron production in this experiment:

Results of neutron activation analysis (NAA) reported in #TP-108743 appear to show production of LENR transmutation products starting from ULM neutron capture on Lithium (adsorbed on the cathode surface from the LiOD electrolyte) all the way out to Iron (Fe), as well as transmutation of Pd-108 to Pd-110 via ULM neutron capture on the Palladium (Pd) cathode surface itself. Laboratory work that produced the virgin and post-experiment Pd cathodes analyzed with NAA was conducted in 1998 at a laboratory in France (IMRA) that had been funded and staffed for Pons & Fleischmann by Toyoda family of Japan; ironically, Prof. Stan Pons himself supervised this experiment

N.B. this experimental data is also consistent with Widom-Larsen theory in Pd-seed LENR networks

Commercializing a Next-Generation Source of Safe Nuclear Energy

Conclusions, W-L technical papers, and final quotation

“Widespread global deployment of cost-effective LENR technologies, in parallel with broad deployment of synergistic large- and small-scale photovoltaic and wind-power systems, could create an energy-rich, ‘greener’ energy future for humanity. Importantly, LENRs and the portfolio of carbon-free energy technologies have the potential to democratize access to affordable energy for every inhabitant of this planet.”

“So there it is. Not to decide is to decide. Sooner or later, we must all place our bets on the future.”

Lattice White Paper, April 12, 2010

Image credit: Corbis



Commercializing a Next-Generation Source of Safe Nuclear Energy

Conclusions

- ✓ In gas-phase H_2/Ni experimental systems, capacity for substantial production of excess heat, clear evidence for some sort of a positive thermal feedback mechanism, observed transmutation products, and anomalous absence of energetic neutrons and 'hard' gamma radiation are readily explained by the W-L theory of LENRs and Cr/Fe/Ni 'seed' transmutation networks shown herein
- ✓ Similarly, W-L theory also readily explains transmutation products that have been observed post-experiment in Ni and Pd 'seed' aqueous H_2O or D_2O electrolytic systems, as well as what appear to be LENR transmutation products observed in emissions from precious metal catalytic converters commonly found in cars and trucks worldwide (see SlideShare dtd. June 25, 2010)
- ✓ Positive thermal feedback has been sporadically reported in electrolytic LENR systems. It has also been reported recently by Mizuno & Sawada (2008) in a gas-phase system with stainless steel reaction vessels using Phenanthrene and metal catalyst seeds, "The reaction is reliably triggered by raising temperatures above ... threshold temperature of $600^\circ C$ and ... hydrogen pressures above 70 atm. It can be quenched by lowering the temperature ... below $\sim 600^\circ C$." (see Lattice SlideShare presentation dtd. November 25, 2009, titled, "Mizuno experiments with PAHs")
- ✓ If the apparent positive thermal feedback loop mechanism can be well understood, closely controlled, and incorporated in future LENR-based commercial power generation systems, a wide variety of inexpensive 'seed' nuclei could potentially be 'burned' as nuclear fuels in comparatively simple, relatively unremarkable pressure/temperature/metal reactors employing W-L ULMN-capture LENR nucleosynthetic networks (such as those outlined herein) and without releasing any additional Carbon as CO_2 , 'hard' radiation, or radioactive isotopes into earth's biosphere

Commercializing a Next-Generation Source of Safe Nuclear Energy

Selected Technical Publications

“Ultra Low Momentum Neutron Catalyzed Nuclear Reactions on Metallic Hydride Surfaces”

Eur. Phys. J. C **46**, pp. 107 (March 2006) Widom and Larsen – initially placed on arXiv in May 2005 at http://arxiv.org/PS_cache/cond-mat/pdf/0505/0505026v1.pdf; a copy of the final *EPJC* article can be found at: <http://www.newenergytimes.com/v2/library/2006/2006Widom-UltraLowMomentumNeutronCatalyzed.pdf>

“Absorption of Nuclear Gamma Radiation by Heavy Electrons on Metallic Hydride Surfaces”

http://arxiv.org/PS_cache/cond-mat/pdf/0509/0509269v1.pdf (Sept 2005) Widom and Larsen

“Nuclear Abundances in Metallic Hydride Electrodes of Electrolytic Chemical Cells”

http://arxiv.org/PS_cache/cond-mat/pdf/0602/0602472v1.pdf (Feb 2006) Widom and Larsen

“Theoretical Standard Model Rates of Proton to Neutron Conversions Near Metallic Hydride Surfaces”

http://arxiv.org/PS_cache/nucl-th/pdf/0608/0608059v2.pdf (v2. Sep 2007) Widom and Larsen

“Energetic Electrons and Nuclear Transmutations in Exploding Wires”

http://arxiv.org/PS_cache/arxiv/pdf/0709/0709.1222v1.pdf (Sept 2007) Widom, Srivastava, and Larsen

“Errors in the Quantum Electrodynamic Mass Analysis of Hagelstein and Chaudhary”

http://arxiv.org/PS_cache/arxiv/pdf/0802/0802.0466v2.pdf (Feb 2008) Widom, Srivastava, and Larsen

“High Energy Particles in the Solar Corona”

http://arxiv.org/PS_cache/arxiv/pdf/0804/0804.2647v1.pdf (April 2008) Widom, Srivastava, and Larsen

“A Primer for Electro-Weak Induced Low Energy Nuclear Reactions” Srivastava, Widom, and Larsen

Pramana – Journal of Physics **75** pp. 617 (October 2010) <http://www.ias.ac.in/pramana/v75/p617/fulltext.pdf>

Commercializing a Next-Generation Source of Safe Nuclear Energy

Lattice Energy LLC

“Make no mistake: Rising powers/shrinking planet is a dangerous formula. Addressing the interlocking challenges of resource competition, energy shortages, and climate change will be among the most difficult problems facing the human community. If we continue to extract and consume the planet's vital resources in the same improvident fashion as in the past, we will, sooner rather than later, transform the earth into a barely habitable scene of desolation. And if the leaders of today's Great Powers behave like those of previous epochs - relying on military instruments to achieve their primary objectives - we will witness unending crisis and conflict over what remains of value on our barren wasteland.”

Michael Klare, “Rising Powers, Shrinking Planet: The New Geopolitics of Energy” page 261

Image credit: Strano, MIT, carbon nanotube rope, *Nature Materials*